PB88-174347

REPORT NO.
UCB/EERC-87/14
SEPTEMBER 1987

EARTHQUAKE ENGINEERING RESEARCH CENTER

EXPERIMENTAL STUDY OF REINFORCED CONCRETE COLUMNS SUBJECTED TO MULTI-AXIAL CYCLIC LOADING

by

STANLEY S. LOW
JACK P. MOEHLE

Report to the National Science Foundation

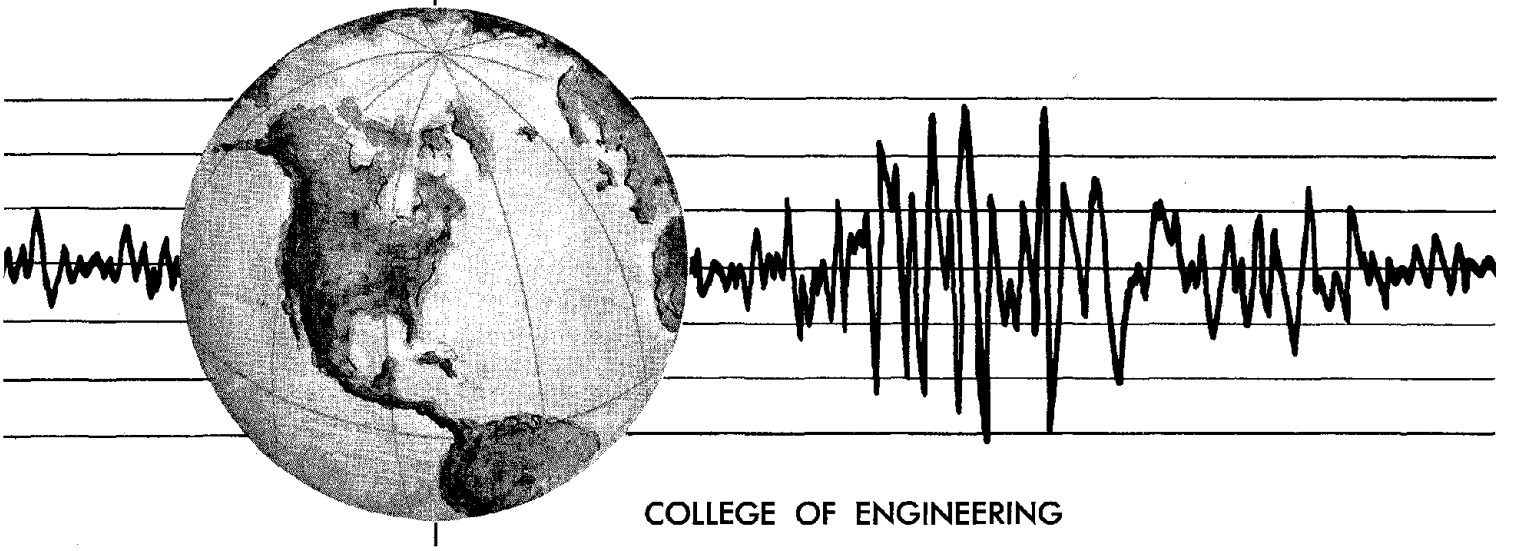

COLLEGE OF ENGINEERING

UNIVERSITY OF CALIFORNIA · Berkeley, California

For sale by the National Technical Information Service, U.S. Department of Commerce, Springfield, Virginia 22161.

See back of report for up to date listing of EERC reports.

50272-101

REPORT DOCUMENTATION PAGE	1. REPORT NO. NSF/ENG-87039	2.	3. Recipient's Accession No. PB88 174347/AS
4. Title and Subtitle: Experimental Study of Reinforced Concrete Columns subjected to Multi-Axial Cyclic Loading			5. Report Date: September 1987 6.
7. Author(s): Stanley S. Low and Jack P. Moehle			8. Performing Organization Rept. No. UCB/EERC-87/14
9. Performing Organization Name and Address: Earthquake Engineering Research Center, University of California, 1301 South 46th Street, Richmond, California 94804			10. Project/Task/Work Unit No. 11. Contract(C) or Grant(G) No. (C) (G) CEE-8316662
12. Sponsoring Organization Name and Address: National Science Foundation, 1800 G. Street, N.W., Washington, D.C. 20550			13. Type of Report & Period Covered 14.

15. Supplementary Notes

16. Abstract (Limit: 200 words)

Five nominally identical quarter-scale reinforced concrete columns were constructed and tested using multiaxial cyclic loading histories. The columns were detailed to satisfy requirements of current North American building codes for reinforced concrete structures in regions of high seismic risk. The columns were loaded as cantilevers attached to stiff foundation blocks. The primary variable was the load history. Load histories included (1) uniaxial cyclic lateral loads with constant axial load, (2) biaxial cyclic lateral loads with constant axial load, and (3) biaxial cyclic lateral loads with cyclicly-varying axial loads.

Measured responses indicate that inelastic deformations in these tests were due primarily to effects of flexure and reinforcement slip from the foundation blocks. Visible damage, stiffness, and resistance were markedly affected by the load history. Existing procedures for computing stiffness and strength under biaxial loading correlated reasonably well with the measured behavior.

This report documents the experiments and measured data, and presents comparisons between measured and calculated responses.

17. Document Analysis a. Descriptors

concrete columns
stiffness
inelastic deformation
flexure
reinforcement slip
uniaxial cyclic load
biaxial cyclic load

b. Identifiers/Open-Ended Terms

c. COSATI Field/Group

18. Availability Statement: Release unlimited	19. Security Class (This Report): Unclassified	21. No. of Pages: 135
	20. Security Class (This Page): Unclassified	22. Price: A07/MF A01/PC $6.95

(See ANSI-Z39.18) See Instructions on Reverse

OPTIONAL FORM 272 (4-77)
(Formerly NTIS-35)
Department of Commerce

EXPERIMENTAL STUDY OF REINFORCED CONCRETE COLUMNS SUBJECTED TO MULTI-AXIAL CYCLIC LOADING

by

Stanley S. Low
Research Assistant

and

Jack P. Moehle
Assoc. Professor of Civil Engineering

A Report to Sponsor:
National Science Foundation

Report No. UCB/EERC-87/14
Earthquake Engineering Research Center
College of Engineering
University of California
Berkeley, California
September 1987

ABSTRACT

Five nominally identical quarter-scale reinforced concrete columns were constructed and tested using multiaxial cyclic loading histories. The columns were detailed to satisfy requirements of current North American building codes for reinforced concrete structures in regions of high seismic risk. The columns were loaded as cantilevers attached to stiff foundation blocks. The primary variable was the load history. Load histories included (1) uniaxial cyclic lateral loads with constant axial load, (2) biaxial cyclic lateral loads with constant axial load, and (3) biaxial cyclic lateral loads with cyclicly-varying axial loads.

Measured responses indicate that inelastic deformations in these tests were due primarily to effects of flexure and reinforcement slip from the foundation blocks. Visible damage, stiffness, and resistance were markedly affected by the load history. Existing procedures for computing stiffness and strength under biaxial loading correlated reasonably well with the measured behavior.

This report documents the experiments and measured data, and presents comparisons between measured and calculated responses.

ACKNOWLEDGMENTS

The research reported herein was funded by the National Science Foundation under Grant No. CEE-8316662 and by the generous contributions from individuals of the Industrial Liaison Program of the College of Engineering of the University of California at Berkeley. (The views presented in this report are those of the authors, and do not necessarily represent the view of the sponsors.)

The authors thank the support staff of the Department of Civil Engineering for their expert assistance in fabricating the test specimens, conducting the tests, and reducing the experimental data. The authors also acknowledge the following for their advice and encouragement: Professors F. Filippou and S. Mahin, and graduate research assistants Xiaoxuan Qi and Shyh-Jiann Hwang, all of the Department of Civil Engineering at the University of California at Berkeley.

The research described in this report is based primarily on work conducted by the first author in partial fulfillment of requirements for the degree of Master of Engineering under the supervision of the second author.

TABLE OF CONTENTS

LIST OF TABLES

Tables

LIST OF FIGURES

Figures

CHAPTER 1

INTRODUCTION

1.1 General

Conventional seismic design of reinforced concrete buildings is carried out considering one direction of seismic loading at a time. Usually, the analysis model assumes elastic behavior and monotonically applied loads. However, during an actual severe earthquake, a building is loaded simultaneously along both axes and may be subject to inelastic deformations with many load reversals. Thus, the capacity of columns in the building to absorb and dissipate energy during multi-axial loading becomes an important factor in the design of the structure.

In conventional design practice, a column is designed explicitly for an ultimate flexural moment, M_u, shear, V_u, and axial load, P_u. The required ductility of a column is assured implicitly by establishing an upper and lower limit on the longitudinal reinforcement ratio and by requiring a minimum amount and spacing of transverse reinforcing. Adequacy of the current design method in providing the required strength and ductility under uniaxial loading reversals has been demonstrated in previous experimental studies [7]. Although behavior of columns under biaxial loading has been studied previously [5], adequacy of the design method for columns subjected to multi-axial loadings has not been fully investigated.

1.2 Scope

To further investigate behavior under multi-axial cyclic loading, an experimental study was carried out in which five one-quarter scale reinforced concrete columns were subjected to inelastic load histories with reversals. The columns were nominally identical, and satisfied major requirements of current codes for design of lateral load resisting columns in regions of high seismic risk [8]. Concrete had compressive strength of approximately 5000 psi. Reinforcement was typical of Grade 60. The longitudinal reinforcement ratio was 0.0226. Average axial load was approximately $0.06f'_cA_g$, in which f'_c = concrete compressive strength at time of test and A_g = gross area of column cross section.

The columns were tested as cantilevers projecting from stiff foundation blocks. Cyclic lateral load histories were either uniaxial along a principal axis of the column, uniaxial along a skewed axis of the column, or a "cloverleaf" biaxial loading. Axial loads were either constant or varied as a function of the lateral load history.

The experiments and measured data are described in later sections of this report. Existing analysis methods are used to compute expected behaviors of the columns, including stiffness, rebar slip effects, monotonic loading curves, and strength under biaxial loading. Computed and measured responses are compared.

1.3 Relevance of Experiment to Current Research

In addition to the importance (as described above) of studying biaxial loading effects in general, it is noted that the columns described in this report are nominally identical to first-story columns of a six-story shake-table model tested in the Earthquake Simulator Laboratory at the Earthquake Engineering Research Center of the Berkeley campus [3]. The shake-table model was subjected to "biaxial" excitations on the earthquake simulator. Column data presented in this report will supplement the study of the shake-table model.

CHAPTER 2

DESCRIPTION OF THE EXPERIMENT

2.1 TEST SPECIMENS

The columns are approximately one-quarter scale models of columns considered representative of those occurring in modern, moderately-tall, ductile concrete frames located in regions of high seismic risk. The columns had the configuration depicted in Fig. 2.1.

Each column was a 21.5 in. long cantilever, having gross cross section of 5 in. by 6.5 in. Longitudinal reinforcement comprised #3 deformed bars at each corner, two #2 deformed bars (0.049 $in.^2$ cross section) along each long face, and one #2 bar deformed bar along each short face (Fig. 2.1). The longitudinal reinforcement ratio, defined as the ratio between total longitudinal steel area and gross column cross-sectional area, was 0.0226. All longitudinal bars were anchored with 90-degree hooks embedded 7-in. into a 13 -in. by 14-in. by 18-in. reinforced concrete footing. Plain, gage No. 9 wire (0.0123 $in.^2$ cross section) was used as transverse reinforcement in the columns. Starting from the top of footing, tie spacing was 1 in. for the first nine inches followed by ties at 1.5 in. on centers. According to prevailing codes [1], the first tie spacing above the top of footing should have been 0.5 in. rather than 1 in. Apart from this deviation, the columns satisfy current code requirements for columns in ductile moment resisting frames located in regions of high seismic risk [8].

The test specimens will be designated as specimens 1 through 5, corresponding to chronology of the individual test dates. As described in Sections 2.2 and 2.5, the designation also indicates variations in concrete materials and test load histories. A chronology of construction and testing is in Table 2.1.

2.2 Materials

The test specimens were cast in a horizontal position in two batches, specimens 1 through 3 in the first batch, and 4 and 5 in the second. Photographs of the reinforcing cages and forms before and after casting are in Fig. 2.2 and 2.3, respectively.

Details of the materials are given in the following tables and figures: Concrete mix proportions (Table 2.2), concrete and steel mechanical properties (Tables 2.3 through 2.5), and stress-strain curves (Fig. 2.4 and 2.5). It is noted that mechanical properties of the longitudinal reinforcement were characteristic of those usually obtained for Grade 60 reinforcement, with mean yield stresses ranging from 60 to 73 ksi. Mean concrete compressive strengths were approximately 5300 psi for specimens 1 through 3, and 4600 psi for specimens 4 and 5 at time of testing.

2.3 Loading Apparatus

The columns were tested in a horizontal position with the weak direction (short column cross-sectional dimension) parallel to the laboratory floor as shown in Fig. 2.6 and 2.7. The footing block was shimmed and prestressed to a massive reinforced concrete block before testing. Two 40-kip hydraulic actuators

(for lateral loads) and a hydraulic jack (for axial load) were then attached to the "free" end of the column through a specially-fabricated universal joint. The joint allowed forces to be applied at the column end with negligible rotational restraint.

The hydraulic pressure for the actuators and jack was provided by three portable Haskel hydraulic pumps. The pumps were controlled manually, with applied loads varied to follow approximately the prescribed displacement or force histories.

2.4 Instrumentation and Data Acquisition

Instrumentation measured lateral column displacements, column loads, deformations of the column near the base, and strain of longitudinal reinforcement. The instrument locations are shown schematically in Fig. 2.6, with a photograph of the test setup in Fig. 2.7.

Displacements of the column were measured near the free end of the column using LVDTs (linear voltage displacement transducers). The LVDTs were mounted to a stiff reference frame attached to the footing blocks, so that recorded displacements are relative to the footing. Thus, any movement of the footing blocks during testing does not influence the recorded displacements.

Deformations of the column near the base were measured with clip gages attached between the top of the foundation block and an aluminum yoke that was fixed to the column concrete a distance

of 5 in. from the top of the foundation block. Three clip gages were used, one at each of three corners of the yoke. Average rotations about each axis along this length were calculated by dividing the differences in relative displacements by the distance between clip gages. It is noted that these rotations include both the rotations due to slippage of the longitudinal reinforcement in the footing and the flexural curvature in the lower 5 in. of the column.

The hydraulic actuators and jack were mounted to strain-gaged load cells that were calibrated to obtain the applied column load. Column base moments (at the top of footing) were computed as the sum of (1) the primary moment due to lateral load and (2) the secondary moment due to the axial load acting through lateral deflections. The primary moment was calculated as the product between lateral load and loading height. The secondary moment (P-delta moment) was calculated according to the procedure outlined in Fig. 2.8. As noted in the equation given in that figure, the P-delta moment includes both the effect of the axial load acting through lateral displacement of the column and the effect of the horizontal component of the "axial" load acting through column height.

Weldable strain gages having 1-in. gage length were installed on two longitudinal bars located along a diagonal of the column cross section (Fig. 2.1 and 2.6). The gages were centered 0.5 in. from the face of the footing block.

Signals from all electronic instruments were scanned at

discrete intervals using a low-speed scanner box. The signals were stored digitally on a computer disk. In addition, signals from displacement and load gages were recorded in analog form on X-Y and X-Y-Y' plotters. The test program was controlled manually by monitoring the plotted signals.

All specimens were whitewashed to make cracks in the concrete more visible. Cracks were marked when the peak displacement in each direction of a given cycle was reached. Maximum crack width was also recorded at this time.

2.5 Test Procedure

The footing block of a specimen was shimmed and then prestressed to a massive concrete block prior to testing. Instrumentation was then installed and zero values set, followed by attachment of the loading jack and actuators. Testing began within an hour of setting zero values for the instruments and attaching the jack and actuators. The load history was different for the different test specimens. The target load/deformation histories for the specimens are shown in Fig. 2.9. Brief descriptions of the load history of each specimen follow.

SPECIMEN 1: Uniaxial lateral loading about the weak axis, with constant axial load of 10 kips

SPECIMEN 2: Biaxial lateral loading with column tip displacements along an axis at 45 degrees relative to the principal axes of the column cross section, with constant axial load of 10 kips.

SPECIMEN 3: Biaxial lateral loading with column tip displacements following a "cloverleaf" pattern, with constant axial load of 10 kips.

SPECIMEN 4: Biaxial lateral loading with column tip displacements along an axis at 45 degrees relative to the principal axes of the column cross section, with axial load varying from 0.5 to 20 kips.

SPECIMEN 5: Biaxial lateral loading with column tip displacements following a "cloverleaf" pattern, with axial load varying from 0.5 to 20 kips.

The axial loads for specimens 4 and 5 varied with the tip displacement in the weak direction. For a given displacement cycle, the axial load varied approximately linearly from 10 kips at zero displacement to 20 kips at the maximum positive displacement for that cycle. For loading in the negative direction, the axial load varied approximately linearly from 10 kips at zero displacement to 0.5 kips at the most negative displacement for that cycle.

In the early stages of loading before reinforcement yielded, loading was controlled by the applied lateral load. For all specimens, the first cycles were at forces corresponding approximately to first cracking, followed by loading to approximately 40% of yielding, followed by loading approximately to initial yielding of reinforcement, as determined for specimen 1. After reinforcement yielded, loading was controlled by the magnitude of the measured tip displacement.

Two complete cycles were carried out at each level of loading (Fig. 2.9). The tip displacement was increased progressively until lateral displacement reached 0.96 in. (5.3% of specimen height measured from top of footing). After reaching the maximum displacement for each cycle, the hydraulic equipment was not manually adjusted for the period of time (approximately

ten minutes) that damage was observed and recorded. Some drop in hydraulic pressure typically was observed during this time.

CHAPTER 3

EXPERIMENTAL RESULTS

3.1 Summary of Data

Observed damage is summarized in photographs and crack diagrams in Fig. 3.1 and 3.2, respectively. Measured load histories are presented in Fig. 3.3 through Fig. 3.7 (in these figures, one unit of "time" is defined to pass whenever data readings are taken). Lateral load versus lateral displacement along each principal axis is presented in Fig. 3.8 through Fig. 3.12. Similarly, relations between base moment (corrected to account for second-order effects) and base rotation along the lower five inches of the column are presented in Fig. 3.13 through Fig. 3.17. Reinforcement strain gage readings are plotted versus time in Fig. 3.18 through Fig. 3.22. A summary of selected experimental results is in Table 3.1.

3.2 Visible Damage

Several observations are made regarding crack patterns, and apparent failure modes (Fig. 3.1 and 3.2).

(1) Primary cracks were generally perpendicular to the longitudinal axis of the columns, and were apparently due to flexural effects.

(2) As the load increased to yield in either direction, minor diagonal tension cracks were observed. For specimen 1, the diagonal cracks formed only on the two faces parallel to the direction of lateral load. For the other specimens, the diagonal cracks formed on all faces. Although flexural cracks

predominated, the diagonal tension cracks indicate that shear was a contributing factor in behavior of the test specimens.

(3) Cracks generally closed when the loading fell below approximately the load that first caused cracking. This is probably attributable to the presence of axial load on the column.

(4) Between column end displacements of 0.32 in. and 0.64 in., and thereafter, development of new cracks slowed. As larger displacements were applied in this range of loading, crack width in existing cracks became larger.

(5) The widest crack in all specimens was at the intersection between the column and the footing block, indicating the occurrence of slip of longitudinal bars from the footing. However, the width of these cracks could not be determined because the crack grew partially below the footing surface.

(6) For specimens 2 through 5, spalling of concrete cover initiated at the corners of the column near the footing during displacement cycles of 0.32 in. or 0.64 in. Specimen 1 did not begin spalling until the displacement cycle to 0.96 in.

(7) For specimens 2 through 5, total spalling of concrete cover near the corners occurred for displacements in the range between 0.64 in. 0.96 in. In specimens 2 and 4, only two diagonal corners spalled, whereas in specimens 3 and 5, all four corners spalled and small portions of cover adjacent to diagonal tension cracks showed minor spalling.

(8) The primary failure mode of all specimens was by flexure. As gaged by the amount and distribution of diagonal cracks, shear

also played a minor role in the failure of specimens 3 and 5. Examination of the specimens revealed that longitudinal reinforcement did not buckle.

3.3 Lateral Load-Displacement Relations

Relations between lateral load and displacement are plotted in Fig. 3.8 through 3.12. Lateral loads reported in those figures are readings obtained directly from load cells in the lateral-load actuators, without a correction for the lateral component of the force in the axial load jack. Lateral displacements were determined directly from readings of LVDTs (Fig. 2.6), and reflect displacement of the column tip relative to a rigid reference frame mounted to the footing block. Twist of the column end about the column longitudinal axis could be determined from the available LVDT readings, and was observed to be negligible.

Based on the envelope of load-displacement responses in Fig. 3.8 through 3.12, three distinctly different ranges of stiffness can be observed, the first corresponding roughly to loading before flexural cracking, the second corresponding to the range between cracking and yield of longitudinal bars, and the third after yield. After the column longitudinal bars had yielded, and for displacement cycles that did not significantly exceed prior displacement maxima, a reduction in both stiffness and resistance were noticeable. When subjected to increased displacements, resistance was mostly regained.

Hysteretic responses for specimens 1, 2, and 4 are similar to those commonly observed for reinforced concrete elements subjected to axial loads and not having significant shear or anchorage deterioration [7]. Hysteretic relations for specimens 3 and 5 show loads "relaxing" for lateral displacements near the maximum and near zero, without significant change in displacement. The relaxation is attributed to the nature of the biaxial loading history, as follows. As shown in Fig. 2.9, drift was first imposed in one direction while ideally fixing displacement in the transverse direction, and then the axes of loading were switched. The relaxation shown in Fig. 3.10 and 3.12 is concurrent with commencement of loading in the perpendicular direction. Section 4.5 of this report discusses this phenomenon further.

3.4 Base Moment-Base Rotation Relations

Measured relations between base moment and base rotation are in Fig. 3.13 through 3.17. As noted in Section 2.4 and illustrated in Fig. 2.8, base moment includes second-order effects of the axial load acting through lateral displacements. Base rotations are the total rotation of the column cross-section at 5 in. from the top of the footing relative to the top of the footing (Section 2.4 and Fig. 2.6). Thus, the reported rotations include effects both of column flexure and reinforcement slip from the footing.

In general, the shape of the moment-rotation relation for each specimen (Fig. 3.13 through 3.17) appears similar to the

corresponding lateral load-displacement relation (Fig. 3.8 through 3.12). The similarity supports a hypothesis that flexural and bond slip deformations in the "plastic-hinge" region of the column were the predominant actions contributing to overall specimen deformation. Section 4.4 of this report examines the contribution quantitatively.

3.5 Strain Histories

Strain histories (Fig. 3.18 through 3.22) indicate that corner longitudinal bars experienced greater inelastic compression and tension strains in specimens subjected to the biaxial cloverleaf lateral loading than in the single specimen (specimen 1) subjected to uniaxial lateral loading. The high strain in the corner portion of the column is consistent with the observed damage (Fig. 3.1 and 3.2). The observation that the longitudinal bars did not buckle, despite having undergone many cycles of high inelastic compression and tension, supports a conclusion that current detailing procedures are effective in controlling buckling of reinforcement. The strains developed in the columns loaded along an axis skewed to the principal axes (specimens 2 and 4) were less than in the other specimens because the gaged bars were located (by oversight) on the diagonal axis of the column transverse to the diagonal of lateral loading.

CHAPTER 4

DISCUSSION OF TEST RESULTS

4.1 Introductory Remarks

Data present in Chapter 3 are analyzed and discussed in this chapter. Computed responses are presented and compared with measured responses. Sources of deformation in the columns are analyzed. A summary of the effects of load history on behavior concludes the chapter.

4.2 Computed Monotonic Behavior

Responses of the columns to monotonically-increasing loads were computed for comparison with measured responses. Included in the computed responses are uniaxial and biaxial moment-curvature relations, biaxial moment-axial load interaction diagrams, shear strengths, bar slip relations, and uniaxial load-deflection relations. These are described in the following subsections.

(a) Moment-Curvature Relations

Moment-curvature relations were computed for monotonic loading using conventional assumptions that plane sections remain plane (including perfect bonding between steel and concrete), stresses are related directly to strain, and relations of statics are valid. A computer program was written to facilitate computation of the relations. The computational scheme is as follows:

(1) The cross section is subdivided into a grid of small

rectangular elements (fiber approach [15]). A material property is assigned to each of these small elements. Additional elements on the cross section are defined for the reinforcement.

(2) A strain field is imposed on the cross section, defined by a maximum concrete strain, depth of neutral axis, and inclination of neutral axis. The strain at the center of each element (fiber) of the cross section is computed from geometry considerations.

(3) Given the strain at the center of each element, stress at the center of each element is determined from a predefined stress-strain relation. An average force in each element is defined as the product between the stress at the center of the element and cross-sectional area of the element.

(4) Axial load and moment about each axis are determined by summing effects of averages forces acting on each element of the cross section. A correction is made for concrete displaced by reinforcement. Axial load is defined to be acting at the geometric centroid of the gross concrete cross section. Moments are defined relative to that centroid.

For the columns in this study, unconfined and confined concretes were defined using properties measured from test cylinders, and analytical relations defined by Scott and Park [13]. The assumed curves are plotted in Fig. 4.1. Assumed stress-strain relations for reinforcement are in Fig. 4.2.

Computed moment-curvature relations, for the range of axial loads experienced during the experiments, are in Fig. 4.3. The

relations indicate that strength and ductility are affected by the level of axial load and the orientation of loading. However, as would be expected for well-confined concrete columns with axial loads below the balanced point, the columns exhibit "adequate" ductility for all plotted axial loads.

(b) Biaxial Moment-Axial Load Interaction Diagrams

Interaction diagrams were constructed using the same computer program described in Section 4.2(a). Families of uniaxial interaction diagrams are plotted in Fig. 4.4 for various assumed maximum concrete compressive strains. Biaxial moment interaction diagrams for various assumed maximum concrete compressive strains and for various axial loads are plotted in Fig. 4.5.

(c) Shear Strength

To check if shear could limit the strength of the columns, shear strengths were computed using the beam shear strength equations of the ACI Building Code [1]. Accordingly, a concrete shear strength of $V_c = 2\sqrt{f'_c}\, bd = 2\sqrt{4900}\,(5)(5.8) = 4.1$ kips is computed parallel the long cross-sectional dimension, and $V_c = 2\sqrt{4900}\,(6.5)(4.3) = 3.9$ kips is computed parallel the short dimension. Using a limiting steel yield stress of 60 ksi, strength of steel in the long direction is $V_s = A_v f_y d/s = (0.0369)(60)(5.8)/1 = 12.8$ kips, and in the short direction is $(0.0492)(60)(4.3)/1 = 12.7$ kip. Adding the steel and concrete strengths in each direction, the total nominal shear strengths are 16.9 kips and 16.6 kips in the long and short directions,

respectively. With a moment arm of 21.5 in. used in the experiments, the base moments corresponding to shear failure are 363 kip-in. and 357 kip-in. in the long and short directions, respectively. These strengths are approximately double the computed flexural strengths (Fig. 4.5). Thus, shear failures are not anticipated.

(d) Bar Slip Relations

The presence of "wide" cracks at the base of the columns suggests that slip of longitudinal reinforcement may have contributed significantly to deformations of the columns. To estimate the contribution, slip of reinforcement from the footings was calculated assuming a uniform bond stress acting over the stressed lead-in length of the reinforcement anchorages. For No. 3 deformed bars, anchored in confined concrete similar to that occurring in the footings, and subjected to monotonic tension loading, an average uniform bond stress of 1300 psi was estimated to be effective [6]. For this bond-stress model, the length, l, of rebar required to develop the tension T in the loaded end of the bar is given by Eq. 4.1.

$$l = \frac{T}{u_b d_b \pi} \quad \ldots\ldots\ldots\ldots\ldots\ldots\ldots\ldots\ldots\ldots\ldots\ldots \quad (4.1)$$

in which u_b = average uniform bond stress and d_b = nominal bar diameter. The elongation, D, of the bar over the length l is given by Eq. 4.2.

$$D = \frac{T^2}{2\pi u_b d_b A_b E_s} \quad \ldots\ldots\ldots\ldots\ldots\ldots\ldots\ldots\ldots\ldots\ldots\ldots \quad (4.2)$$

in which A_b = cross-sectional area of the bar and E_s = Young's modulus for the bar.

Values for l and D are tabulated in Table 4.1 for different values of the steel stress, f_s, and with T in Eq. 4.1 and 4.2 taken equal to the product between f_s and A_b. Even when stressed to yield (approximately 70 ksi in Table 4.1), the length l does not exceed the available lead-in length for the bars in the footing (Fig. 2.1). Thus, deformations along the bent portion of the hook and beyond need not be considered according to the analytical model. Accordingly, total slip of the bar from the footing is equal to the value of D.

Displacement at the end of the column due to bar slip is computed as the product between column height and rotation due to bar slip. Rotation due to bar slip is computed as the ratio between bar slip, D, and the distance between the bar and the neutral axis for bending. The distances are taken equal to 3.1 in. and 4.1 in. for bending about the weak and strong axes, respectively. Computed column end displacements, D_x and D_y, for bending about the weak and strong axes, respectively, are tabulated in Table 4.1.

(d) Calculated Monotonic Load-Displacement Relations

Relations between load and displacement at the column end were computed by numerically integrating calculated curvatures over height and adding calculated displacements due to bar slip from the foundation (Table 4.1). The relations are plotted in

Fig. 4.6. It is noted that the computed displacement due to bar slip effects is approximately 10 to 20 percent of the total computed displacement before yield.

4.3 Comparison Between Computed and Measured Quantities

(a) Failure Mode

According to computed responses, each specimen is anticipated to fail in flexure after developing deformations well in excess of yield. The measured results support this expectation. Cracks were primarily flexural (Fig. 3.1 and 3.2). Longitudinal reinforcement showed strain histories consistent with inelastic flexural response (Fig. 3.18 through 3.22). Load-deformation relations (Fig. 3.8 through 3.12) are characteristic of flexural response, and shear distortions were at no time visible during testing. At the final load stages, concrete cover spalled near the base only, with patterns of spalling consistent with expected compression forces from flexural effects.

Shear, although apparently resulting in some inclined cracks (Fig. 3.1 and 3.2), did not appear to be a prime contributor. Slip of reinforcement from the footing, although contributing to deformations, did not limit the strength.

(b) Strength

Figure 4.7 compares measured biaxial base moment histories (corrected for second-order effects) and computed biaxial moment envelopes. The computed envelopes were obtained using the computer program described in Section 4.2(a), with maximum

concrete compression strain of 0.01. For specimens 4 and 5, for which axial load during testing varied between 0.5 and 20 kips compression, three computed biaxial moment envelopes are shown, one each for axial compression of 0.0 kip, 10 kips, and 20 kips.

The data in Fig. 4.7 indicate that measured biaxial moment strengths compare well with computed strengths. In general, measured moment strengths exceed computed values. Although no detailed analysis of the overstrengths will be presented in this report, it is possible to attribute the overstrength to a combination of several effects. For one, measured compression strains in reinforcement exceeded the value of 0.01 assumed for concrete in the analysis. As shown in Fig. 4.4, flexural strengths are higher for the range of axial loads under consideration if larger compression strains are assumed. In addition, Bauschinger effects due to inelastic load reversals generally result in higher reinforcement stresses for a given strain than recognized in the scheme used to calculate member strengths under monotonic loading. Reinforcement is also likely to reach higher stresses in the columns than in coupon tension tests because the smaller length under maximum tension in a column is not likely to contain a weak "link" that limits strength in a coupon tension test. Column strength is also increased due to increases in concrete strength and maximum strain capacity that result from high strain gradients and confinement of concrete by the large footing block at the column base. All of these effects are likely to increase the column

strength to values exceeding calculated strength.

(c) Load-Displacement Relations

Measured and calculated load-displacement relations are compared in Fig. 3.9 through 3.12, with calculated relations shown by broken curves. The calculated relations are identical to those described in Section 4.2(d) and Fig. 4.6, and include effects of reinforcement slip from the footings as described in Section 4.2(d). For columns loaded biaxially, computed relations are shown for lateral load assumed to be uniaxial and parallel to the direction for which the response is shown, and for lateral loads resulting in displacement response at 45 degrees to the direction being shown.

Calculated responses assuming uniaxial load for specimen 1 or biaxial load for the remaining four specimens compare well with measured responses, suggesting that existing analytical models are adequate for this purpose. For the biaxially-loaded columns, it is apparent by comparison with computed uniaxial load-displacement relations that the biaxial loading results in reduced effective moment resistance along the principal axes of the column.

4.4 Source of Deformation at Final Loading Stage

The appearance of the columns following testing (Fig. 3.1) suggests that the majority of column tip displacement was due to

inelastic rotations occurring at the base of the columns. In support of this observation, column tip displacements about both principal axes due to rotations measured by clip gages at the base of the column were computed for comparison with measured displacements. For this purpose, the rotation measured over a five-in. gage length by the clip gages was assumed to be concentrated at the center of the five-in. length as shown at the top of Fig. 4.8. Computed displacements due to base rotations are compared with actual measured maximum displacements at the bottom of Fig. 4.8. According to this calculation, base rotations along the bottom five in. of the column contributed between 82 and 92 percent of the total maximum tip displacement.

A conventional design practice [11] is to assume that all inelastic action is attributable to uniform flexural curvature within a plastic hinge region at the end of an element. For the columns of this study, a plastic hinge length equal to approximately five in. is appropriate. Hence, rotations inferred from the clip-gage readings at the base of the column are effectively the equivalent plastic hinge rotations.

If the measured base rotations are assumed to be attributable to uniform flexural curvature over the plastic hinge length, then for specimen 1, for example, the computed curvature is equal to (0.06 rad)/(5 in.) = 0.012 rad/in. In addition, if the distance from the neutral axis to the tension reinforcement is taken equal to the distance between extreme layers of

longitudinal reinforcement, that is, 3.0 in., then the expected strain in longitudinal reinforcement is equal to (0.012 rad/in.)(3 in.) = 0.036 in./in. Actual maximum measured strain for specimen 1 was 0.029 in./in. Thus, the method for estimating strain produces fairly good estimates of maximum expected strain.

It is noted in relation to the preceding paragraph that the calculated strain exceeds the measured strain, even though the measured strain is likely to be a maximum value whereas the calculated strain is an average. A plausible reason for this apparent inversion of magnitudes is that the calculation method does not consider the effect of rebar slip from the footing blocks. Because of slip of the reinforcement, the column base rotation is developed by reinforcement strains over a longer length, thereby reducing the actual required reinforcement strain over that length.

4.5 Effect of Load History on Load-Displacement Response

As described in Chapter 2, the columns were loaded to effect displacement histories that followed prescribed patterns (Fig. 2.8 and 3.3 through 3.7). Under uniaxial lateral loading, either along one principal axis as for specimen 1 or along an inclined axis as for specimens 2 and 4, the resulting hysteretic relations between lateral load and displacement (Fig. 3.8, 3.9, and 3.11) show familiar patterns of slightly spindle-shaped loops. For specimens 3 and 5, which were loaded in a cloverleaf pattern of displacements, the hysteretic loops (Fig. 3.10 and 3.12) and

biaxial moment interactions (Fig. 4.7c and 4.7e) follow unfamiliar patterns. The hysteretic responses of specimens 3 and 5 are explained qualitatively in the following paragraphs.

Figure 4.9 through 4.12 present an idealized chronological sequence of displacement paths, load-deformation loops, and biaxial moment interaction diagrams. The diagrams are considered representative of specimen 3, with constant axial load, and for lateral loads inducing inelastic response. Similar diagrams can be plotted for specimen 5, but these would be complicated somewhat by the simultaneous variations of axial loads during the loading sequence. To clarify the presentation, the diagrams are plotted successively on several sheets.

The diagram at the upper left of each sheet of Fig. 4.9 through 4.12 represents the displacement path during a selected portion of one complete cloverleaf loading cycle. Points "a" through "m" denoted on the displacement path occur successively. The second pair of diagrams at the bottom of each sheet represents the load-deformation relation along "X" and "Y" axes of the column, with points "a" through "m" from the displacement history designated at appropriate points. The diagram at the upper right of each sheet represents the relation between base moments about each axis, again with points "a" through "m" designated at appropriate points. There is no attempt to present the diagrams to any prescribed scale.

Figure 4.9 plots idealized responses for roughly the first

quarter cycle (points "a" through "c"). At first loading, the displacement is increased in the "X" direction to point "a" (Fig. 4.9a). The load-deformation relation in the "X" direction loads to point "a" (Fig. 4.9c), whereas no loading is noted in the "Y" direction (Fig. 4.9d). The moment interaction diagram (Fig. 4.9b) shows moment only about the "Y" axis (that is, in the "X" direction).

As the displacement progresses to point "b" (Fig. 4.9a), the load in the "Y" direction increases (Fig. 4.9d). As the moment M_x increases for loading in the "Y" direction, flexural strength considerations require that the moment M_y, developed during loading to point "a", must decrease (Fig. 4.9b). The decrease in moment M_y is noted also in the load-deformation relation in the "X" direction (Fig. 4.9c). In addition, the displacement in the "X" direction increases slightly as the load in that direction relaxes (Fig. 4.9c). The magnitude of this increase in displacement is partly a function of the test specimen and partly a function of the loading system used in the experiments. Similarly, moving from point "b" to point "c", the displacement in the "X" direction is decreased, which simultaneously results in an inelastic relaxation of load and displacement in the "Y" direction.

As the loading is continued into the second quarter cycle (points "d" through "f" in Fig. 4.10), similar behavior occurs. Moving from point "c" to point "d", the column is loaded from a

positive "Y" displacement to an equally large negative "Y" displacement (Fig. 4.10a). There is a simultaneous drop in load in the "X" direction (Fig. 4.10c) as the cross section realigns to the newly-imposed strain distribution. Moving to point "e", displacement is applied in the positive "X" direction, as in the first quarter cycle, with the characteristic relaxation of load in the "Y" direction (Fig. 4.10d) as moments follow the biaxial moment interaction diagram (Fig. 4.10b). A familiar pattern is repeated in moving to point "f".

The diagrams in Fig. 4.11 and 4.12 continue the pattern described in the preceding paragraphs. The completed idealized hysteretic loops of Fig. 4.12 are qualitatively similar to those measured for specimens 3 and 5 (Fig. 3.5 and 3.7, 3.10 and 3.12, and 4.7).

The influence of biaxial lateral loading on the load displacement envelopes is illustrated by Fig. 4.13. Figure 4.13a is an envelope relation of lateral load in the weak direction for various loading points for specimens 1, 2, and 3, with loading points illustrated in Fig. 4.13c. As would be expected from well-known principles for columns under uniaxial and biaxial load [11], specimen 2 (with loading applied approximately along a diagonal) has less lateral-load resistance than specimen 1 (with load along the principal axis). For specimen 3, two different points are plotted. Points "3a" correspond to first loading to maximum displacement in the weak ("X") direction (Fig. 4.13c). The envelope for these points is lower than those for specimen 1, indicating that prior biaxial loading has reduced the effective

resistance of specimen 3. Points "3b", occurring after the column has subsequently been loaded in the strong ("Y") direction (Fig. 4.13c), reveal even lower resistance (Fig. 4.13a), indicating that if transverse loads are applied while strength is being maintained in one direction, a further reduction in load resistance will occur. Fig. 4.13b presents similar data for the strong ("Y") direction of loading.

The loading history also influences the loading stiffness. Figure 4.14 plots loading paths (base moment about the "Y" axis versus base rotation in the same direction) in the positive loading direction for all specimens. In those figures, different loading paths are designated with a number. The number corresponds to a specific displacement cycle of the loading program, so that, for example, the number "6" for all specimens corresponds nominally to the same loading cycle "6" for all specimens. It is concluded from the data in Fig. 4.14 that loading stiffness in a given principal direction is reduced significantly by biaxial lateral loading, the biaxial loading either having been applied previous to or simultaneous with the current loading.

4.6 Effect of Load History on Damage

The different load histories resulted in markedly different amounts of damage in the different columns. Photographs of the five specimens at the conclusion of testing are shown in Fig. 3.1. The photographs were taken after loose concrete was removed by hand. Even though the columns were each loaded with the same

number of cycles in the weak direction, and to the same lateral displacement, differences in visible damage are clear. The uniaxially-loaded column, specimen 1, shows very little concrete spalling. The columns loaded along the diagonal, specimens 2 and 4, show significantly greater damage in the corners along the loading diagonal. Once the damage began in the corners for those columns, it spread more readily to other parts of the column perimeter. The columns with cloverleaf displacement histories, specimens 3 and 5, show the most severe damage, with major spalling around the entire perimeter at the base of the column.

In addition to effects of the displacement history, examination of the photographs in Fig. 3.1 reveals that the columns with varying axial load, specimens 4 and 5, had more severe damage than corresponding specimens 2 and 3, respectively, which underwent the same lateral displacement histories with constant axial load.

The greater extent of damage in columns with cloverleaf loading histories (specimens 3 and 5) relative to the uniaxially-loaded column (specimen 1) is also apparent in longitudinal reinforcement strain histories (Fig. 3.18, 3.20, and 3.22). (Strain-history data for specimens 2 and 4 are not indicative of the severity of loading, as the measured strains are for bars not located in the most-severely strained corners of those columns.)

The extensive variation in apparent damage, despite similarities in maximum lateral drift, is an indicator that response levels in real structures cannot be closely approximated

based on visible damage following an earthquake. A biaxially loaded column, as might be found in a real structure following an earthquake, reveals damage significantly different from a similar column subjected in the laboratory to uniaxial loading.

CHAPTER 5

SUMMARY AND CONCLUSIONS

An experimental program was conducted to study the behavior of reinforced concrete columns subjected to inelastic multiaxial loads with reversals. Five nominally-identical, one-quarter scale columns were tested in the program. The test specimens represented columns considered typical of those occurring in moderately tall buildings designed to satisfy current code requirements for reinforced concrete construction in regions of high seismic risk.

The columns were tested as cantilevers projecting from stiff foundation blocks, with lateral and axial loads applied at the end of the cantilever. The main variable in the experiments was the load history. Three columns were tested with constant axial load, one with uniaxial lateral load directed along a principal axis of the column, one with uniaxial lateral load directed along a skew axis of the column, and one with biaxial lateral loads resulting in a "cloverleaf" displacement pattern. Two remaining columns were tested under varying axial loads, with lateral load either applied uniaxially along a skewed axis or applied biaxially to achieve a cloverleaf displacement pattern. Experimental measurements include applied lateral loads, column end displacements, longitudinal reinforcement strains, and column base deformations.

This report documents the experiments and discusses observed behavior both qualitatively and by comparison with analytically

computed responses. Major conclusions include the following.

(1) Lateral deformations of the columns were predominated by rotations occurring within a length equal to approximately one column width measured from the top of the footing. These rotations are attributed to flexural curvature over this length and to slip of reinforcement from the footing.

(2) Based on observed damage, and as supported by calculations, lateral-load strength of the columns was limited by flexural strength.

(3) Reinforcement details, which satisfied current codes for ductile concrete frames in regions of high seismic risk, resulted in satisfactory behavior. Strength under load reversals was sustained through displacements equal to approximately five percent of column height (displacement ductility of approximately six), and could probably have been sustained through larger deformations had the test apparatus permitted further loading. Buckling of reinforcement did not occur, despite spalling of concrete cover and measured reinforcement compressive strains as large as 0.04.

(4) Biaxial lateral loading influenced observed behavior. Visible damage (concrete cracking and crushing) was notably more extensive in the biaxially-loaded columns. Measured strains in reinforcement, particularly in compression, were larger than for the uniaxially-loaded columns. Measured strengths and stiffnesses under biaxial loading were less than under monotonic loading. Even columns loaded uniaxially at a given stage of testing did not reach the uniaxially-measured strengths and

stiffnesses if those columns had been previously subjected to transverse loading. In general, the state of damage worsened for columns also subjected to axial load variations, even though the maximum axial load in these experiments was less than half the balanced axial load.

(5) Hysteretic relations under biaxial loading were strikingly different from those measured for uniaxial loading.

(6) Measured strengths and load-deflection envelopes could be reproduced reasonably well using existing analytical concepts for reinforced concrete sections subjected to monotonic loading. The analytical correlations were better for the columns loaded uniaxially along the principle axis or along a skew axis than for the columns loaded in the cloverleaf pattern.

(6) For columns loaded in the cloverleaf pattern, measured base moments were closely bounded by biaxial moment envelopes calculated assuming monotonically applied loads.

REFERENCES

1. American Concrete Institute, "Building Code Requirements for Reinforced Concrete," (ACI 318M-83), Detroit, Michigan, 1984

2. American Concrete Institute, "Commentary on Building Code Requirements for Reinforced Concrete," (ACI 318-83), Detroit, Michigan, 1983

3. Shahrooz, B. M., "Experimental Study of Seismic Response of R/C Setback Buildings," Ph.D. Dissertation Submitted to the University of California, Berkeley, September 1987.

4. Bertero, V.; Popov, E. and Wang, T., "Hysteretic Behavior of Reinforced Concrete Flexural Members With Special Web Reinforcement," Report No. UCB/EERC-74/09, Earthquake Engineering Research Center, University of California, Berkeley, California, 1974.

5. Desai, J. A. and Furlong, R. W., "Strength and Stiffness of Reinforced Concrete Rectangular Columns Under Biaxially Eccentric Thrust," University of Texas, Austin, Texas, January 1976.

6. Filippou, F. C.; Popov, E. and Bertero, V.,"Effects of Bond Deterioration on Hysteretic Behavior of Reinforced Concrete Joints," Report No. UCB/EERC-83/19, Earthquake Engineering Research Center, University of California, Berkeley, California, August 1983.

7. Gill, W. D.; Park, R., and Priestley, M. J. N., "Ductility of Rectangular Reinforced Concrete Columns With Axial Load," Department of Civil Engineering, University of Canterbury, Christchurch, New Zealand, February 1979.

8. International Conference of Building Officials, Uniform Building Code, Whittier, Ca., 1982.

9. Lai, S.; Will, G. and Otani, S., "Model For Inelastic Biaxial Bending of Concrete Members," JOURNAL OF STRUCTURAL ENGINEERING, Vol. 110 No. 11, November 1984, pg. 2563 - 2584.

10. Maruyama, K.; Ramirez, H. and Jirsa J., "Short RC Columns Under Bilateral Load Histories,: JOURNAL OF STRUCTURAL ENGINEERING, Vol. 110 No. 1, January 1984, pg. 120 - 137.

11. Park, R. and Paulay, ., "Reinforced Concrete Structures," John Wiley & Sons, New York, 1975.

12. Popov, E.; Bertero, V. and Krawinkler, H., "Cyclic Behavior of Three Reinforced Concrete Flexural Members With High Shear," Report No. UCB/EERC-72/05, Earthquake Engineering Research Center, University of California, Berkeley, California, 1972.

13. Scott, B. D.; Park R., and Priestley, M. J. N., "Stress - Strain Relationships For Confined Concrete: Rectangular Sections," Department of Civil Engineering, University of Canterbury, Christchurch, New Zealand, February 1980.

14. Umehara, H. and Jirsa, J., "Short Rectangular RC Columns Under Bidirectional Loading," JOURNAL OF STRUCTURAL ENGINEERING, Vol. 110 No. 3, March 1984, PG. 605 - 618.

15. Zeris, C.A., "Three Dimensional Nonlinear Response of Response of Reinforced Concrete Buildings," Ph.D. Dissertation Submitted to the University of California, Berkeley, November 1986.

Table 2.1 Chronology of Experiments

1. Construction of Reinforcing Cage for Specimens 1 to 5

   a.) Reinforcing Cages
   b.) Attaching Strain Gages

2. Casting of Specimens 1 to 3 (2/7/86)

3. Casting of Specimens 4 and 5 (3/7/86)

4. Setup of Testing Apparatus

   a.) Loading Apparatus
   b.) Instrumentations

5. Testing of Specimen 1 (4/17/86)

   a.) Uniaxial Lateral Loading with Constant Axial Load

6. Testing of Specimen 2 (4/28/86)

   a.) Biaxial Lateral Loading at 45 Degrees with Constant Axial Load

7. Testing of Specimen 3 (5/6/86)

   a.) Biaxial "Cloverleaf" Lateral Loading with Constant Axial Load

8. Testing of Specimen 4 (5/16/86)

   a.) Biaxial Lateral Loading at 45 Degrees with Varying Axial Load

9. Testing of Specimen 5 (5/30/86)

   a.) Biaxial "Cloverleaf" Lateral Loading with Varying Axial Load

10. Reduction of Experimental Data and Analytical Analysis

Table 2.2 Concrete Batch Quantities for One Cubic Yard, Saturated Surface-Dry

Materials	Batch #1 (lb) Specimens 1-3	Batch #2 (lb) Specimens 4-5
Type II Cement Permanente C1028	611	641
Water	342	342
Fine Sand Tidewater Blend	325	325
Course Sand Radum Top	1300	1300
Fine Gravel Radum 3/8" Pea	1315	1315
Total	3893	3923

Table 2.3 Concrete Compressive Strengths

	Cyclinder Size	Age of Concrete (Days)	Cyclinder Strength (psi.)	Average Strength (psi.)
Batch #1	3 x 6	28	5459 4879	5169
		63	5120 5516	5318
	6 x 12	28	5015 5352	5201
		63	5320 5550	5435
Batch #2	3 x 6	28	4802 5064	4933
		70	5000 5143	5071
	6 x 12	28	4500 4440	4470
		70	4556 4562	4559

Table 2.4 Concrete Splitting Tensile Strengths

6 x 12 Cyclinder	Age of Concrete (Days)	Load (lb)	Tensile Strength (psi.)	Avg. Tensile Strength (psi.)
Batch #1	63	67000	592	592
		67100	593	
Batch #2	50	60700	536	493
		50700	449	

Table 2.5 Reinforcement Properties

Properties	#3 Deformed Bar	#2 Deformed Bar (shipment #1)	#2 Deformed Bar (shipment #2)	Guage #9 Transverse Reinforcement
f_y (ksi.)	64.9	64.4	73.1	60.0
f_u (ksi.)	95.7	86.0	96.5	85.5
f_f (ksi.)	95.7	86.0	96.5	85.5
E (ksi.)	29000.0	29000.0	29000.0	29000.0
E_{sh} (ksi.)	1690.0	1200.0	1250.0	2500.0
e_y (in/in)	0.0022	0.0022	0.0025	0.0021
e_{sh} (in/in)	0.0120	0.0300	0.0252	0.0025
e_u (in/in)	0.1310	0.1740	0.1300	0.1000
e_f (in/in)	0.1600	0.2000	0.1640	0.1200

Table 3.1 Summary of Selected Experimental Results

	Specimens				
	#1	#2	#3	#4	#5
YIELD					
My (kip-in)	116.0	81.0		62.0	
Mx		137.0		85.0	
Vx (kips)	5.2	3.4		2.9	
Vy		5.9		4.5	
dx (inches)	0.19	0.14		0.15	
dy		0.15		0.15	
ULTIMATE					
My (kip-in)	136.0	95.0	123.0	142.0	146.0
Mx		161.0	175.0	151.0	168.0
Vx (kips)	5.9	3.8	5.1	4.0	4.8
Vy		6.7	7.6	6.2	7.0
MAXIMUM					
dx (inches)	1.12	1.01	1.01	0.99	1.01
dy		0.99	1.01	0.97	1.01

Table 4.1 Calculated Effect of Bar Slip on Column End Displacements

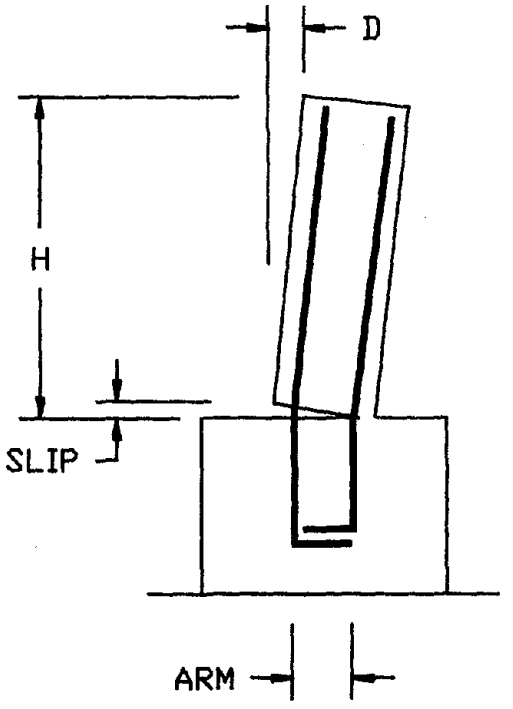

D=[SLIP/ARM]*H ; Dx, Dy

H=20 in.

ARM_x=3.1 in. Weak Direction

ARM_y=4.1 in. Strong Direction

ARM: Denotes the Approximate Distance Between the Neutral Axis and the Bar Where Slip is Occurring

Steel Stress (ksi)	Bond Stress u_b (ksi)	Rebar Slip (in.)	Hook Slip (in.)	Total Pull-out (in.)	End Displacement	
					Dx (in.)	Dy (in.)
70	1.30	0.0061	0	0.0061	0.040	0.030
60	1.30	0.0045	0	0.0045	0.029	0.022
50	1.30	0.0031	0	0.0031	0.020	0.015
40	1.30	0.0020	0	0.0020	0.013	0.010
30	1.30	0.0011	0	0.0011	0.007	0.005
20	1.30	0.0005	0	0.0005	0.003	0.002
10	1.30	0.0001	0	0.0001	0.001	0.000
0	0.00	0.00000	0	0.00000	0.000	0.000

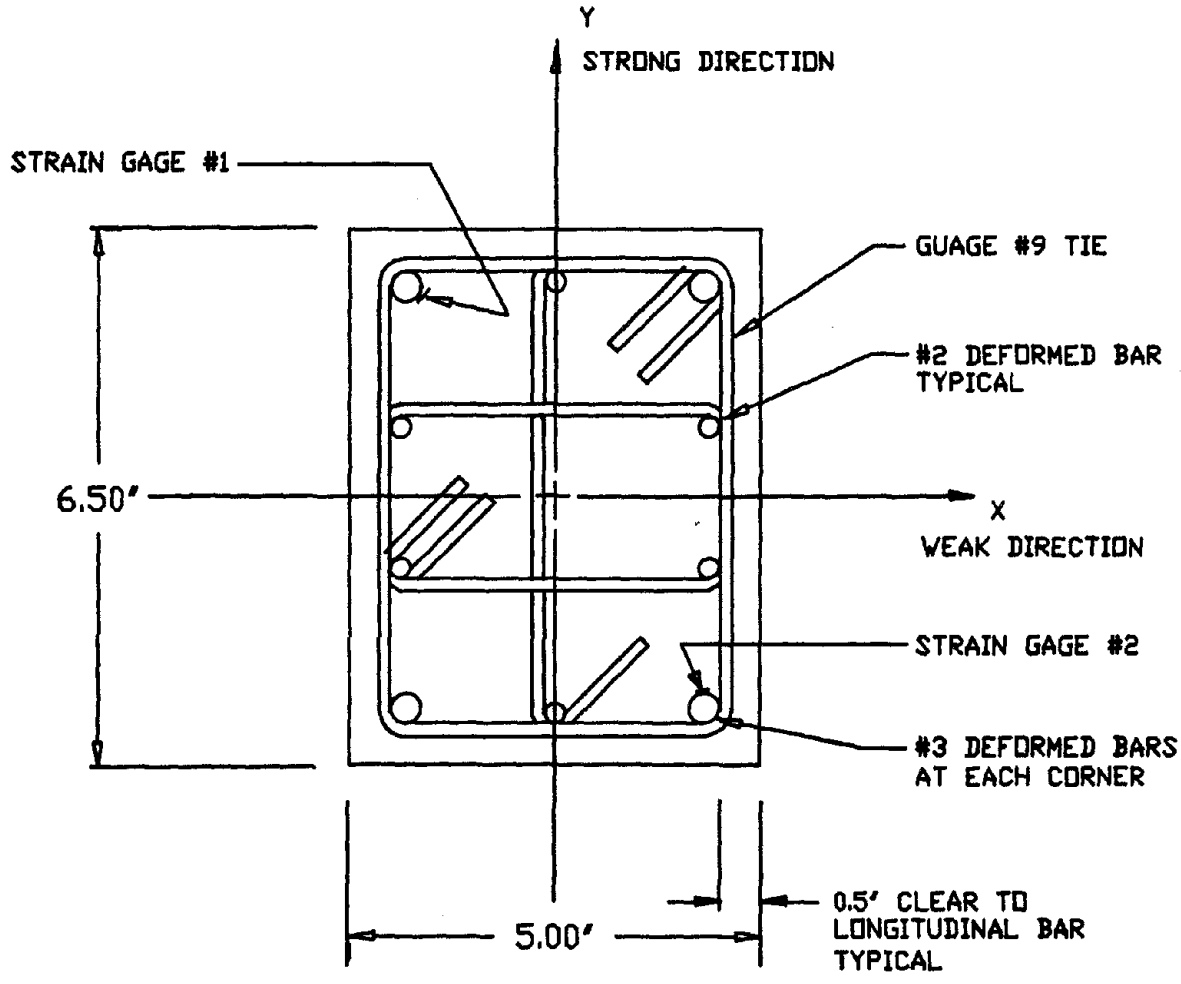

CROSS SECTION

NOTE: #2 DEFORMED BARS ALONG THE "Y" AXIS ARE TYPE "SHIPMENT #1" IN TABLE 2.5. ALL OTHER #2 DEFORMED BARS ARE TYPE "SHIPMENT #2"

FIG. 2.1 Test Specimen Configuration

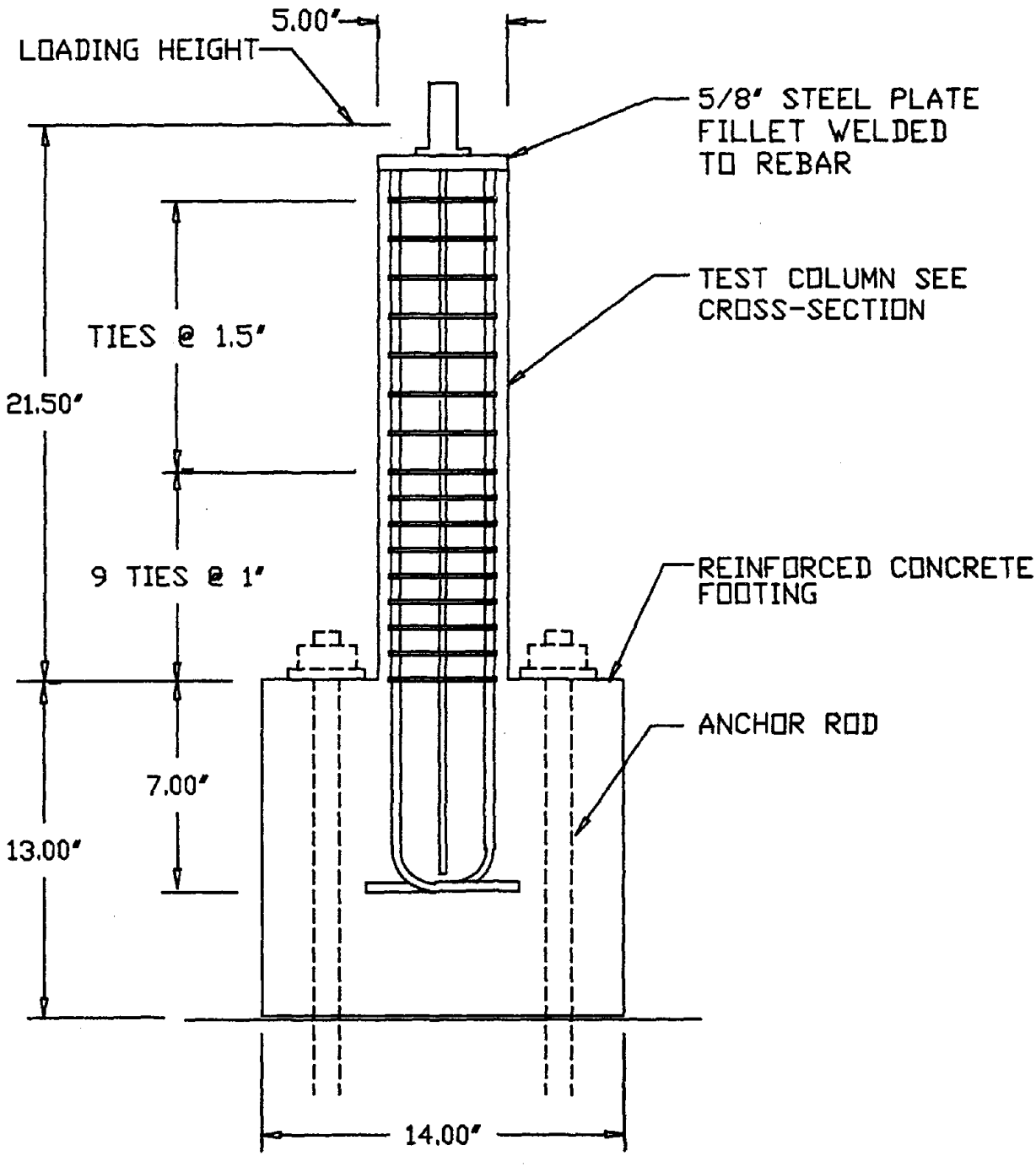

COLUMN ELEVATION "Y" DIRECTION

FIG. 2.1 Continued

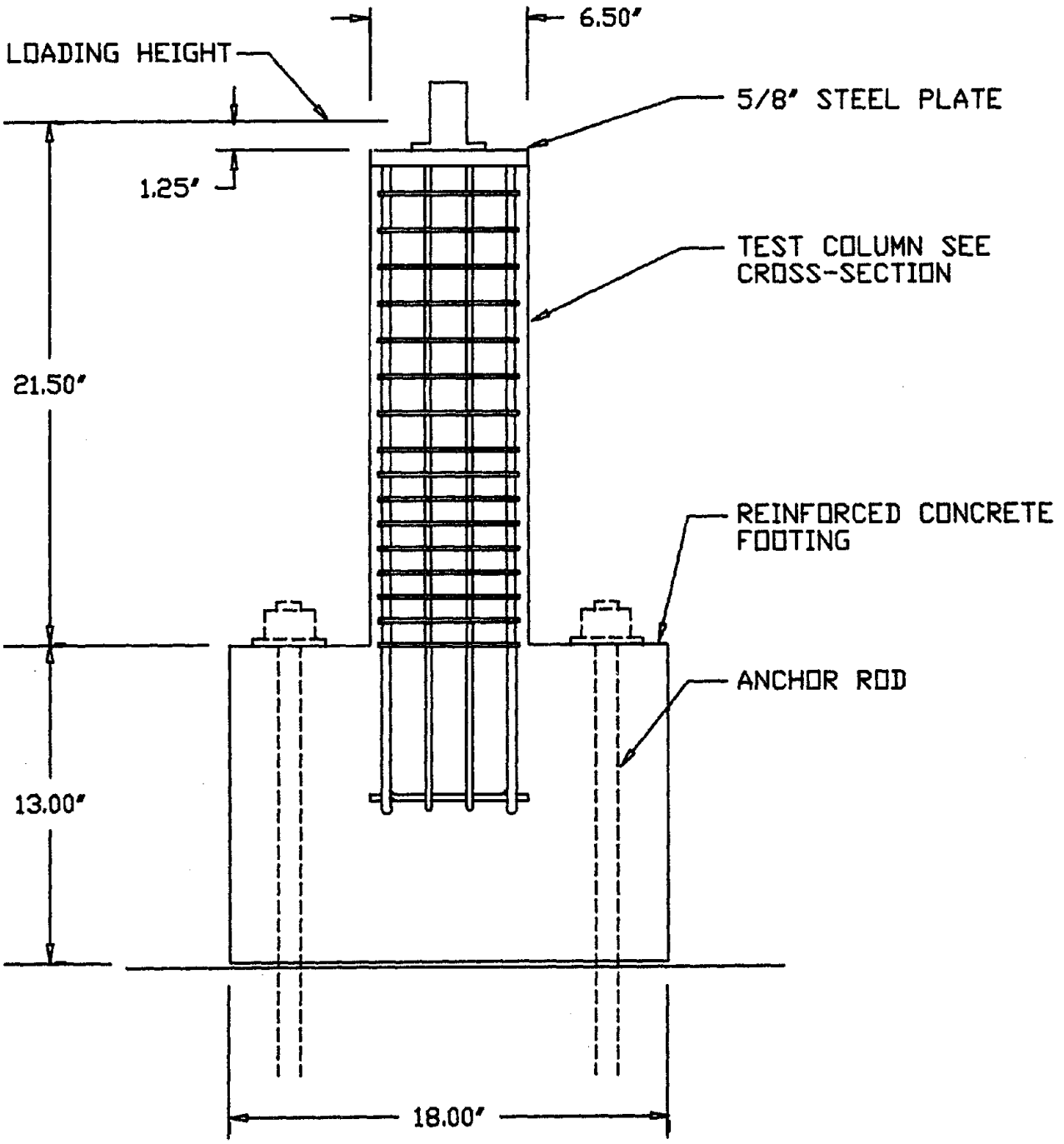

FIG. 2.1 Continued

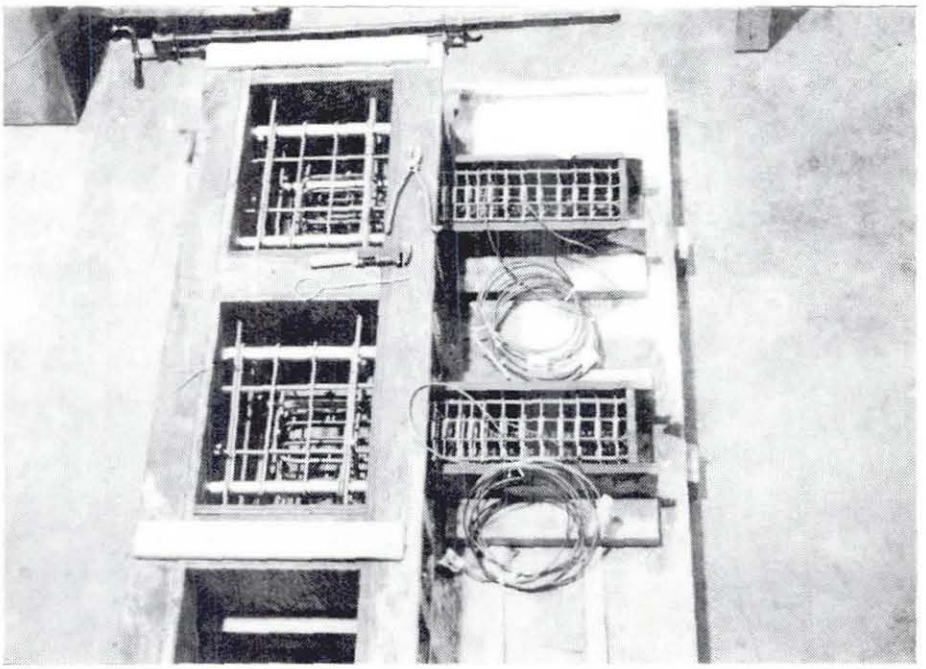

FIG. 2.2 Test Specimens Ready for Casting

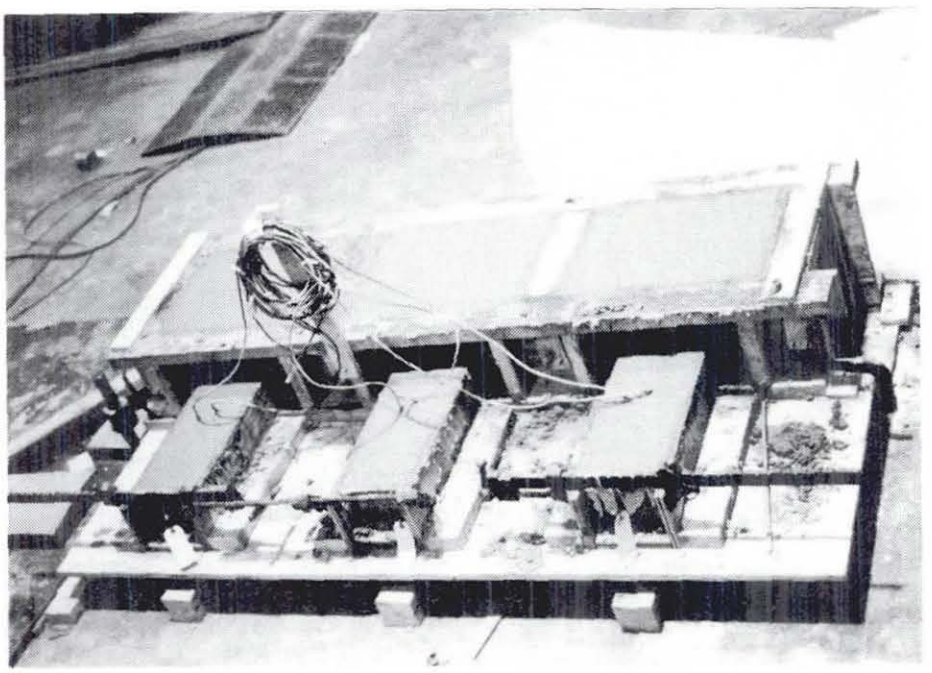

FIG. 2.3 Testing Specimens After Casting

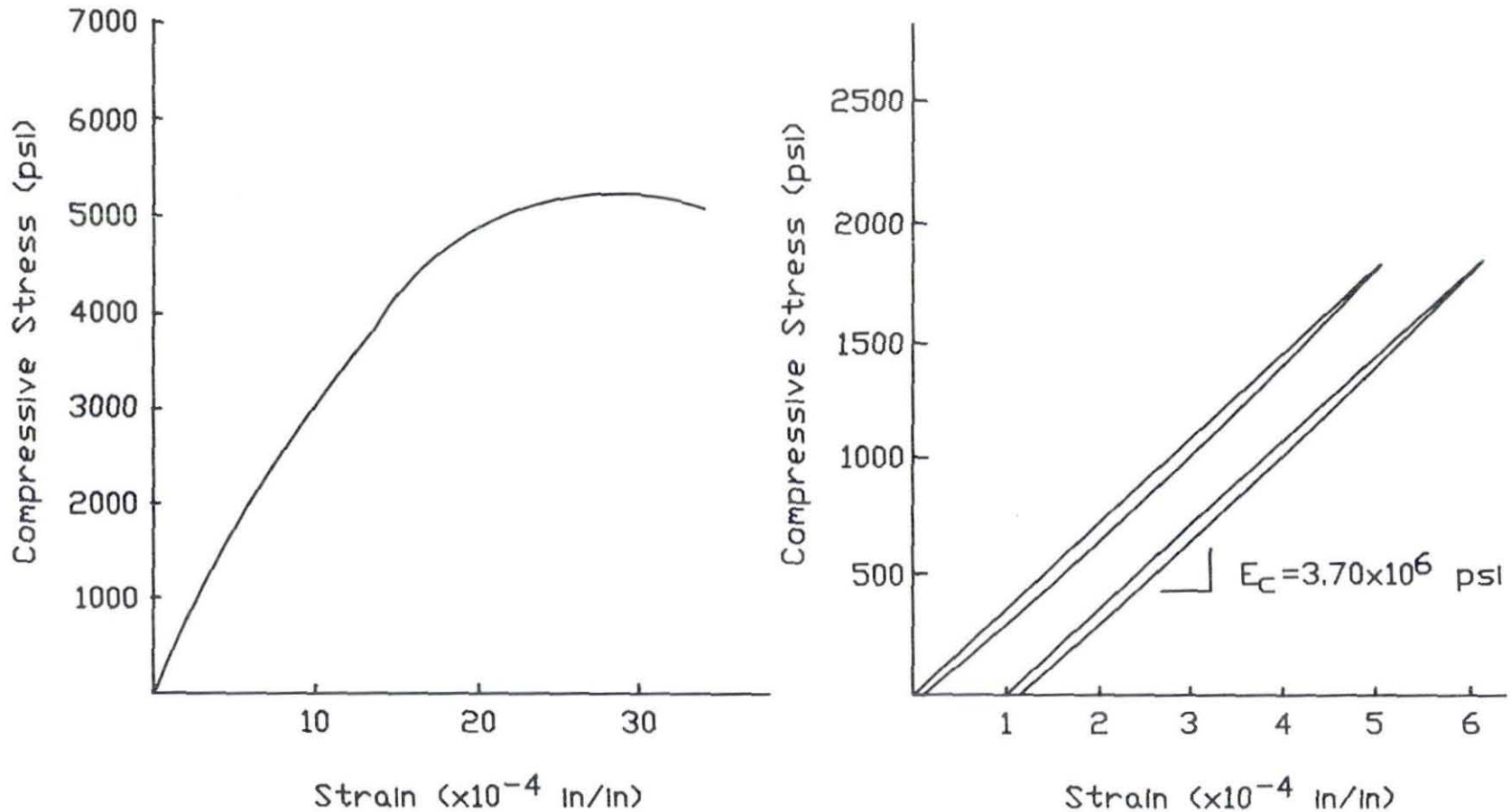

FIG. 2.4 Concrete Stress-Strain Relations

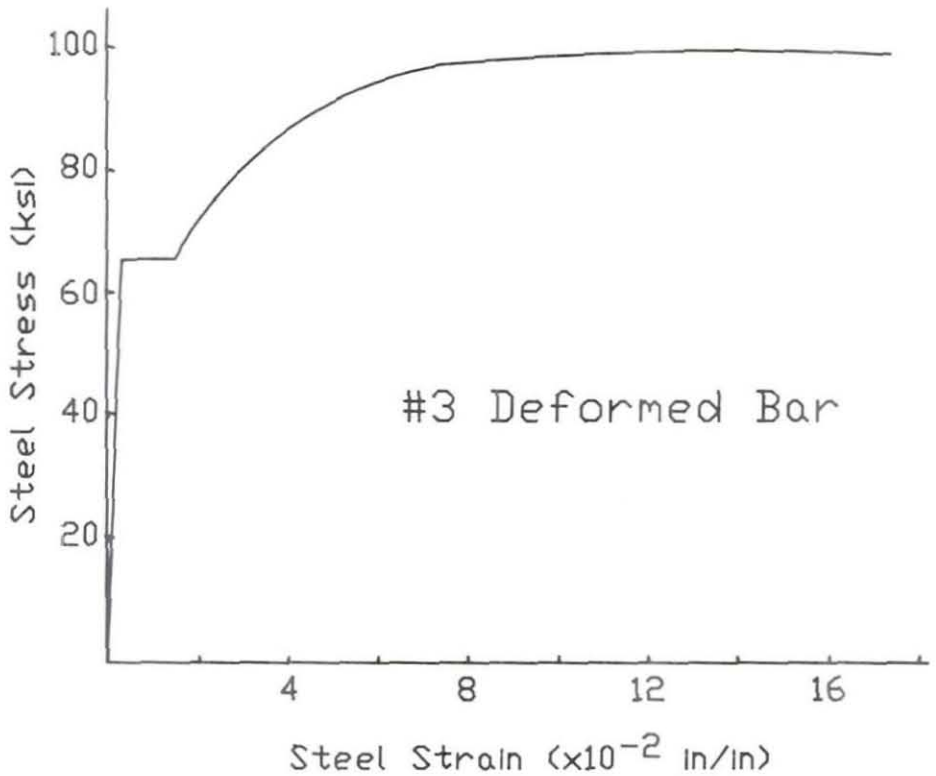

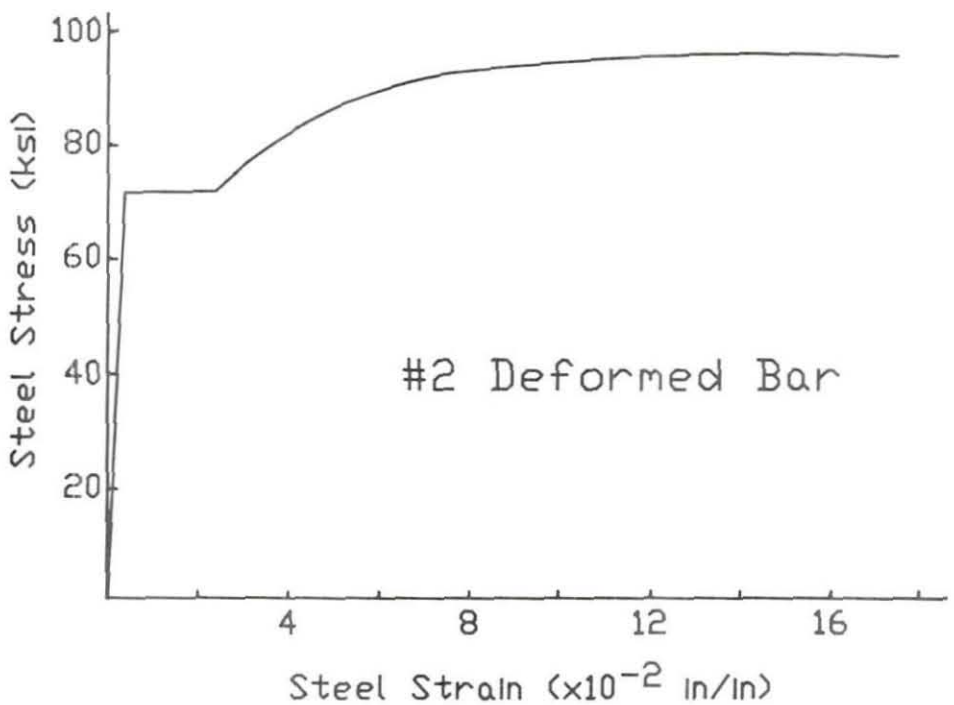

FIG. 2.5 Longitudinal Steel Stress-Strain Relations

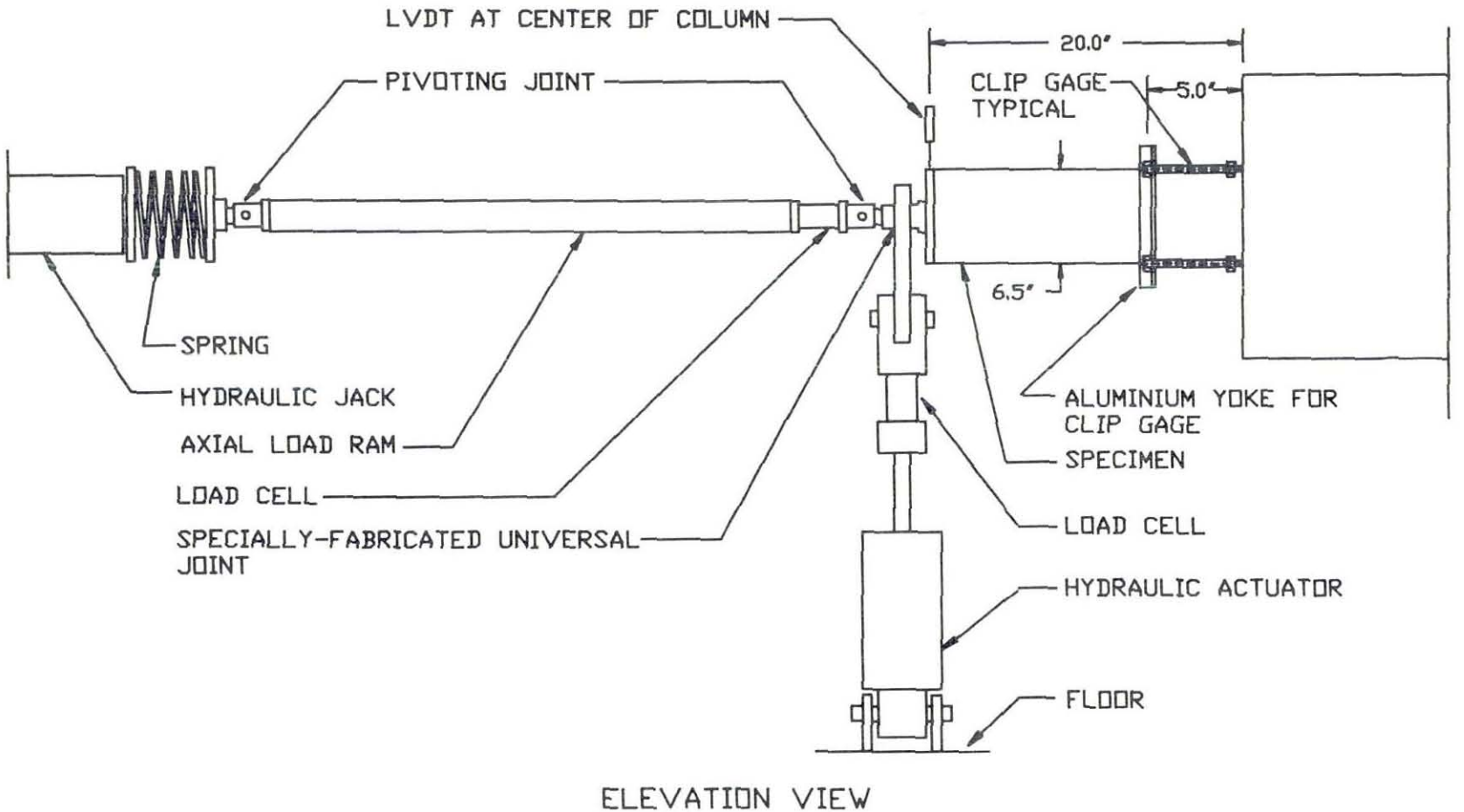

FIG. 2.6 Loading Apparatus and Instrumentation

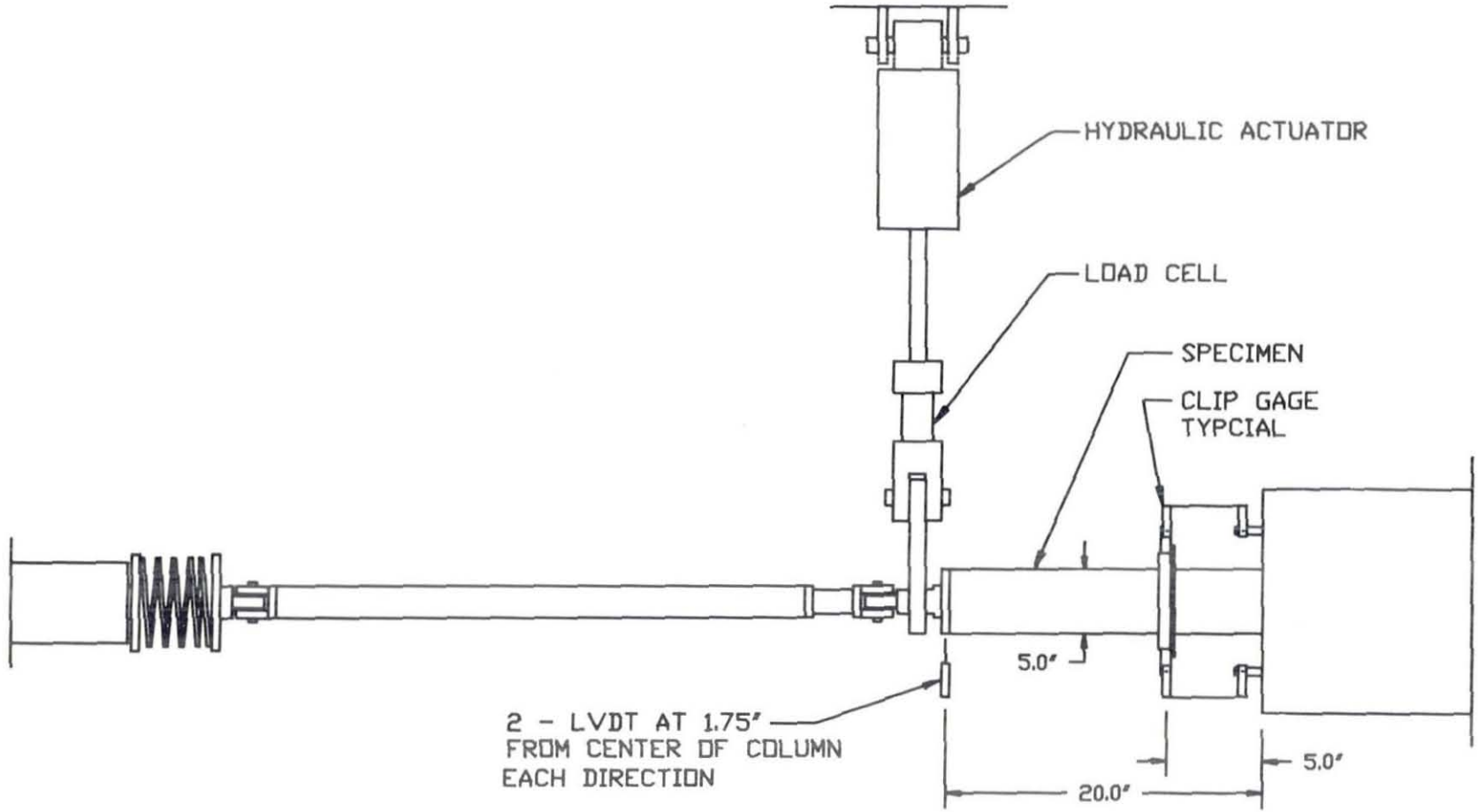

FIG. 2.6 Continued

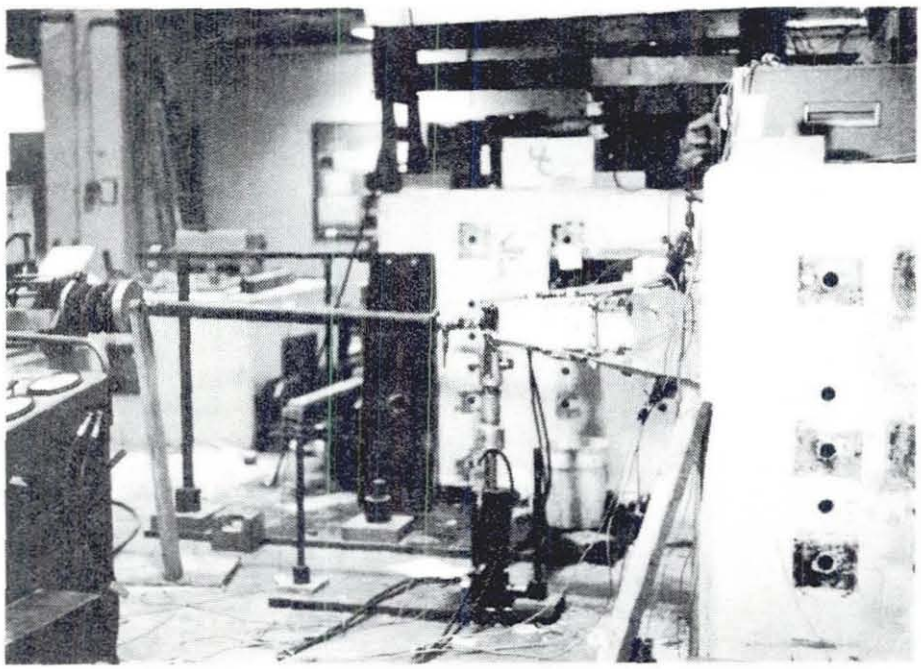

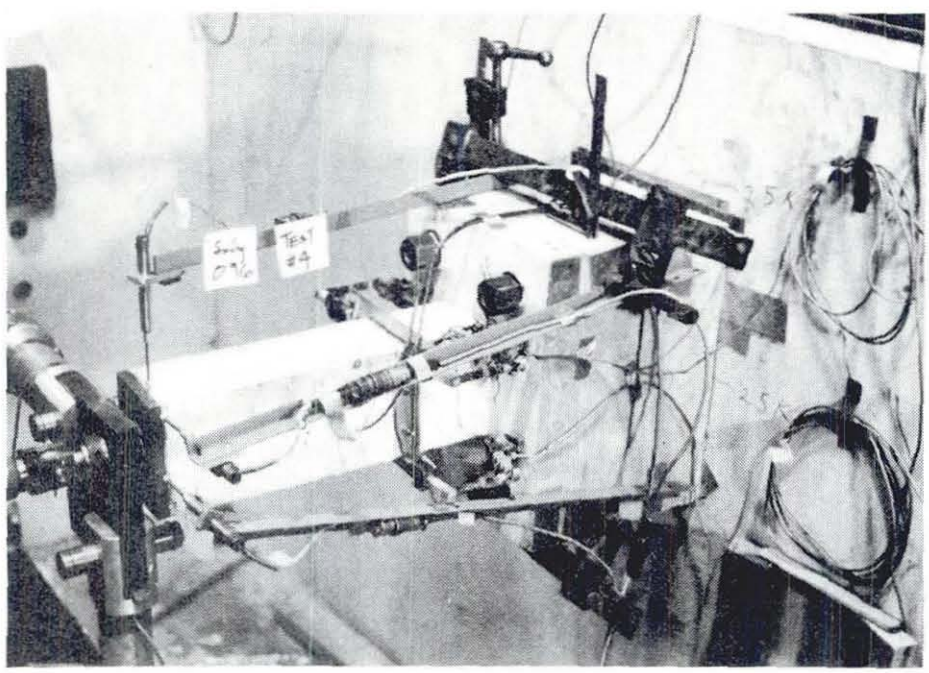

FIG. 2.7 Photographs of Experimental Setup

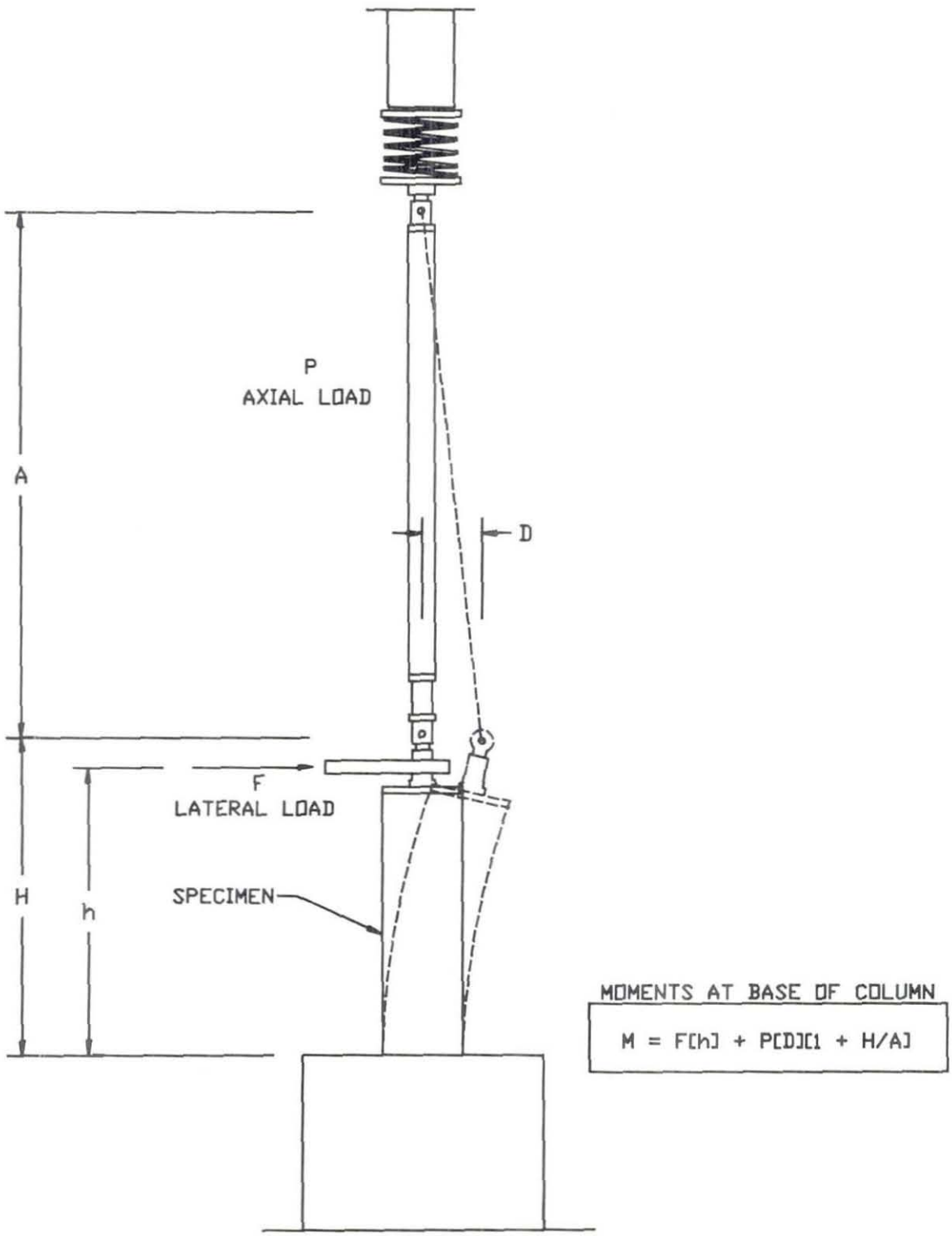

FIG. 2.8 Base Moment Determination

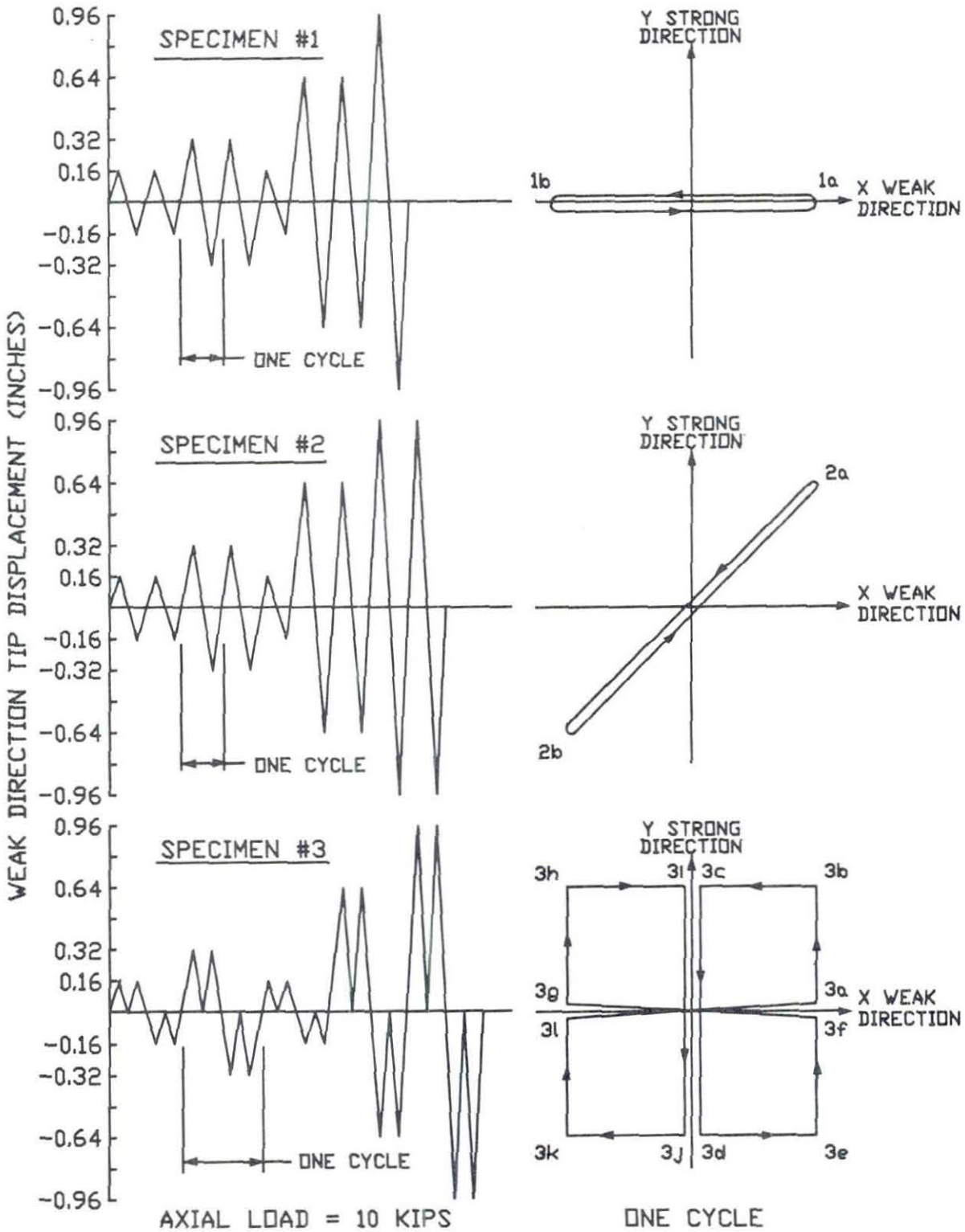

FIG. 2.9 Intended Displacement and Load Histories

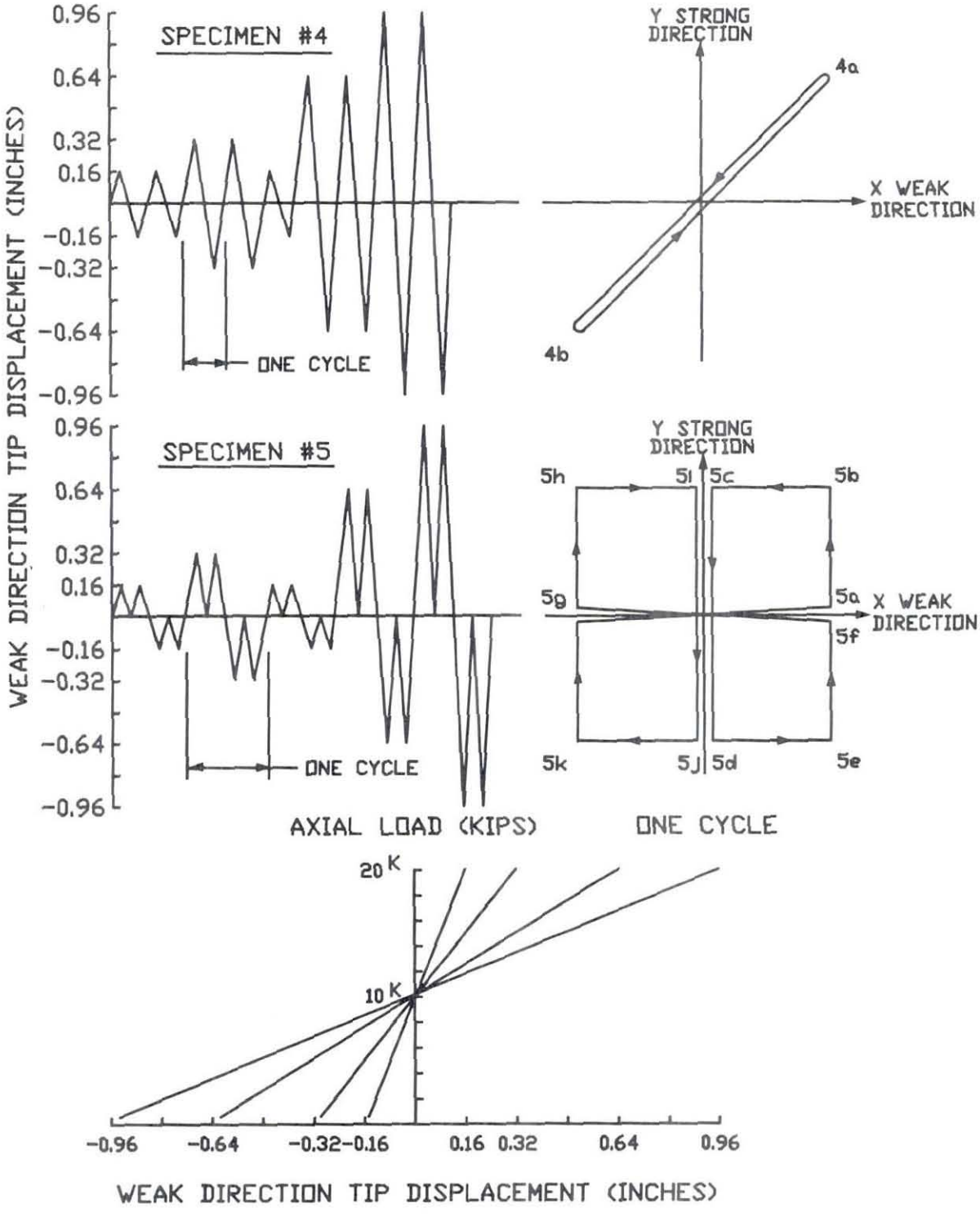

FIG. 2.9 Continued

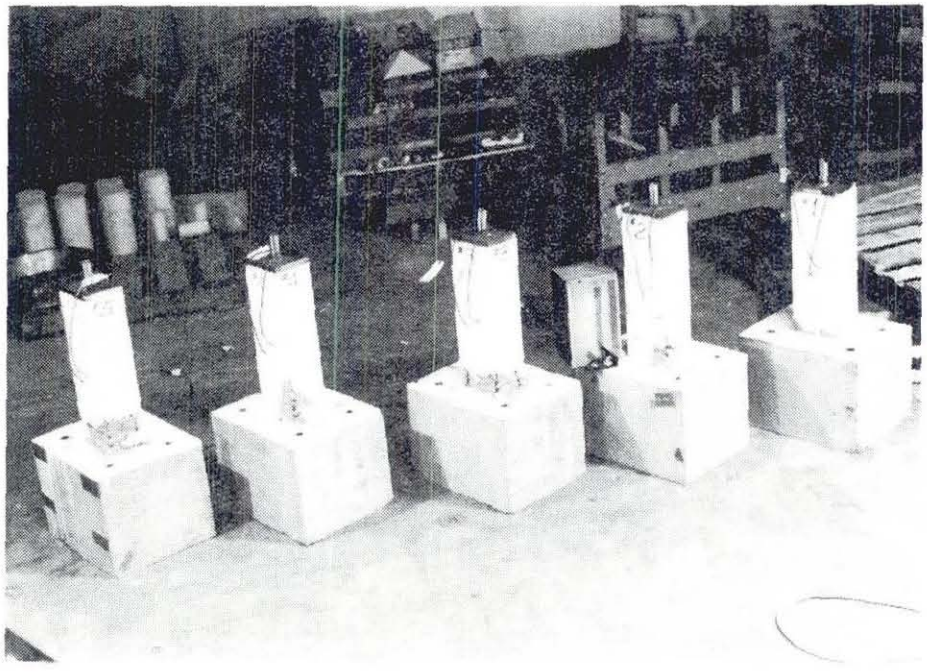

FIG. 3.1 Photograph of Test Specimens at Conclusion of Testing

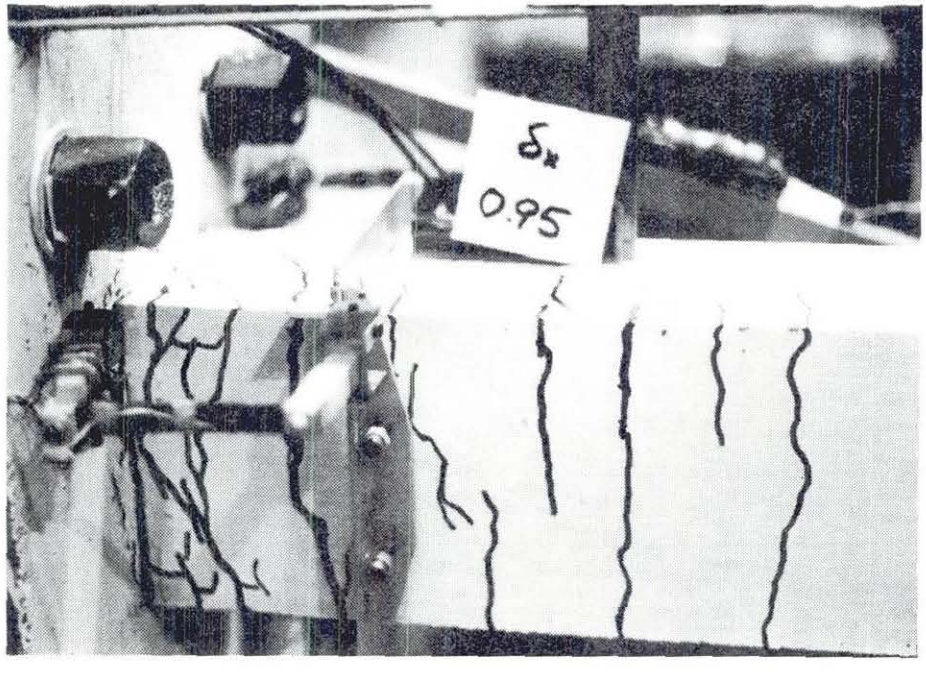

FIG. 3.1a Photograph of Test Specimen 1 at Conclusion of Testing

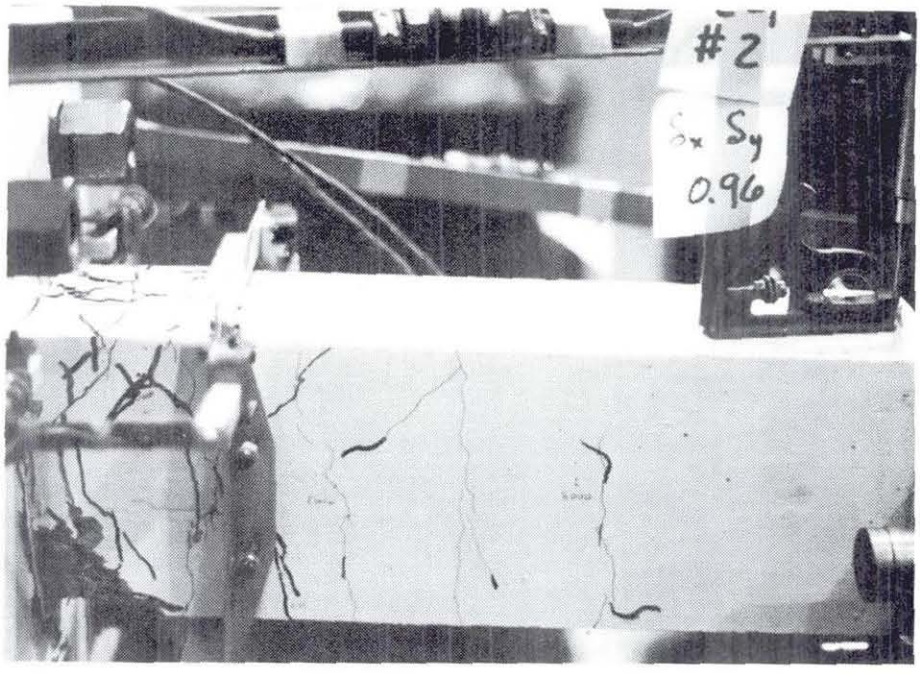

FIG. 3.1b Photograph of Test Specimen 2 at Conclusion of Testing

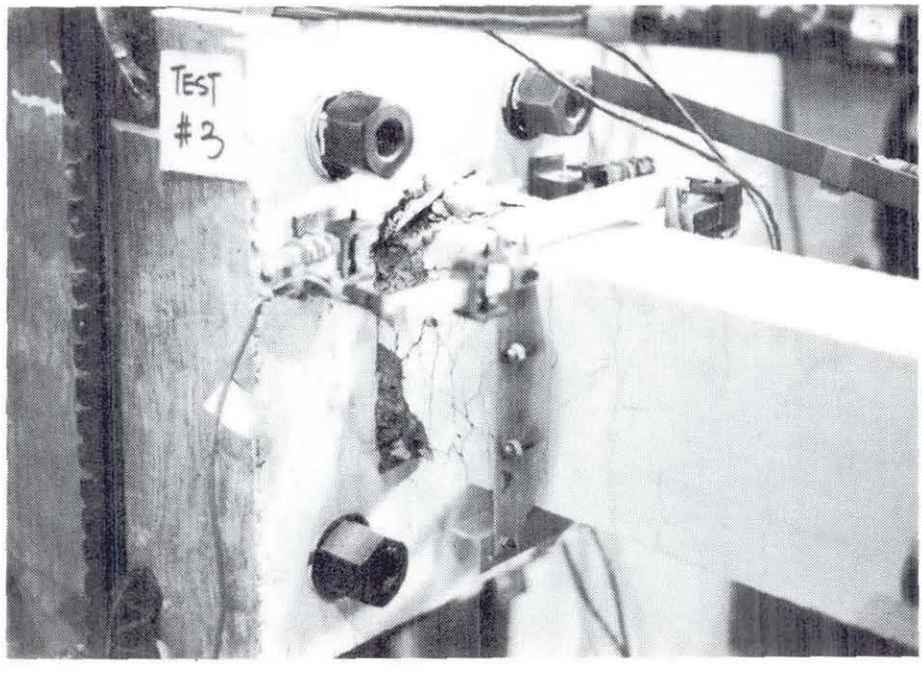

FIG. 3.1c Photograph of Test Specimen 3 at Conclusion of Testing

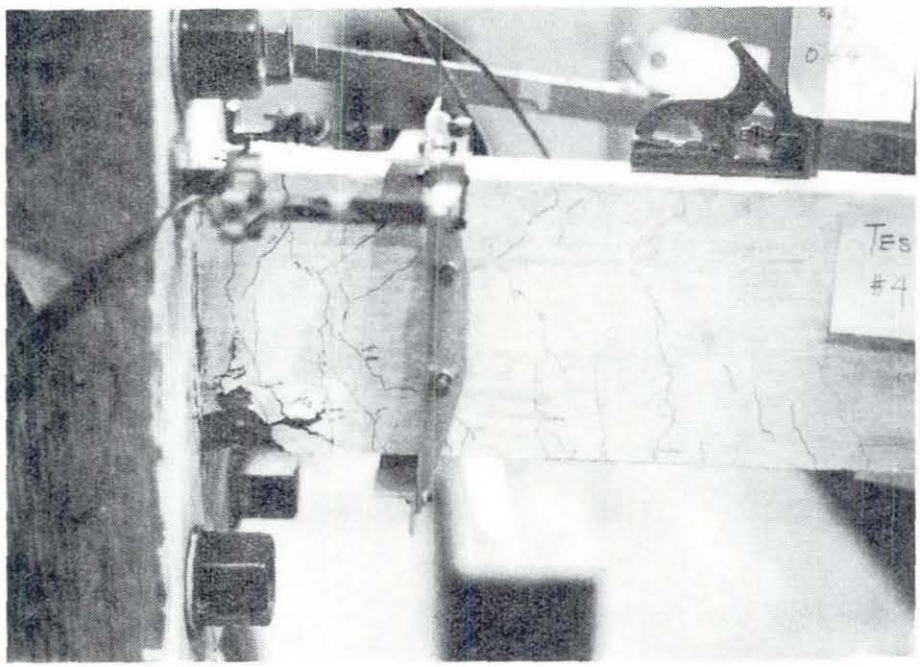

FIG. 3.1d Photograph of Test Specimen 4 at Conclusion of Testing

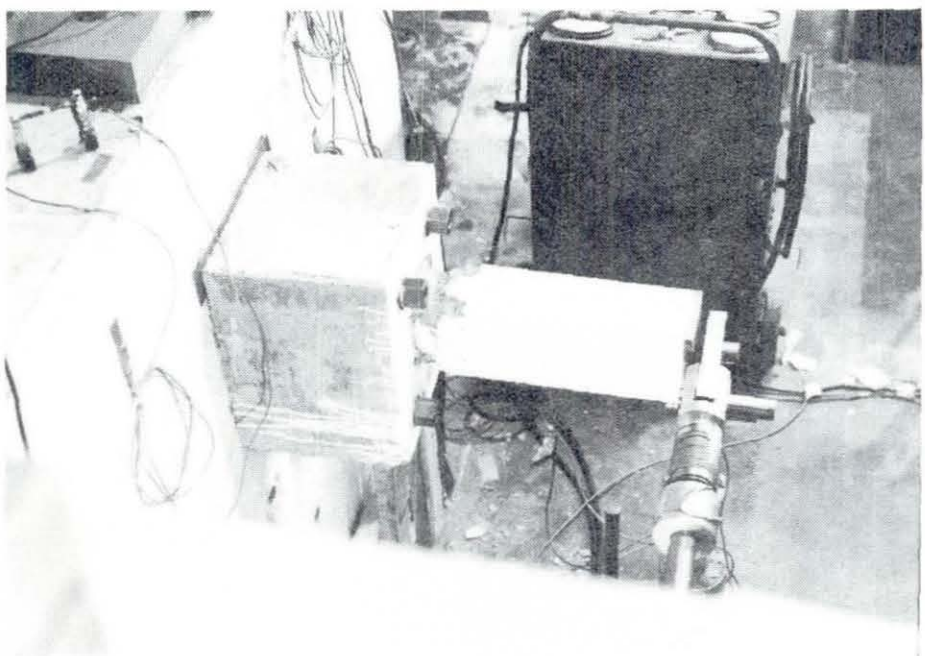

FIG. 3.1e Photograph of Test Specimen 5 at Conclusion of Testing

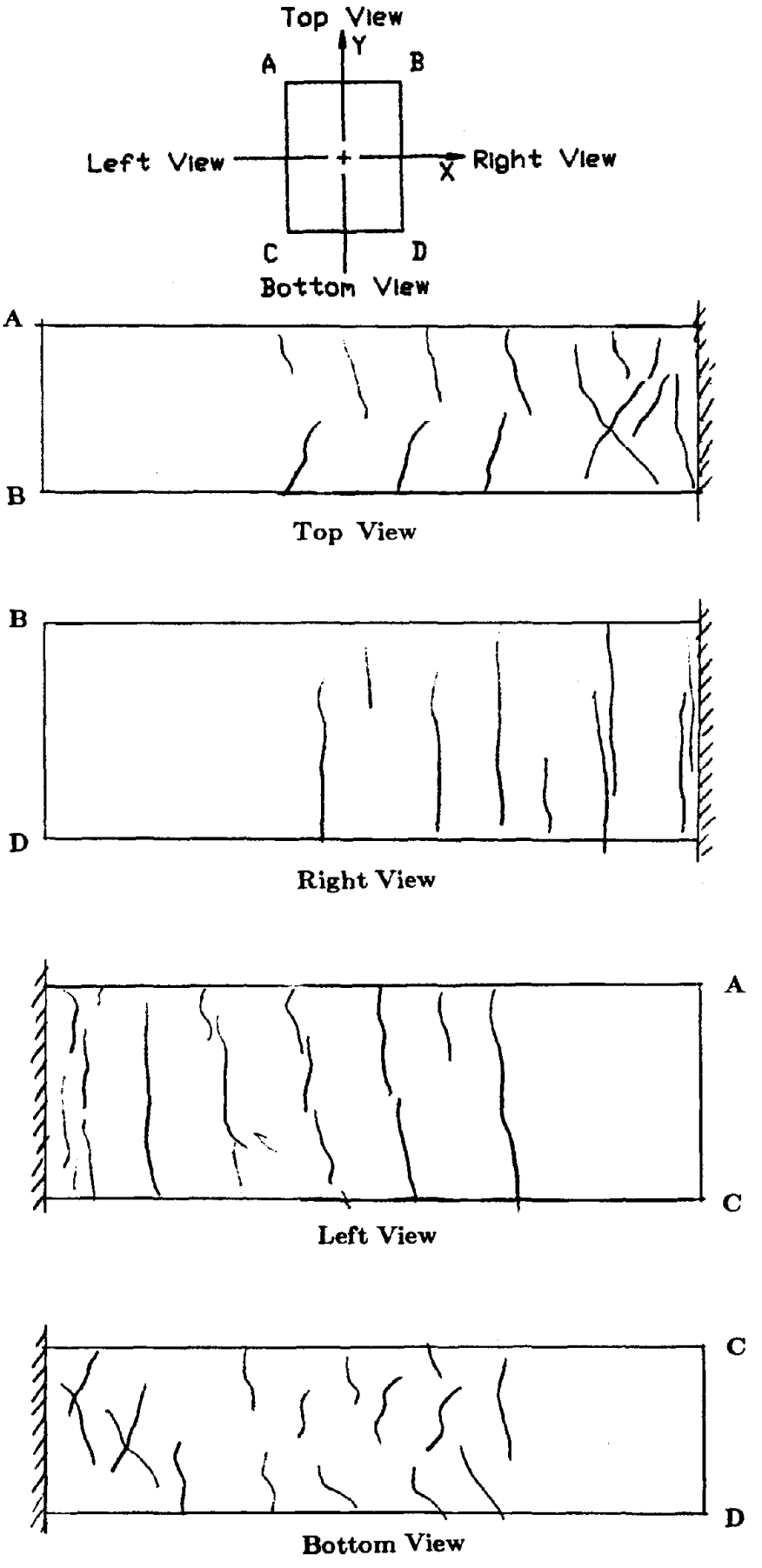

FIG. 3.2 Crack Patterns at Conclusion of Testing - Specimen 1

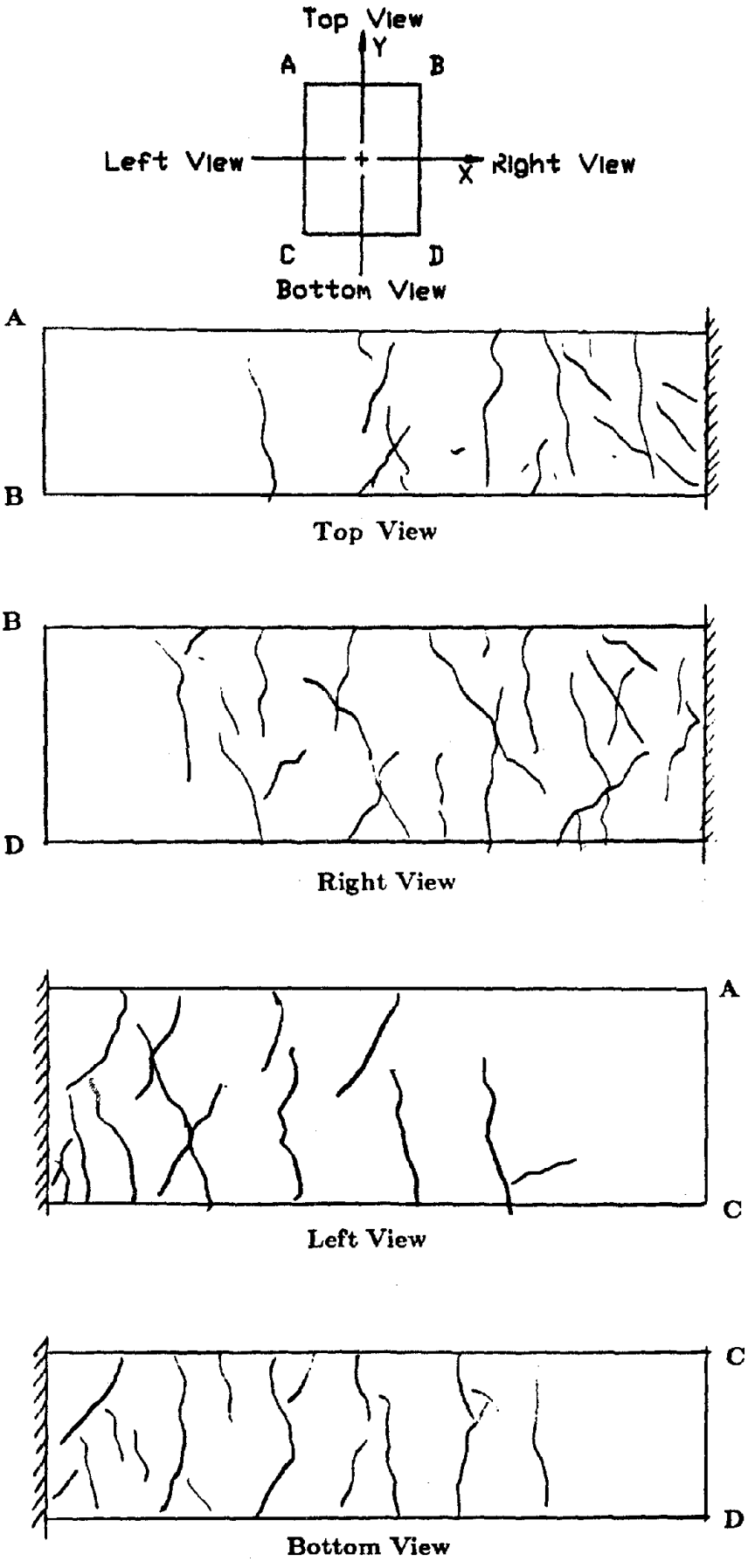

FIG. 3.2a Crack Patterns at Conclusion of Testing - Specimen 2

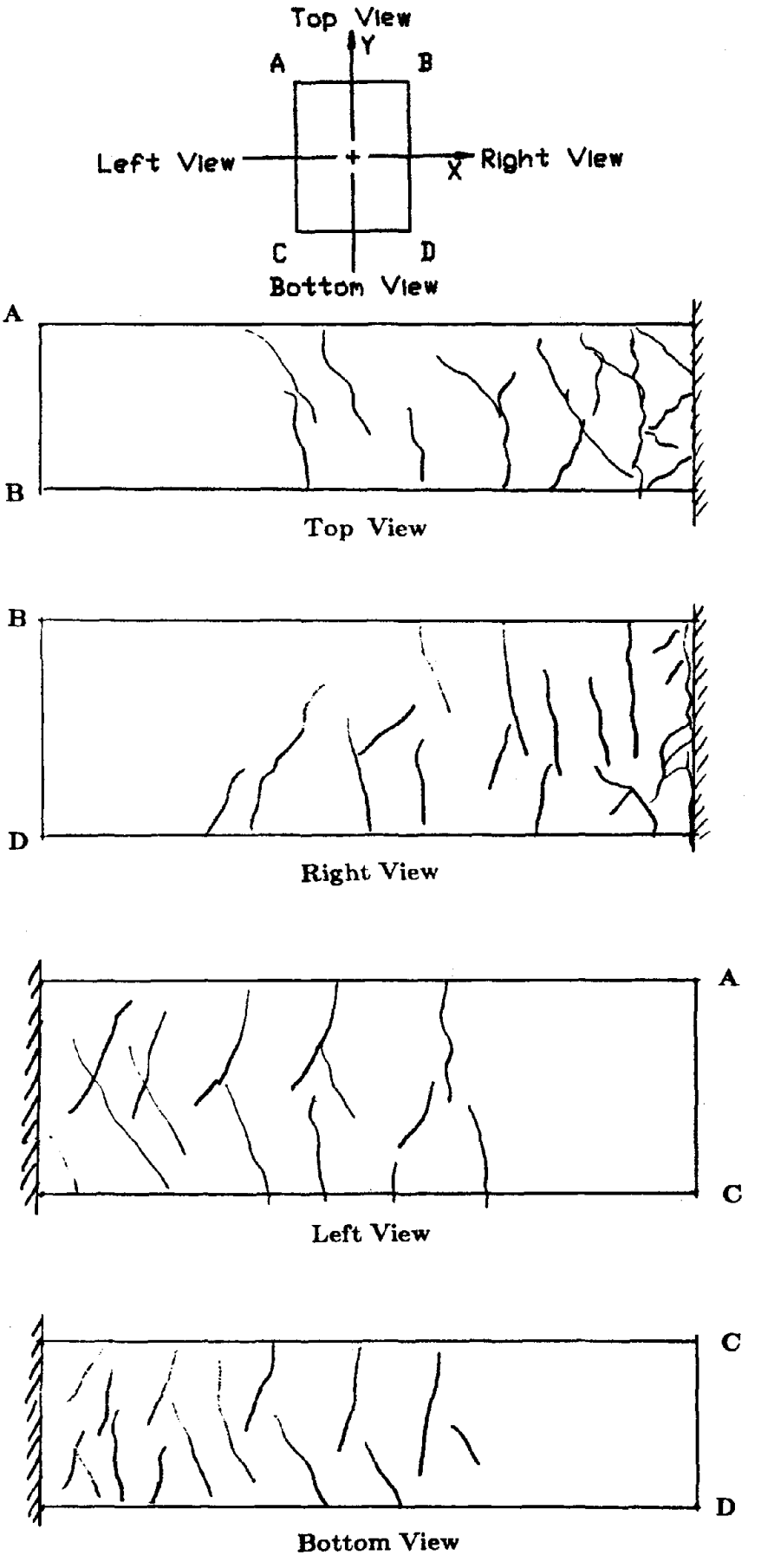

FIG. 3.2b Crack Patterns at Conclusion of Testing - Specimen 3

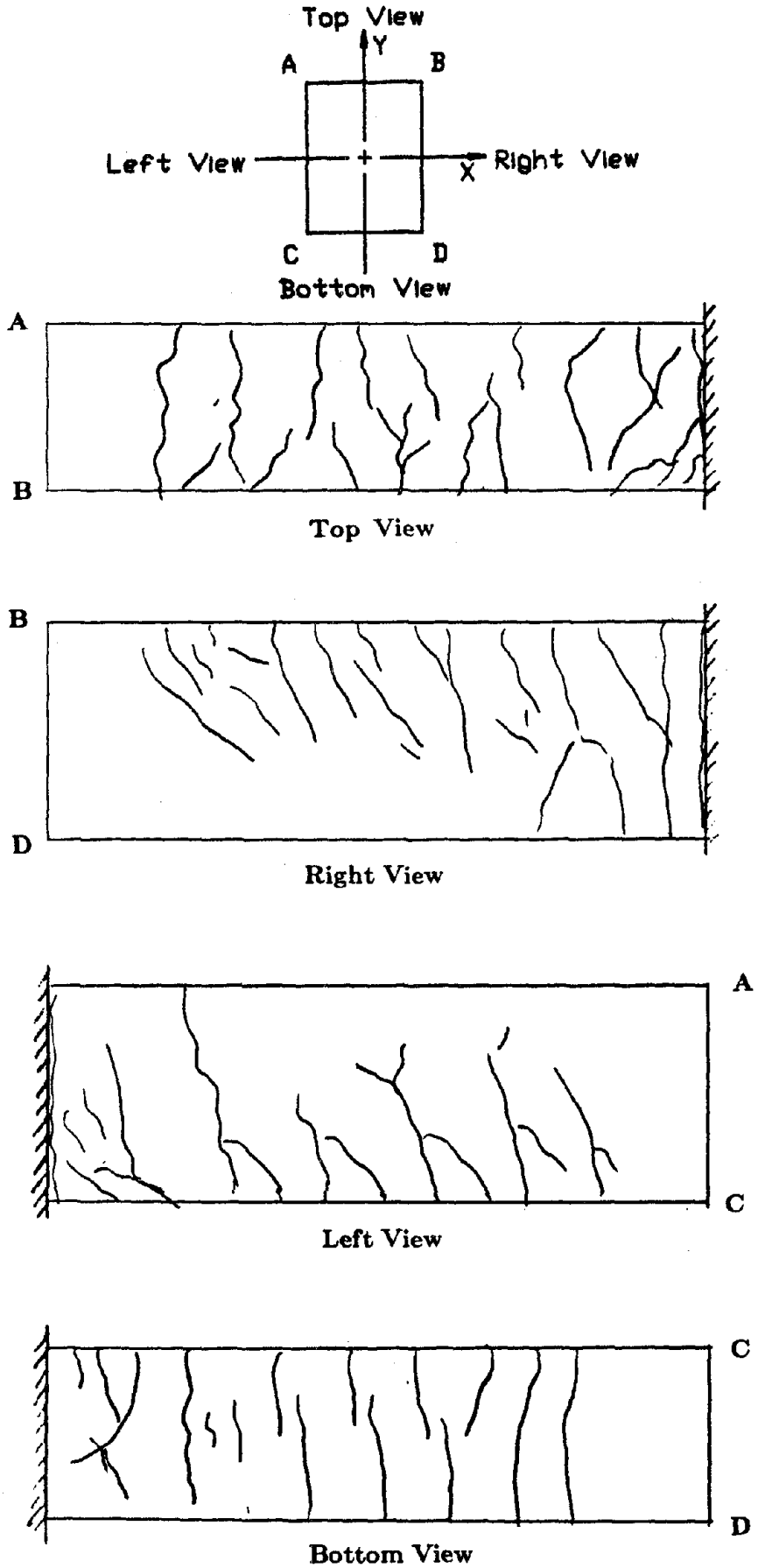

FIG. 3.2c Crack Patterns at Conclusion of Testing - Specimen 4

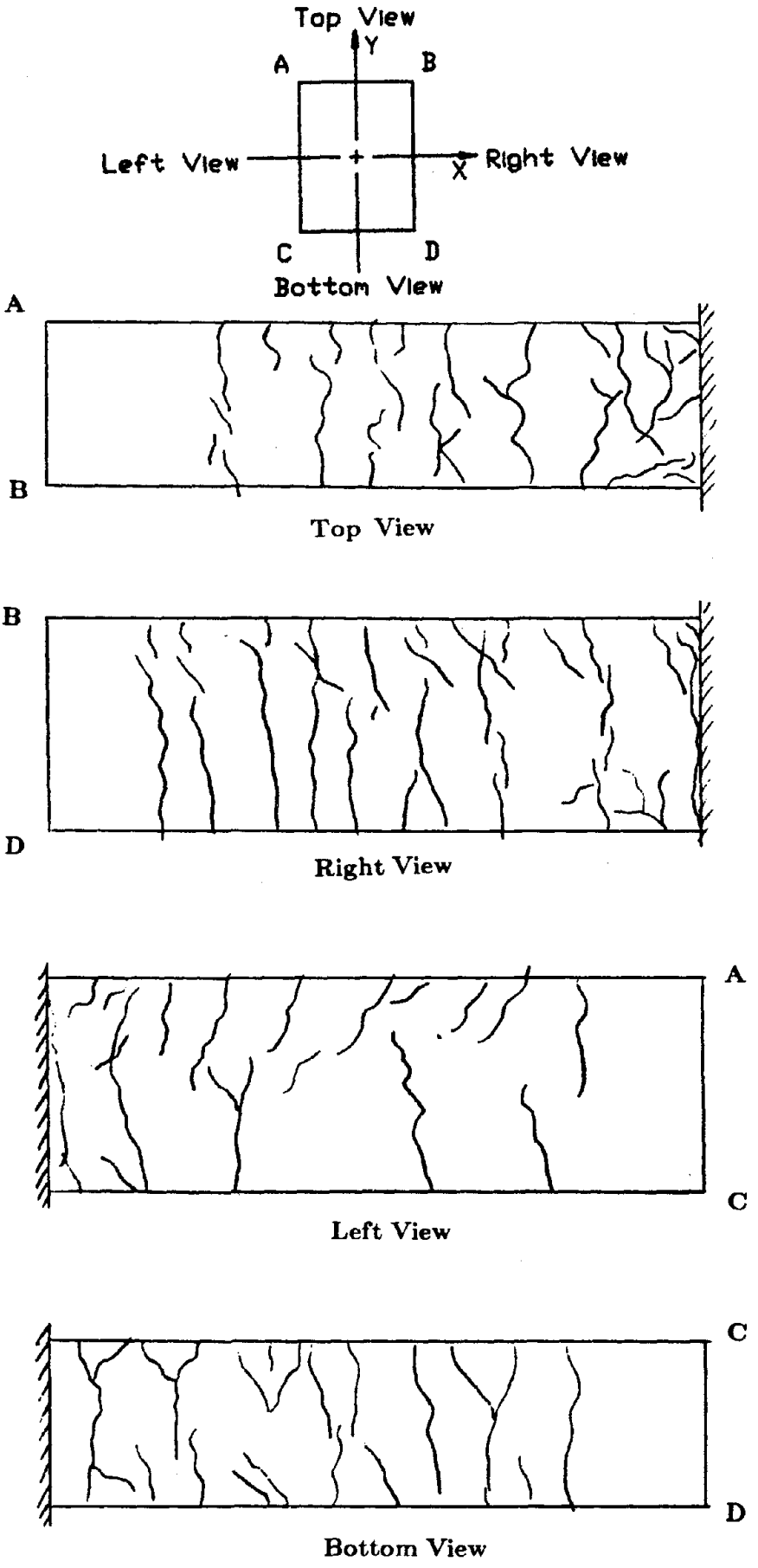

FIG. 3.2d Crack Patterns at Conclusion of Testing - Specimen 5

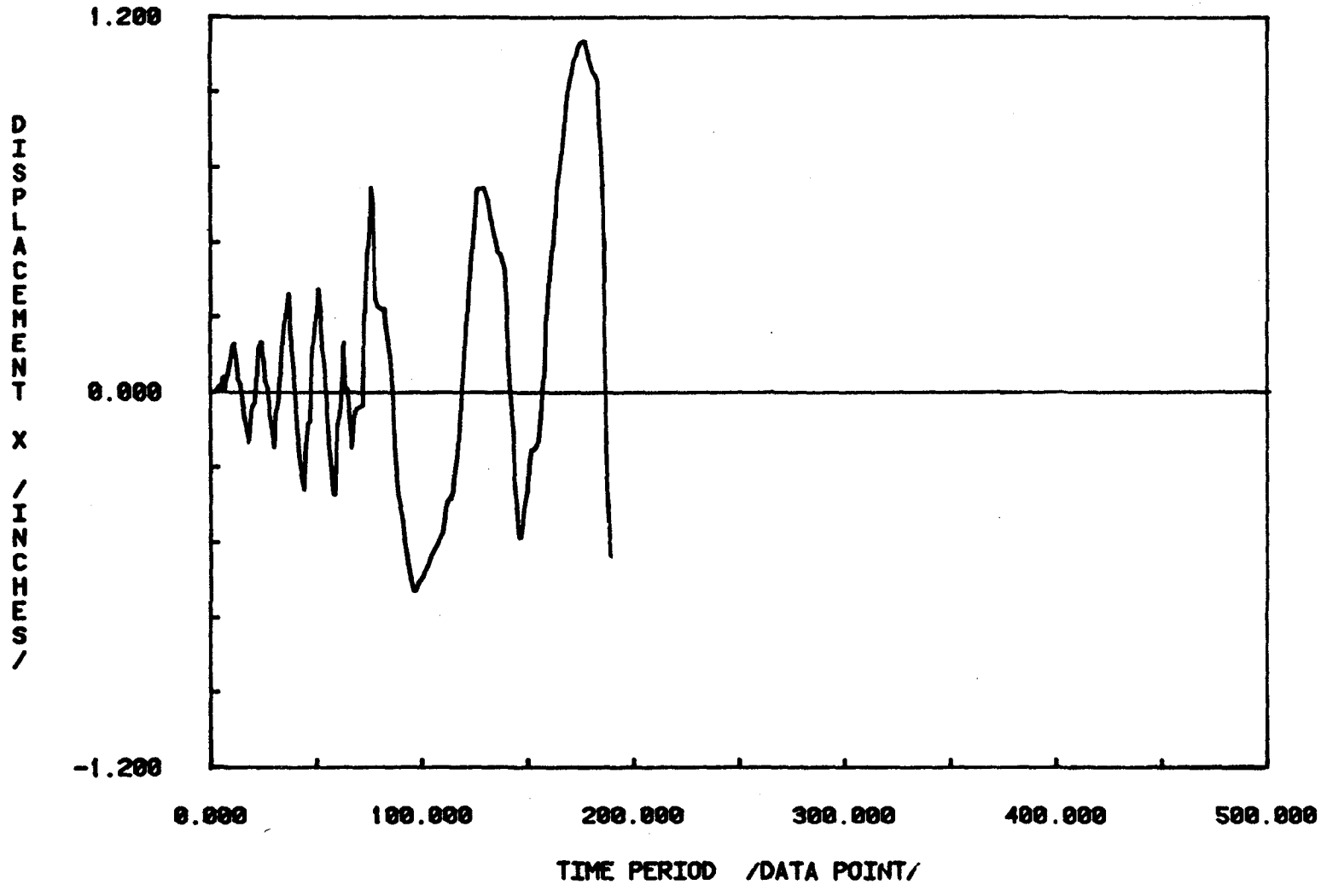

FIG. 3.3 Measured Load History for Specimen 1

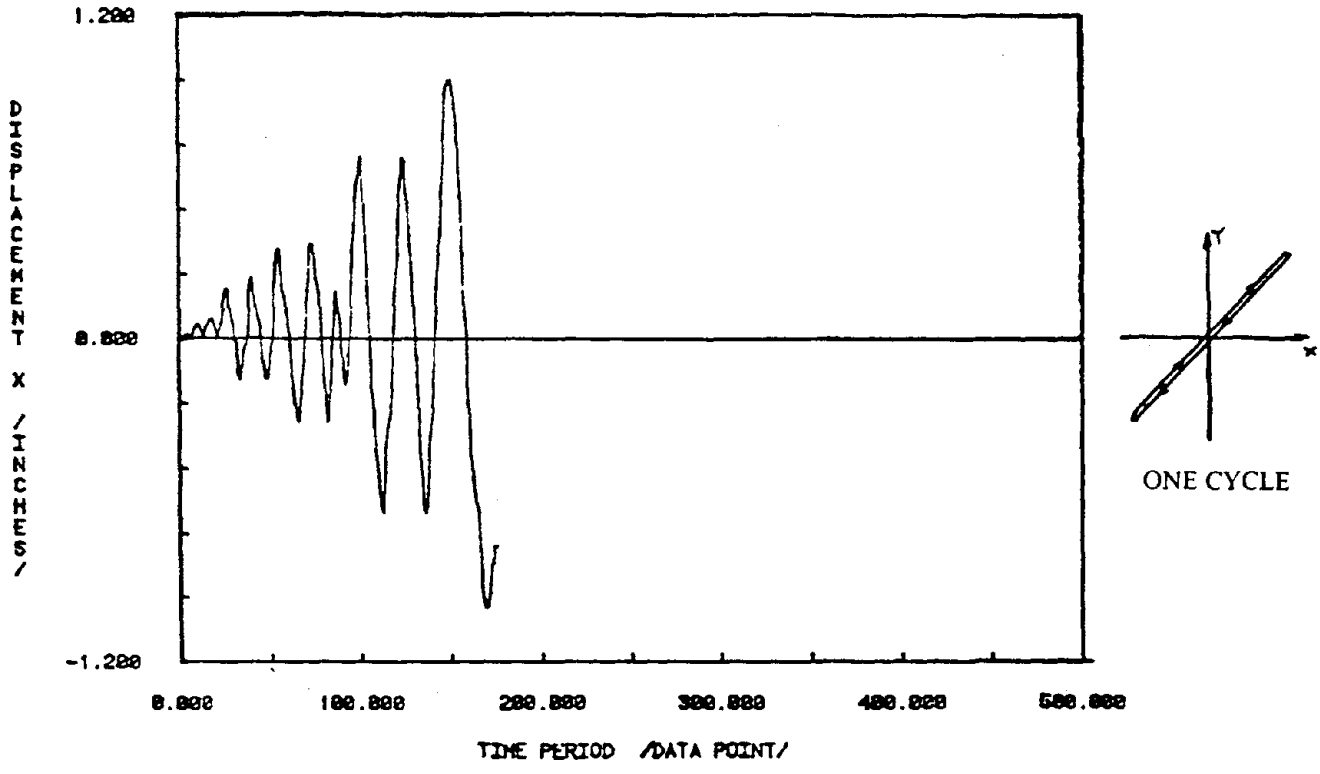

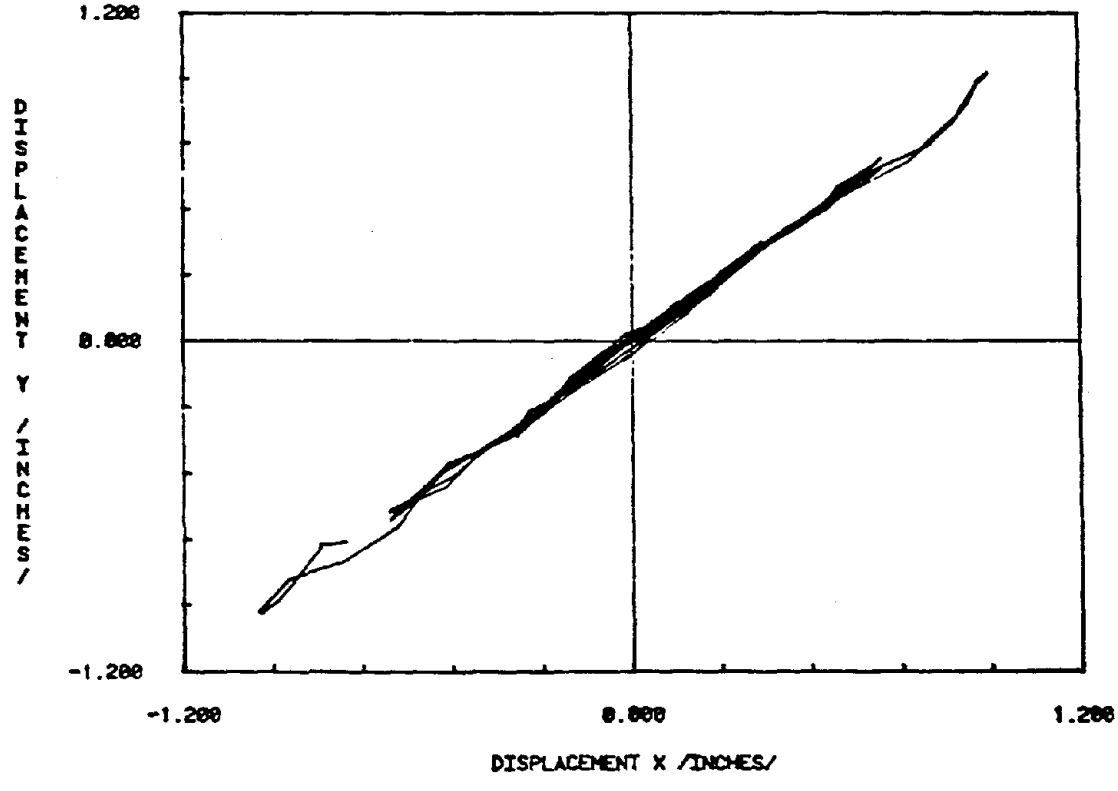

FIG. 3.4 Measured Load History for Specimen 2

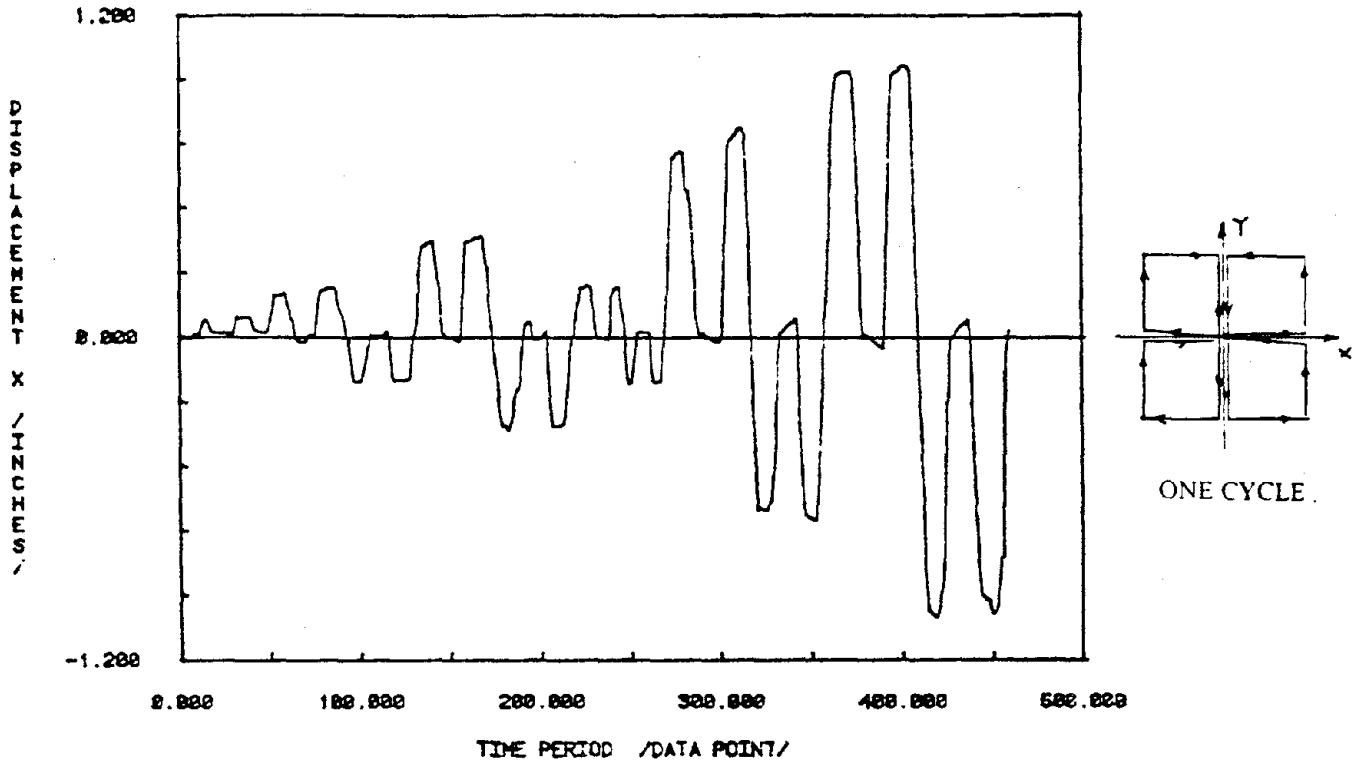

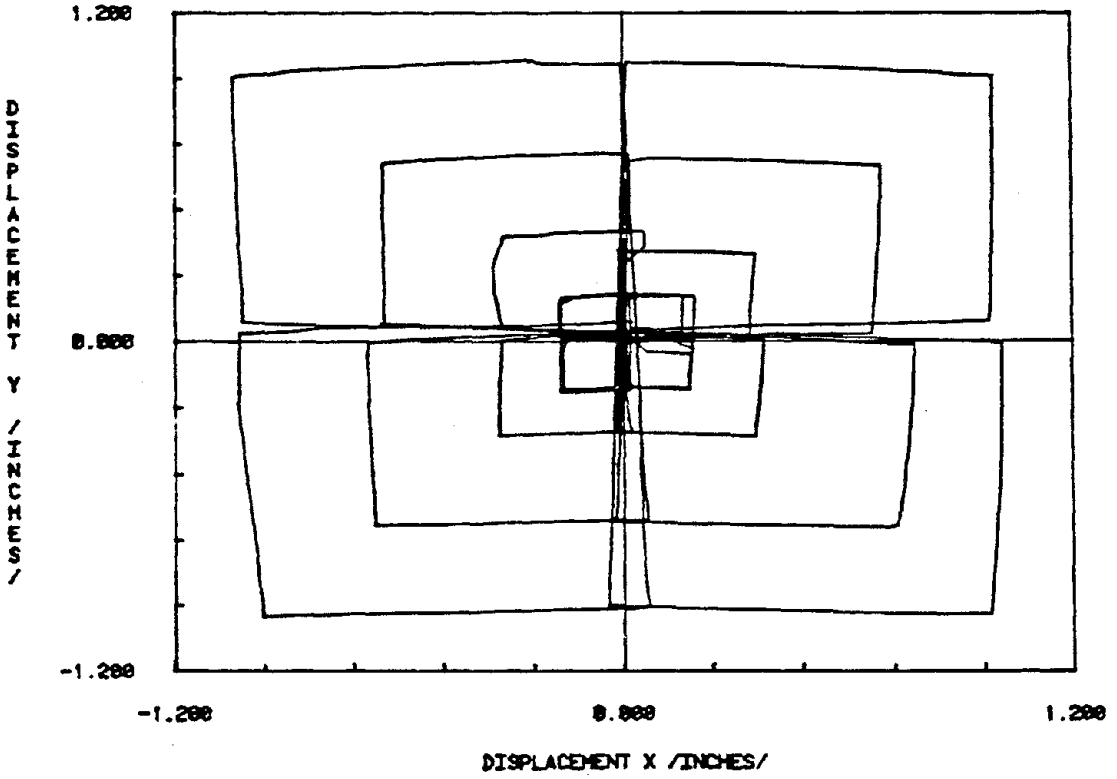

FIG. 3.5 Measured Load History for Specimen 3

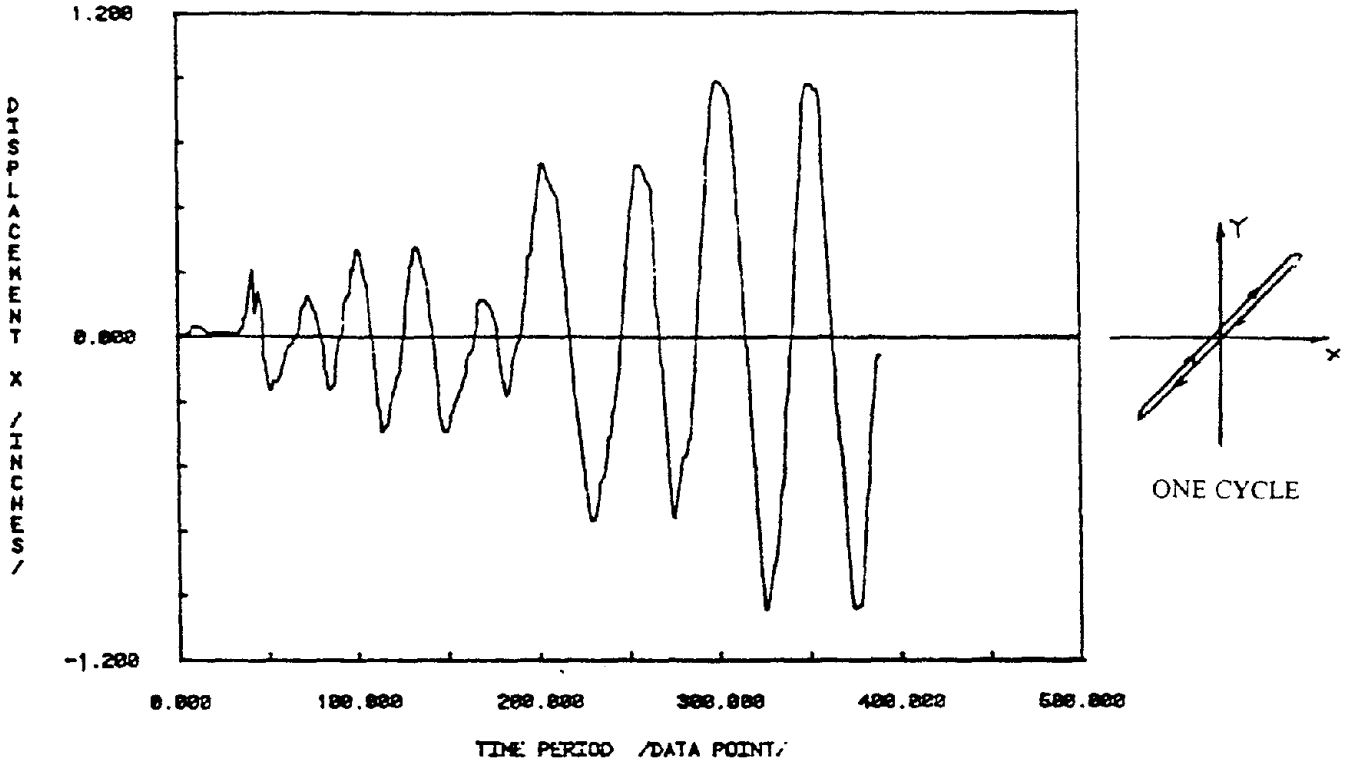

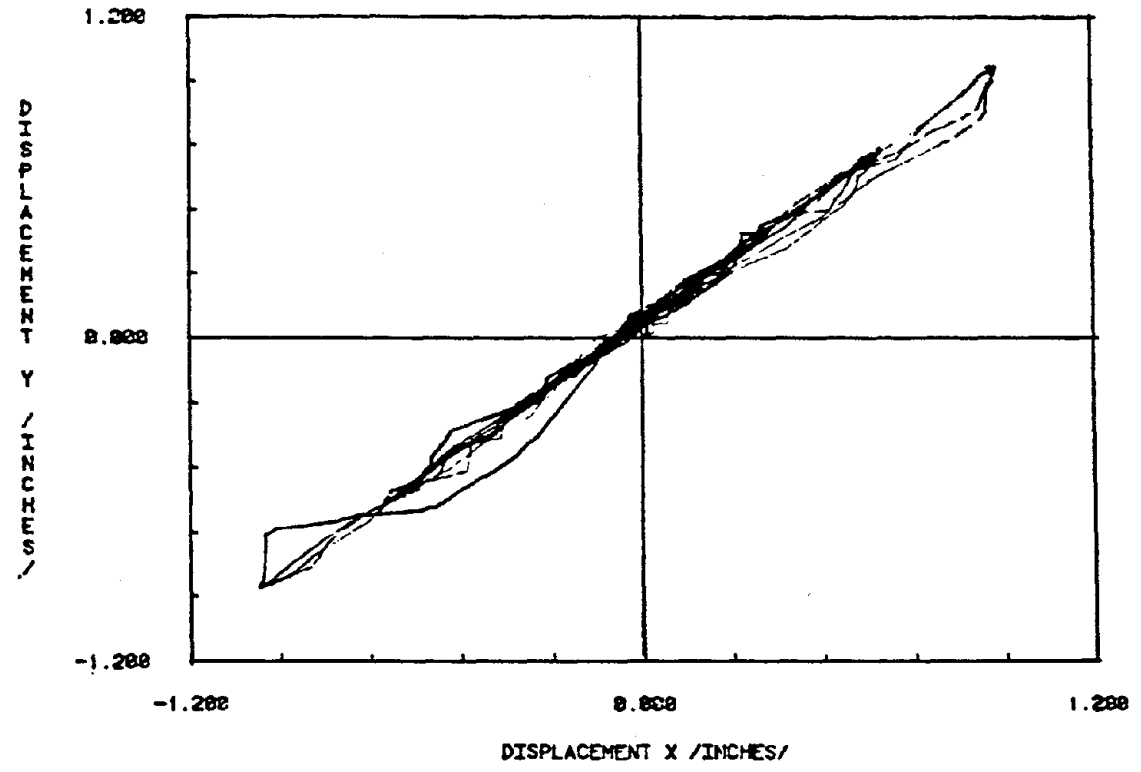

FIG. 3.6 Measured Load History for Specimen 4

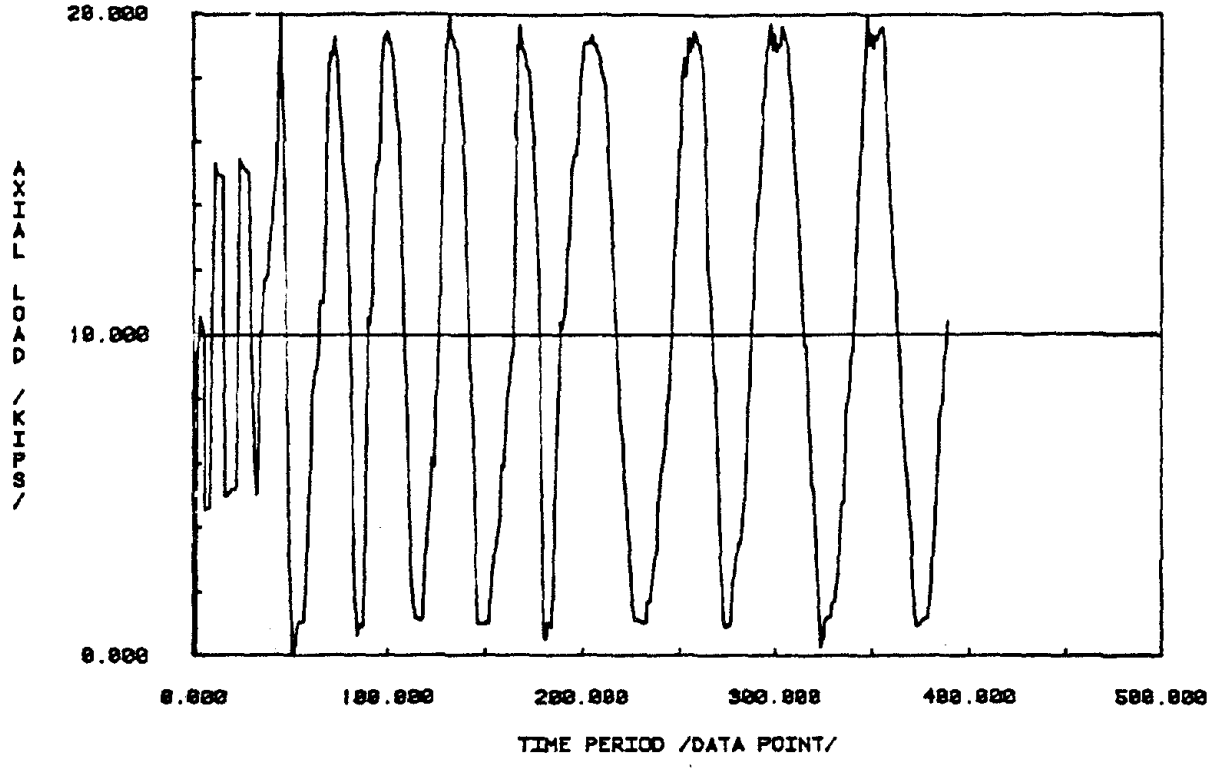

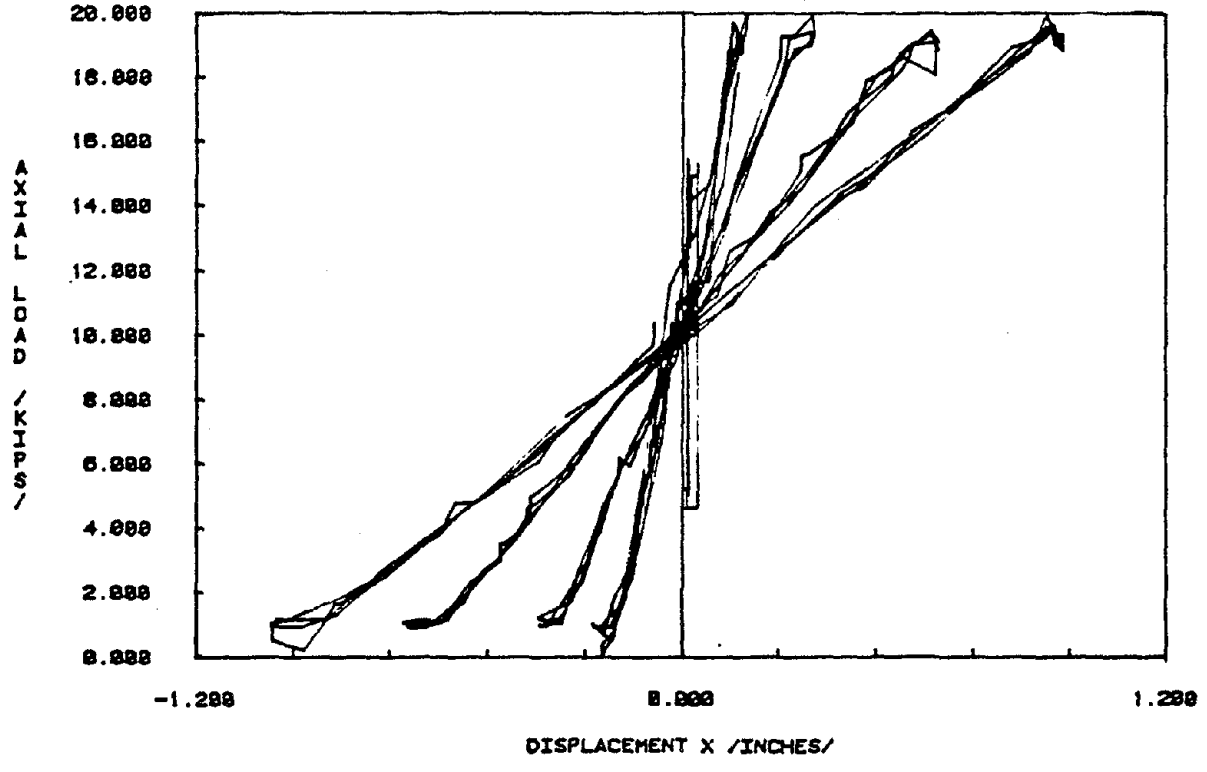

FIG. 3.6 Continued

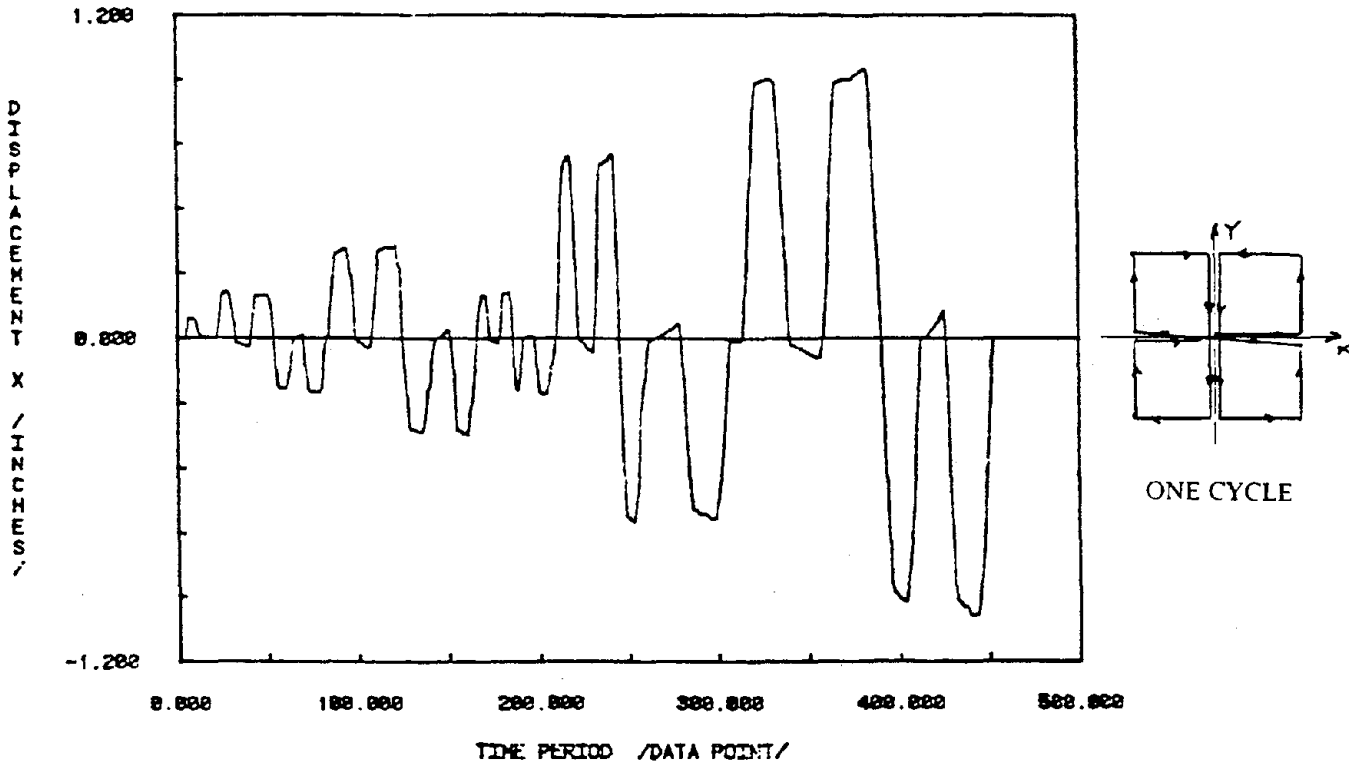

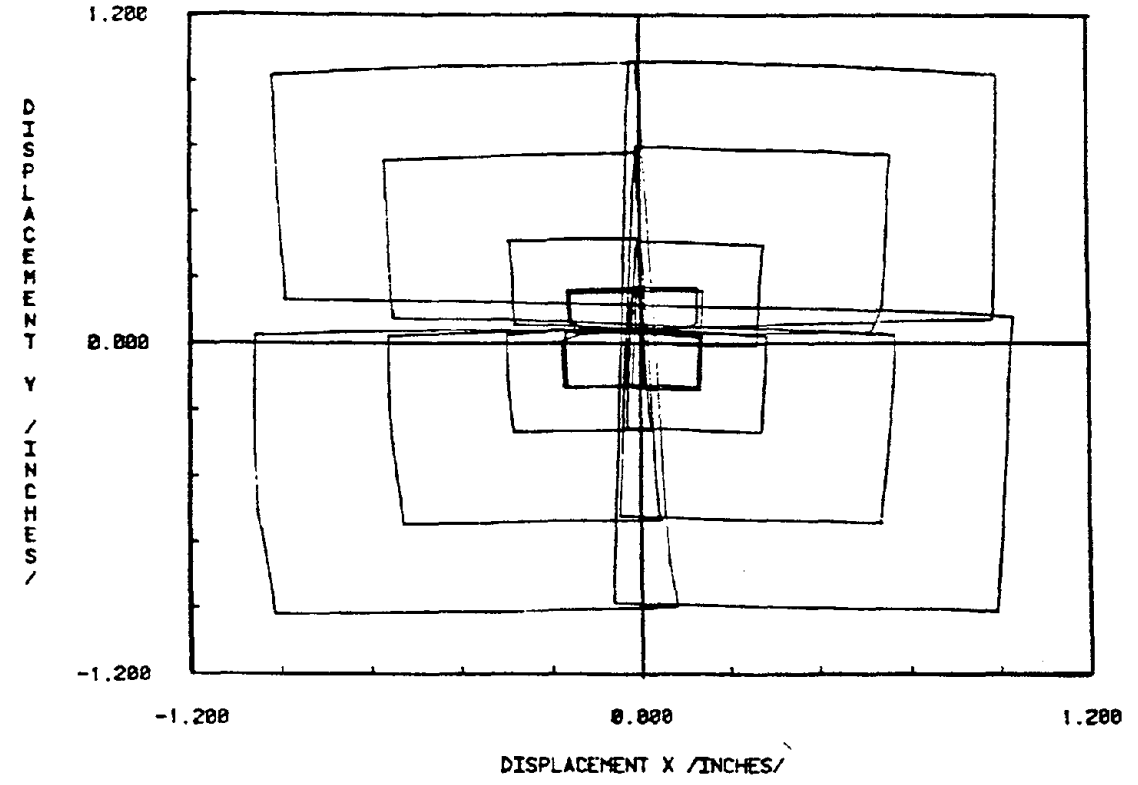

FIG. 3.7 Measured Load History for Specimen 5

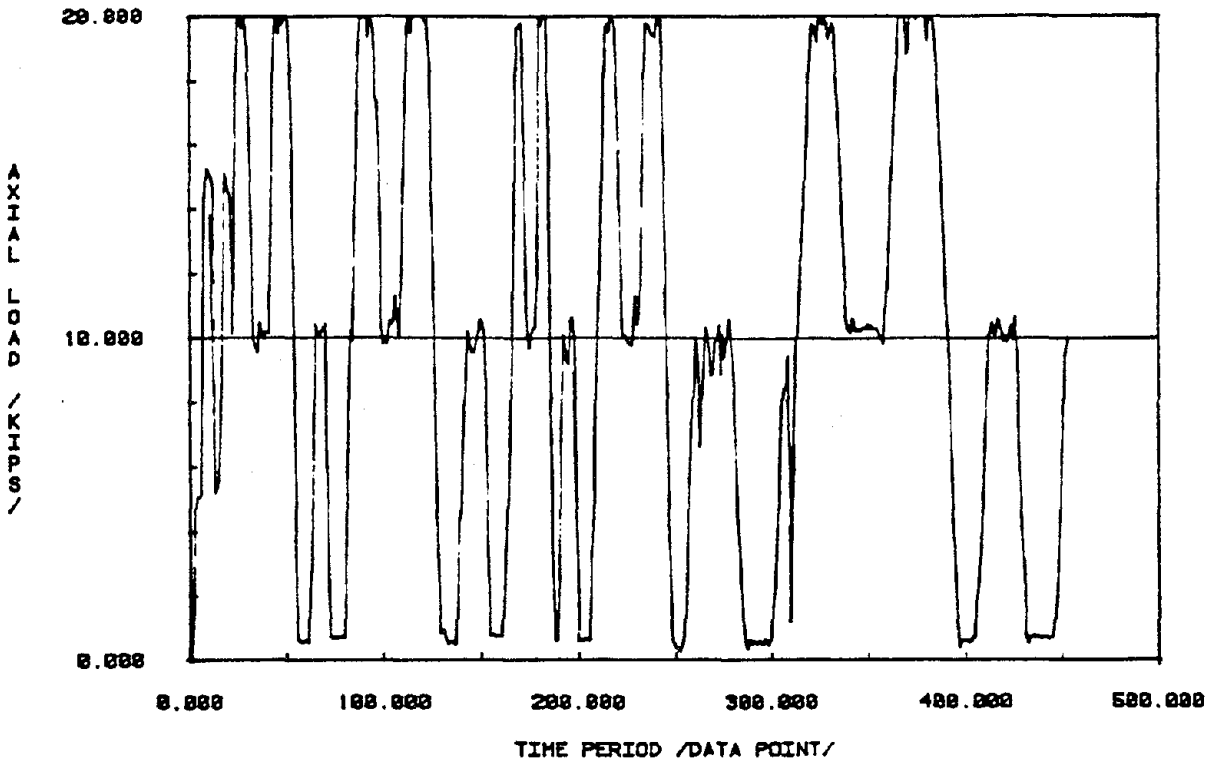

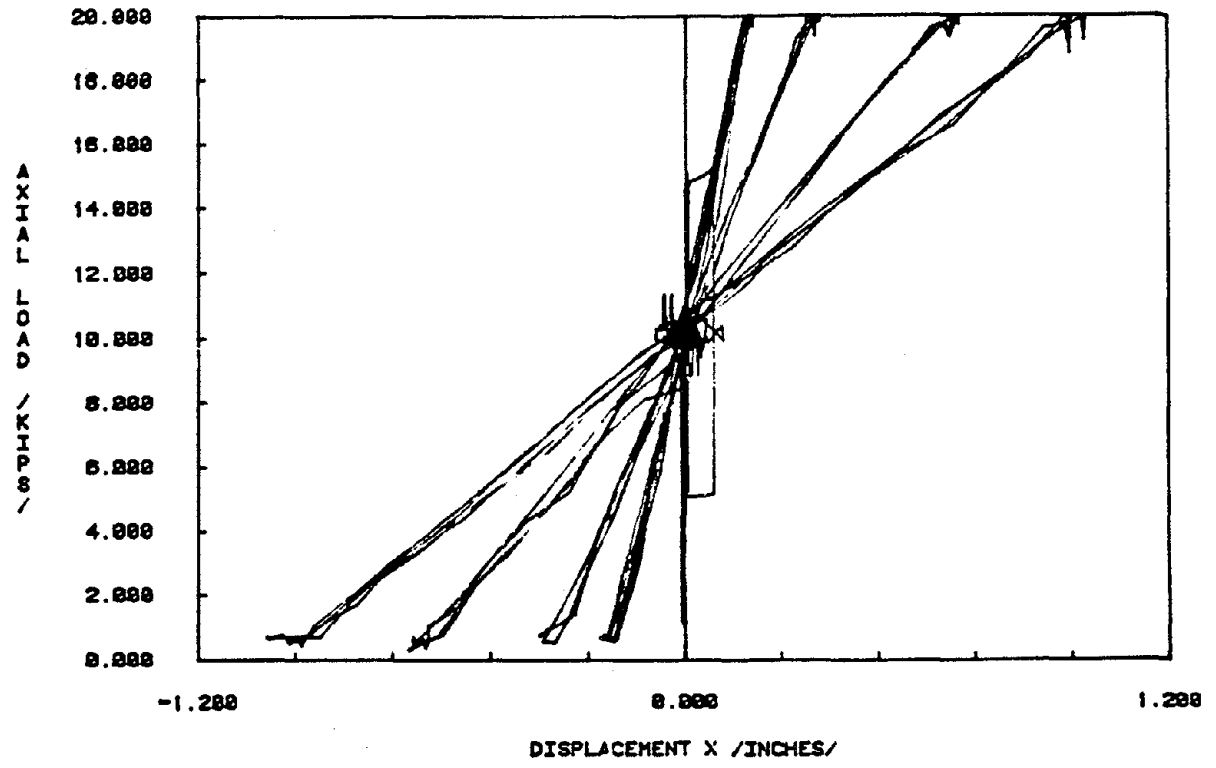

FIG. 3.7 Continued

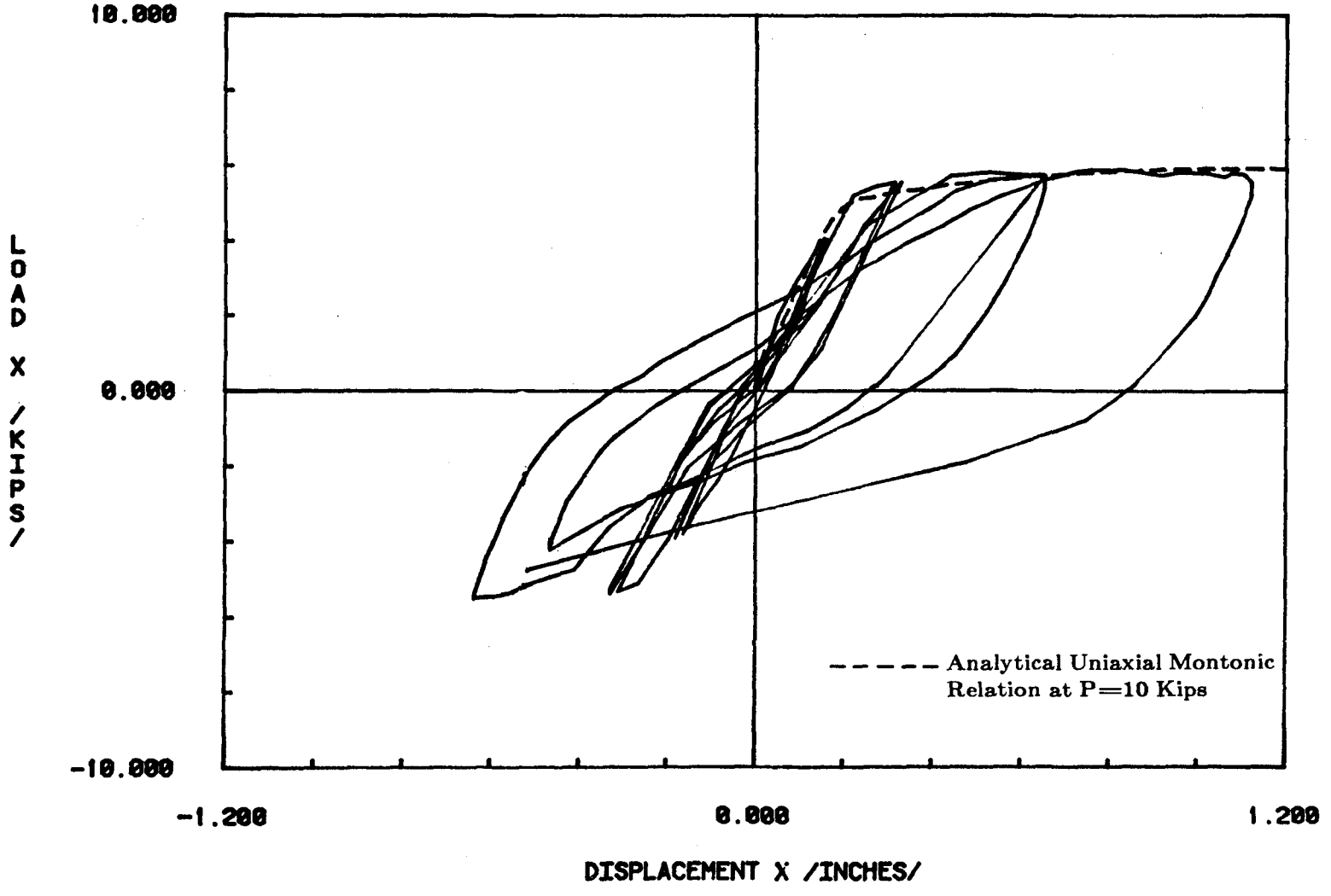

FIG. 3.8 Lateral Load Versus Lateral Displacement for Specimen 1

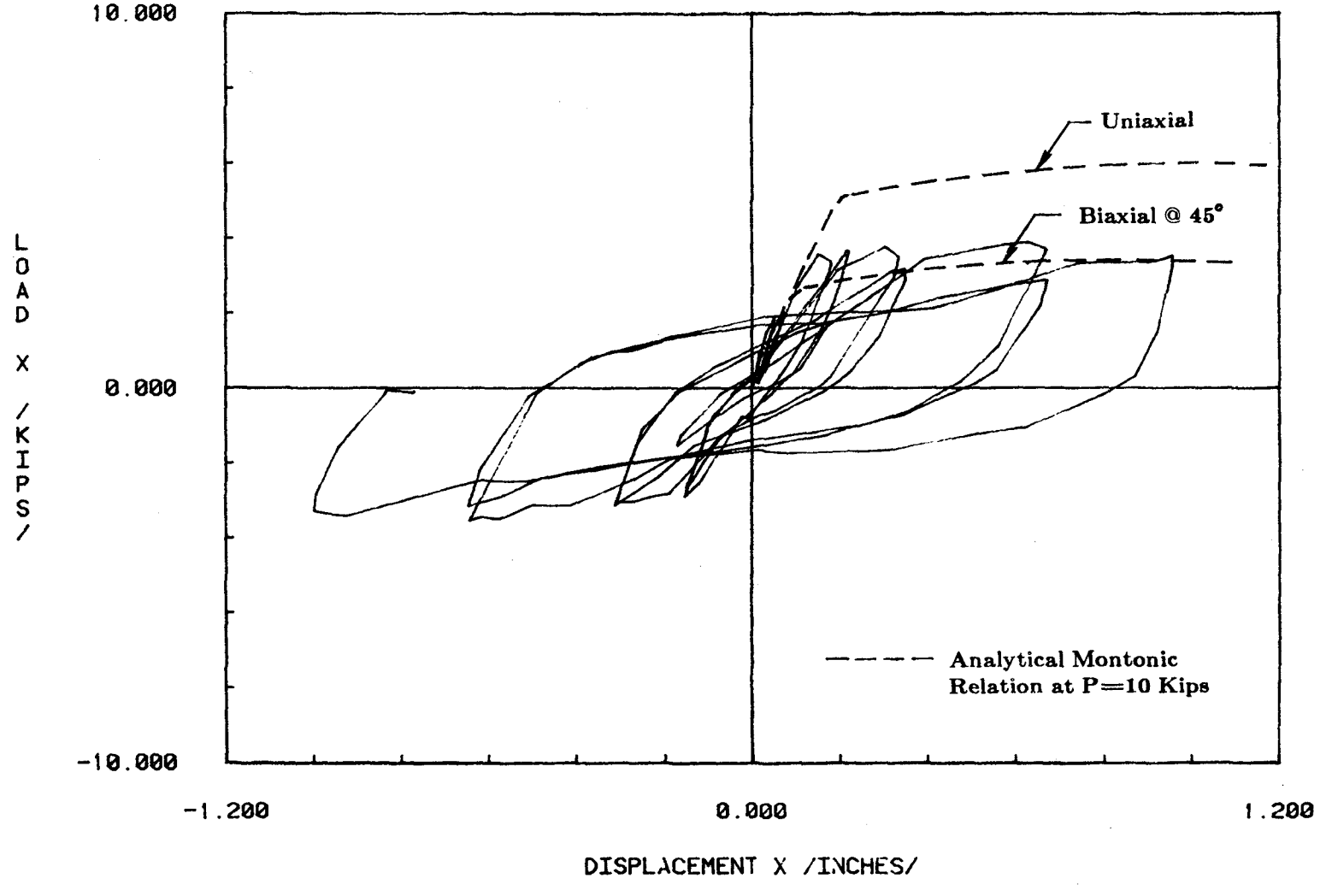

FIG. 3.9 Lateral Load Versus Lateral Displacement for Specimen 2

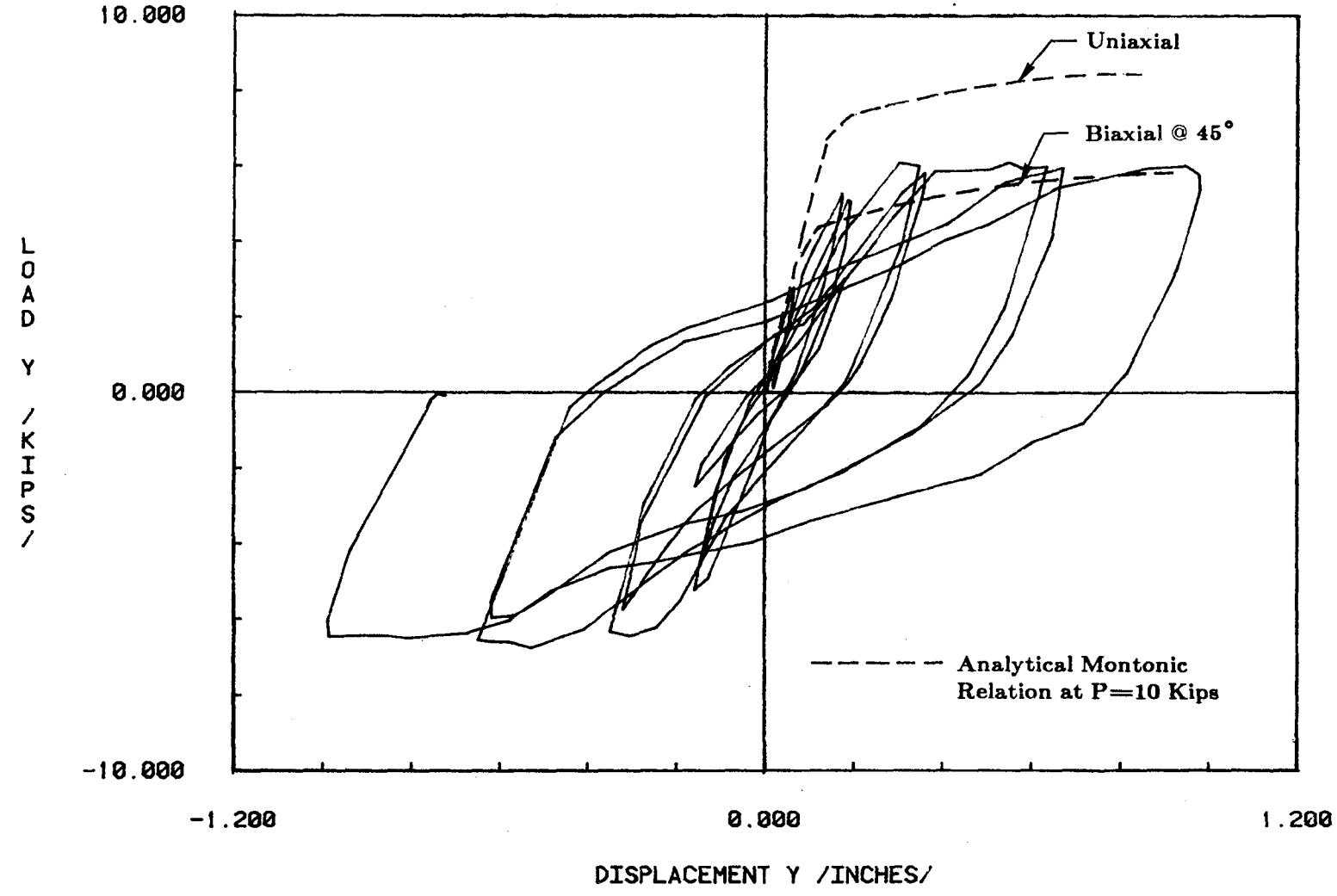

FIG. 3.9 Continued

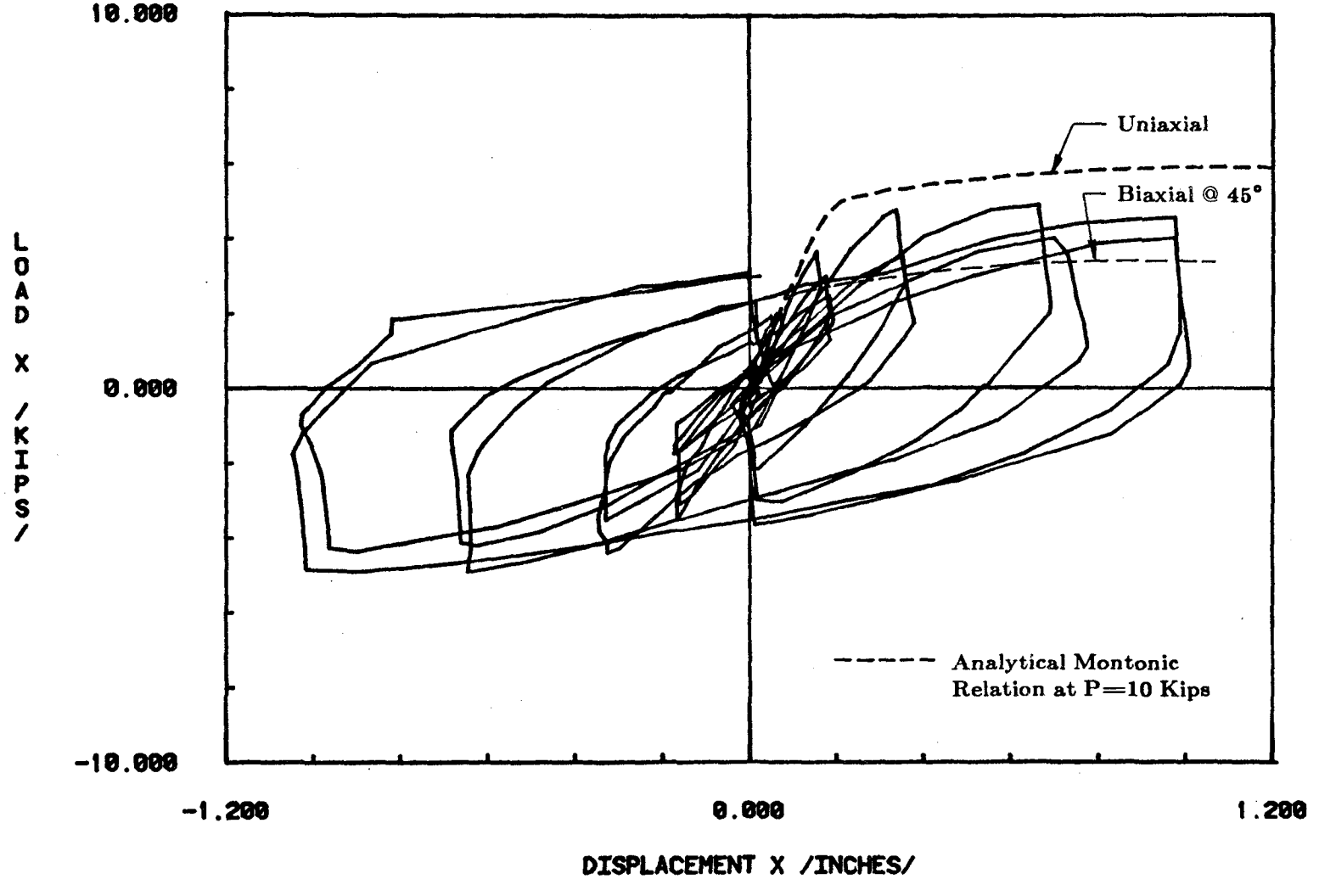

FIG. 3.10 Lateral Load Versus Lateral Displacement for Specimen 3

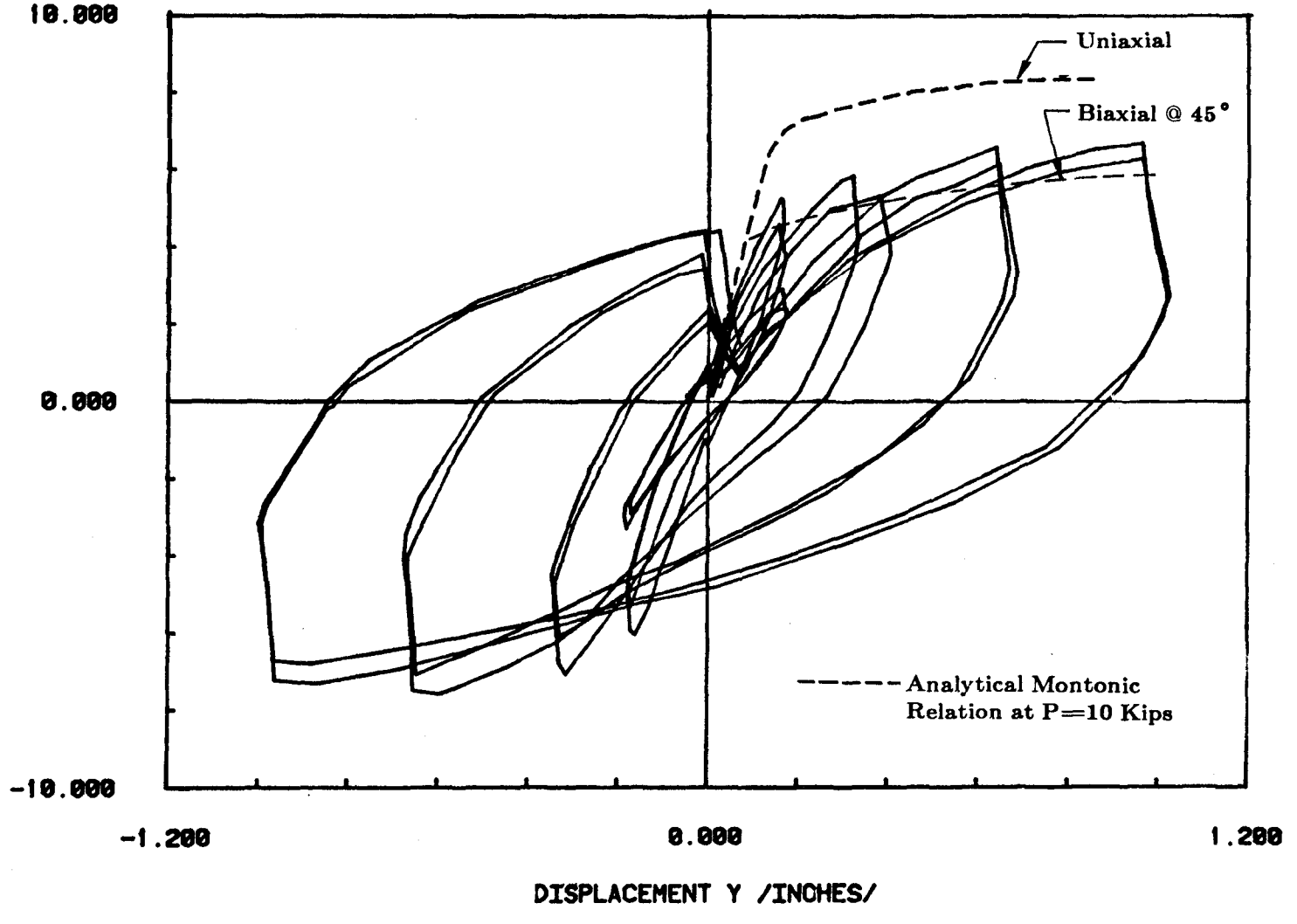

FIG. 3.10 Continued

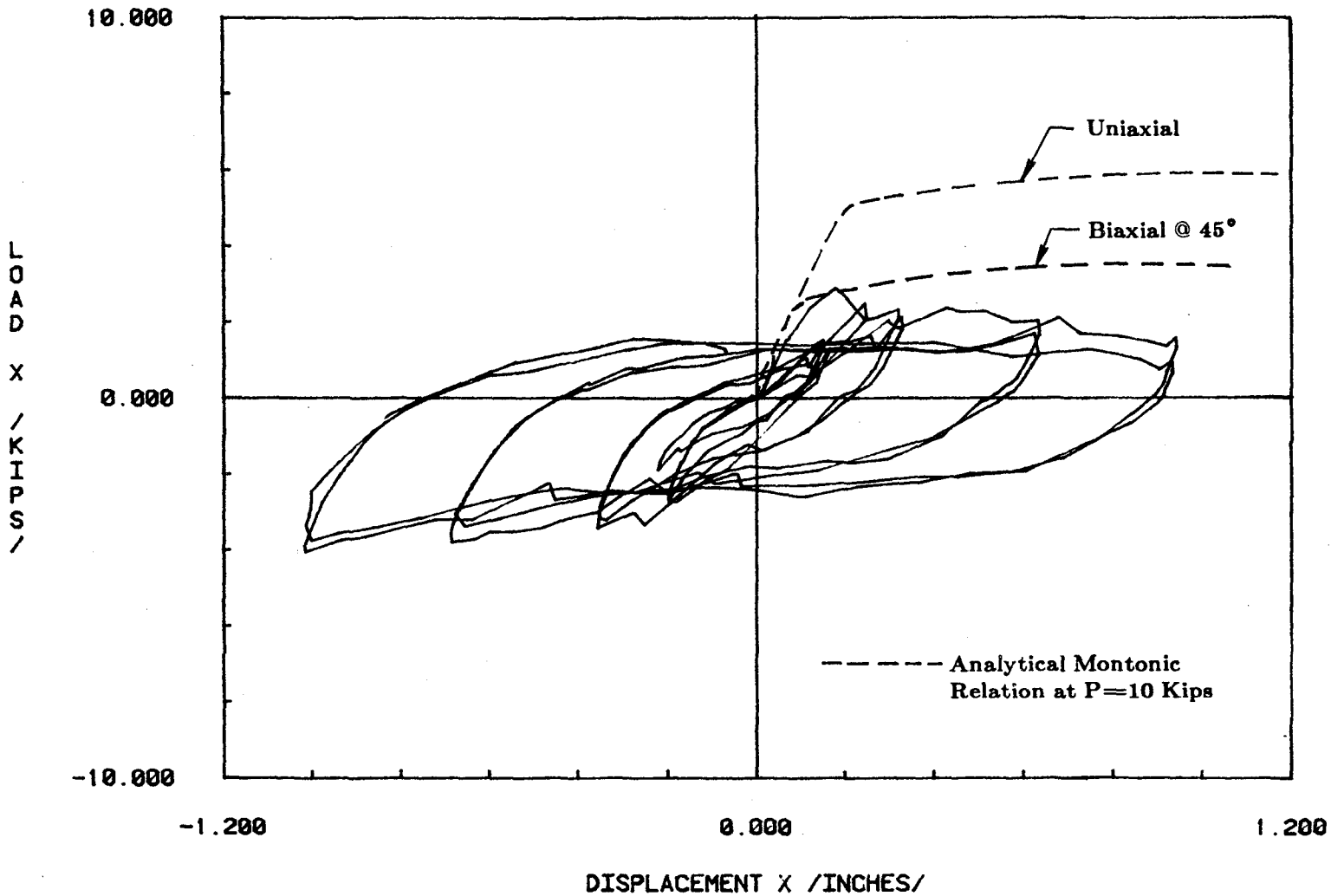

FIG. 3.11 Lateral Load Versus Lateral Displacement for Specimen 4

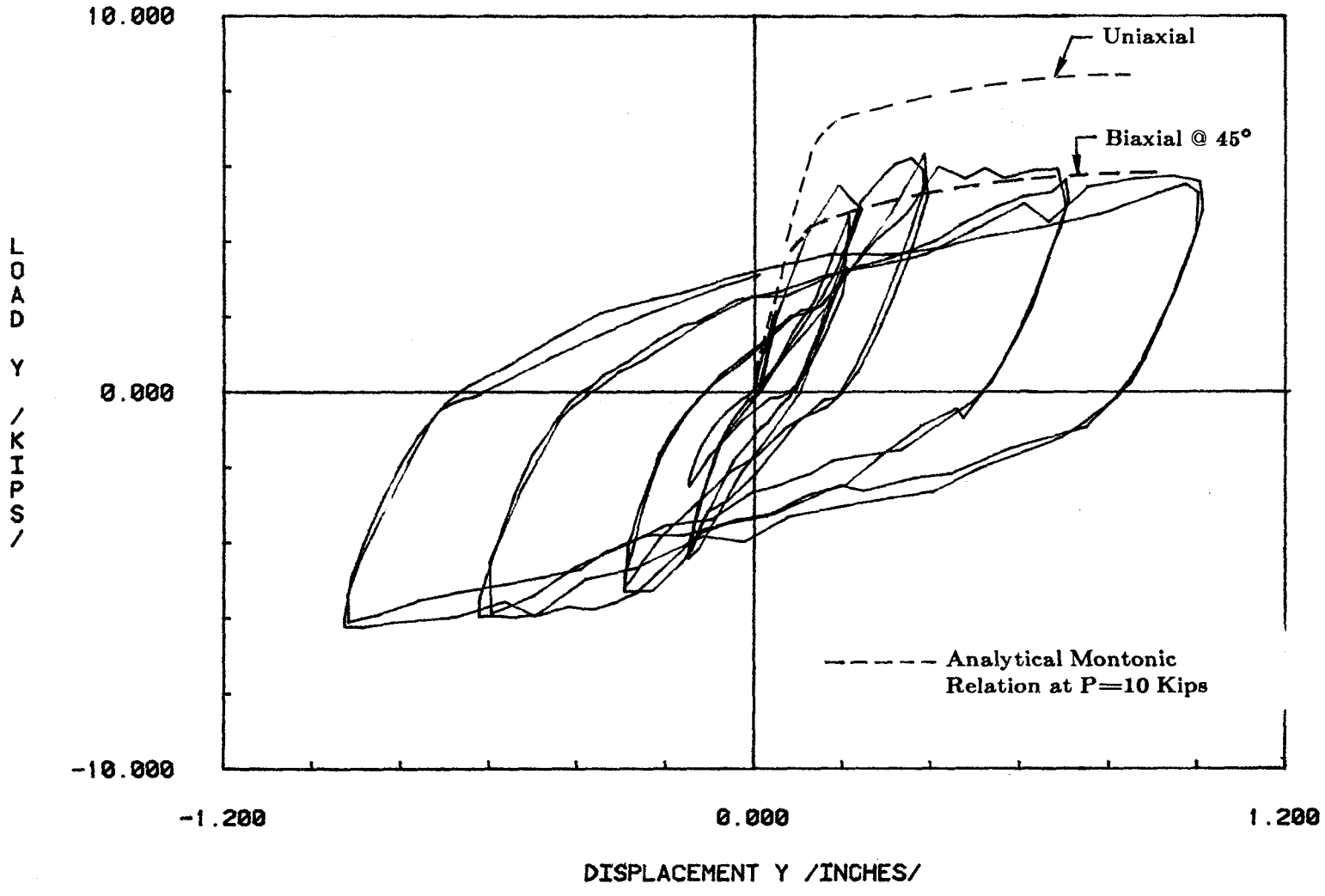

FIG. 3.11 Continued

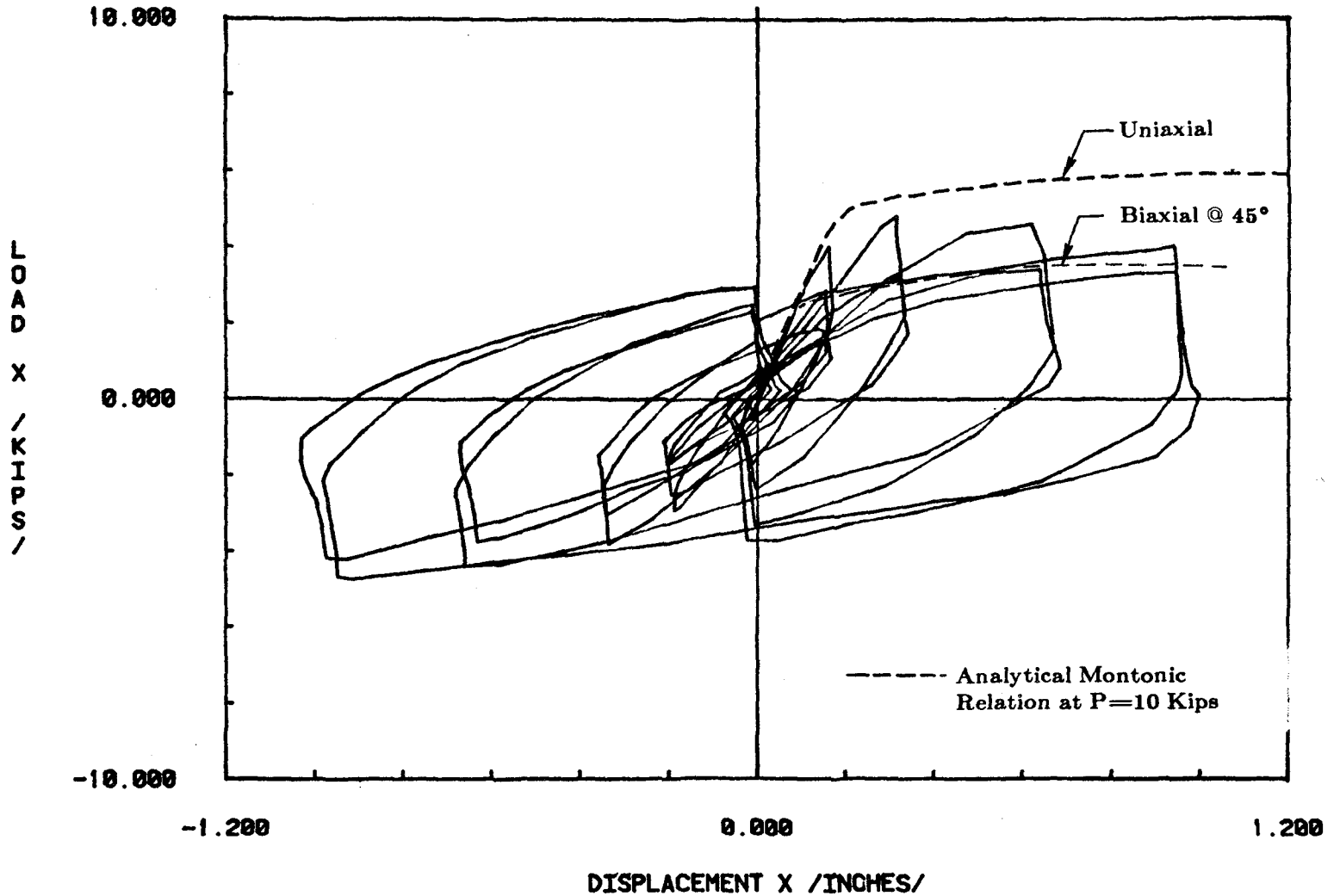

FIG. 3.12 Lateral Load Versus Lateral Displacement for Specimen 5

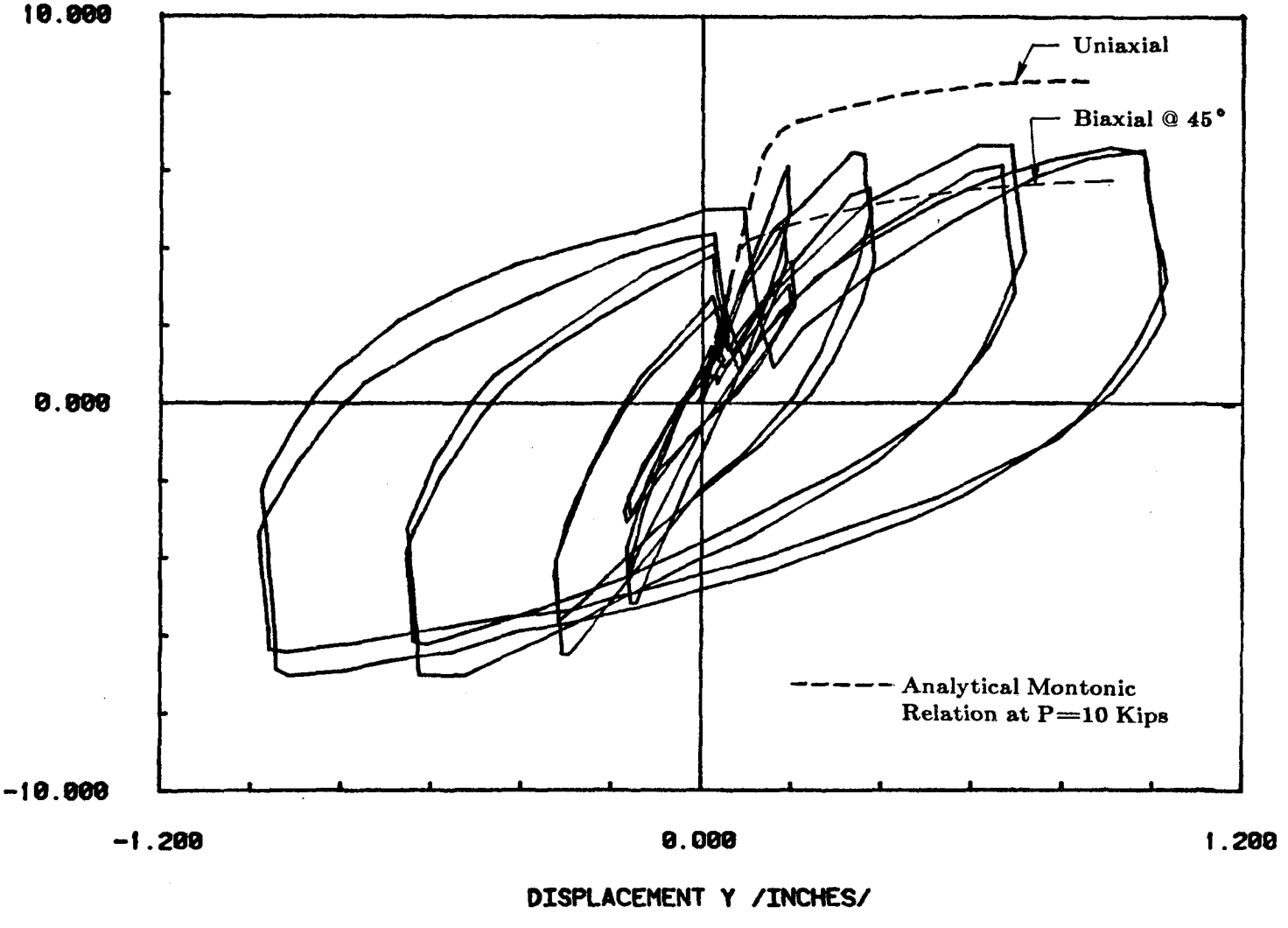

FIG. 3.12 Continued

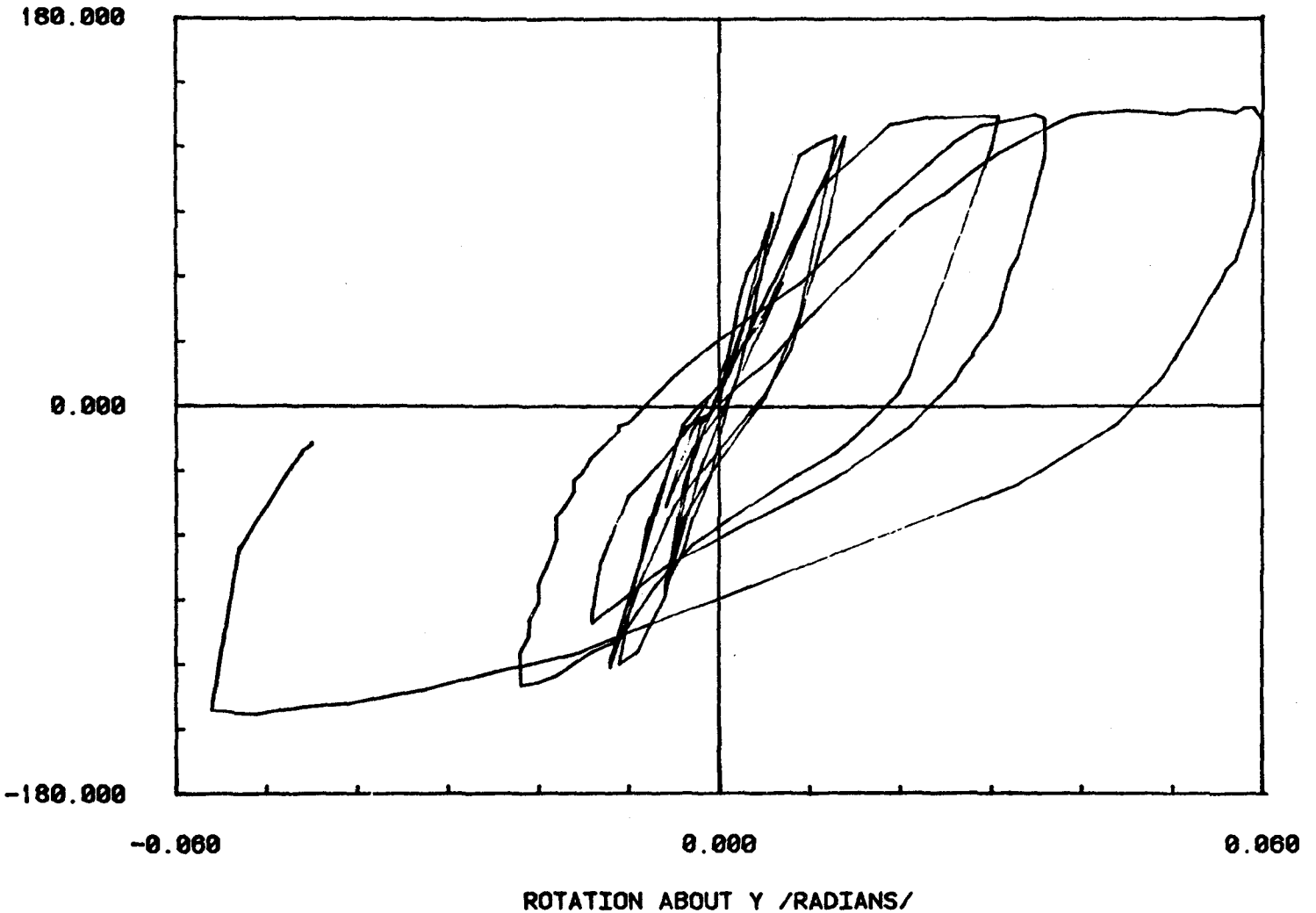

FIG. 3.13 Base Moment Versus Lower Column Rotation for Specimen 1

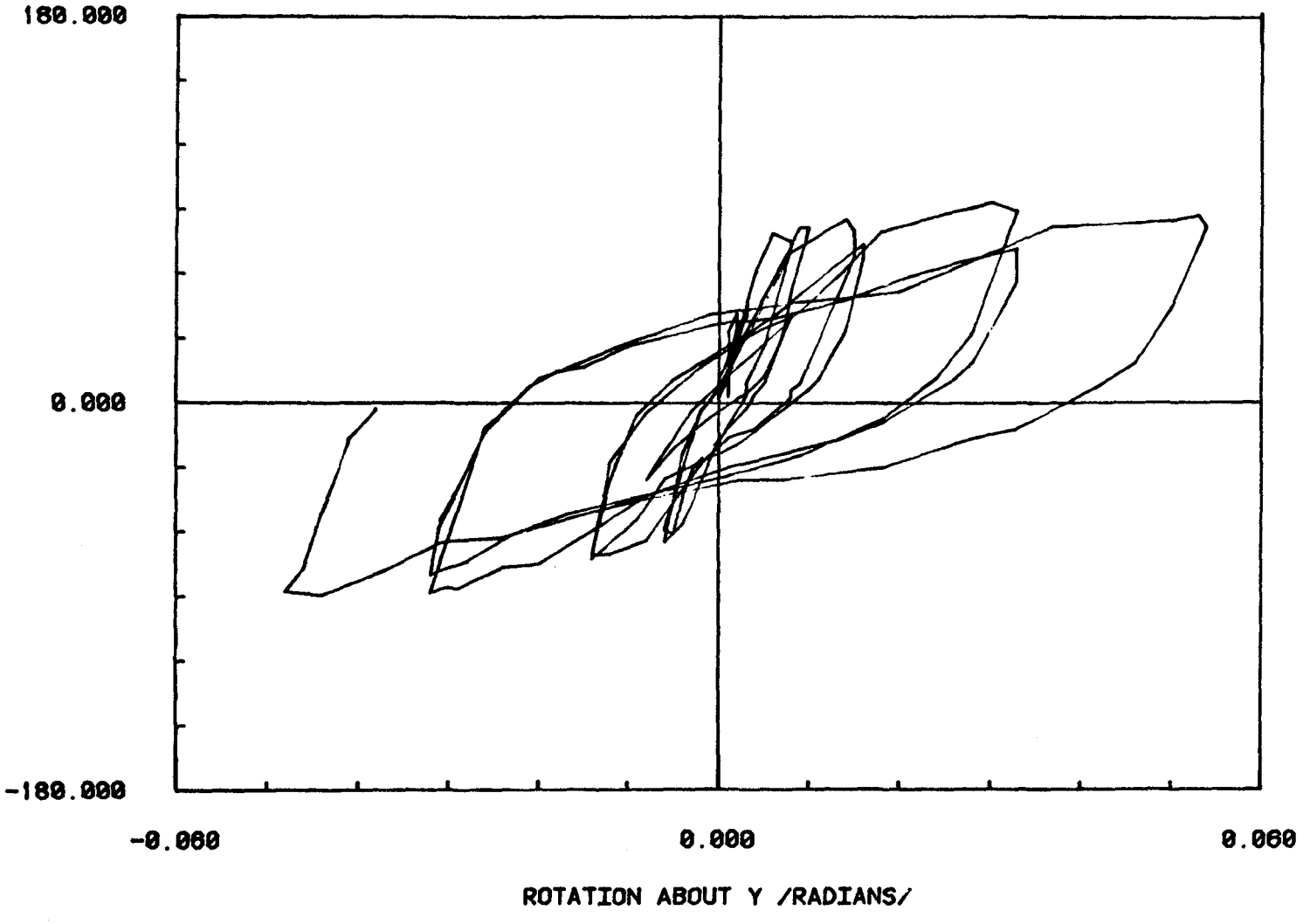

FIG. 3.14 Base Moment Versus Lower Column Rotation for Specimen 2

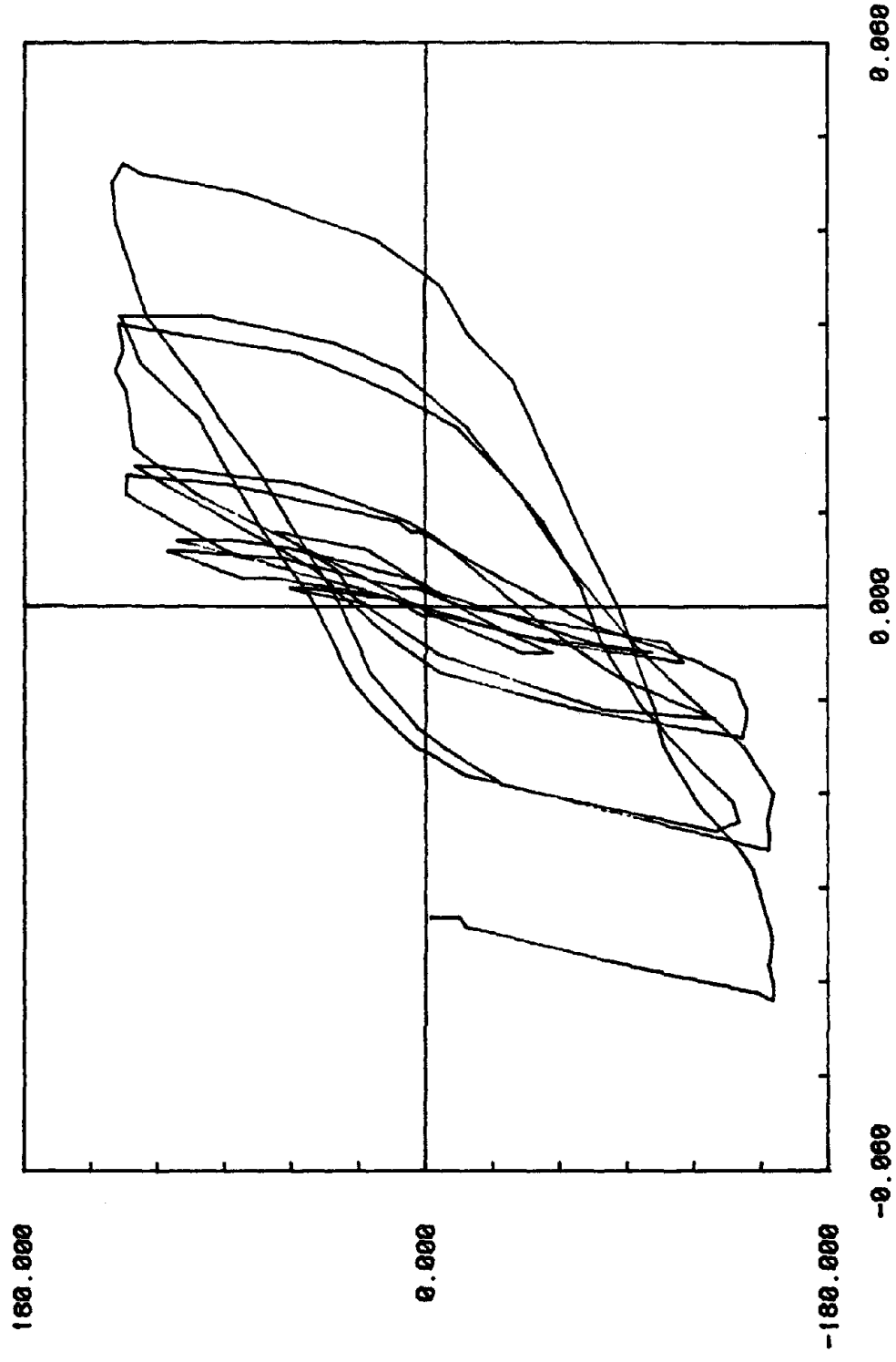

FIG. 3.14 Continued

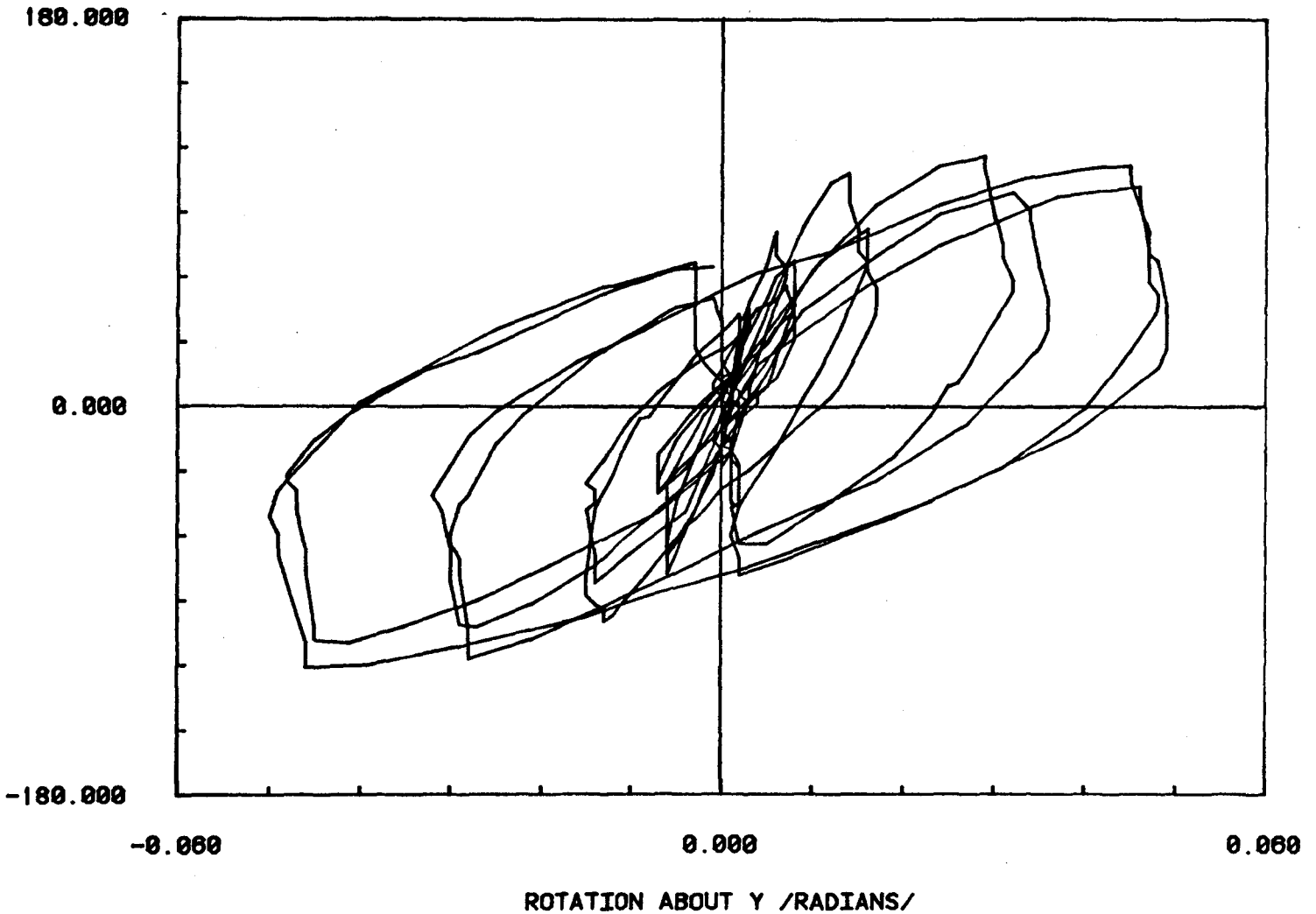

FIG. 3.15 Base Moment Versus Lower Column Rotation for Specimen 3

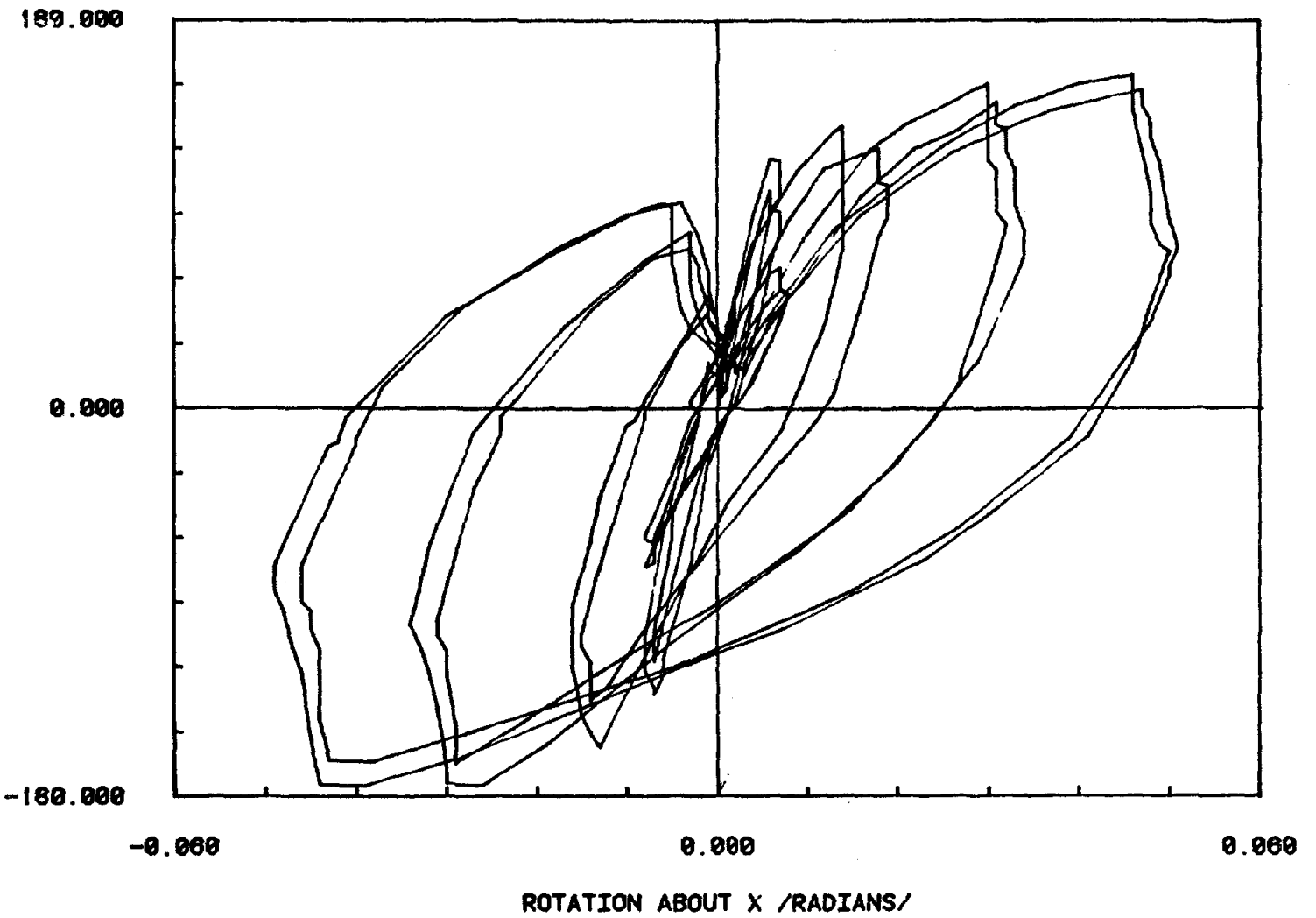

FIG. 3.15 Continued

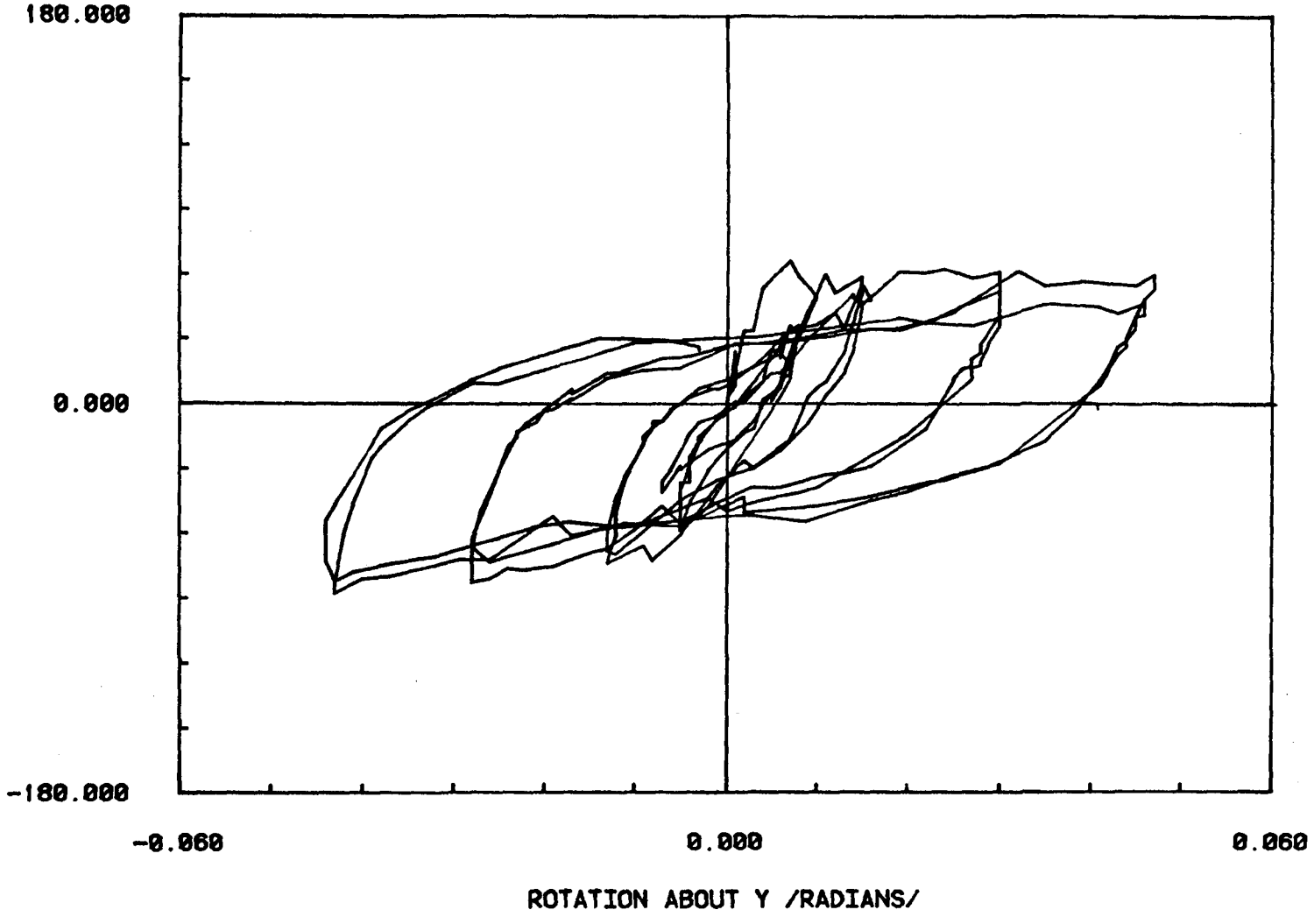

FIG. 3.16 Base Moment Versus Lower Column Rotation for Specimen 4

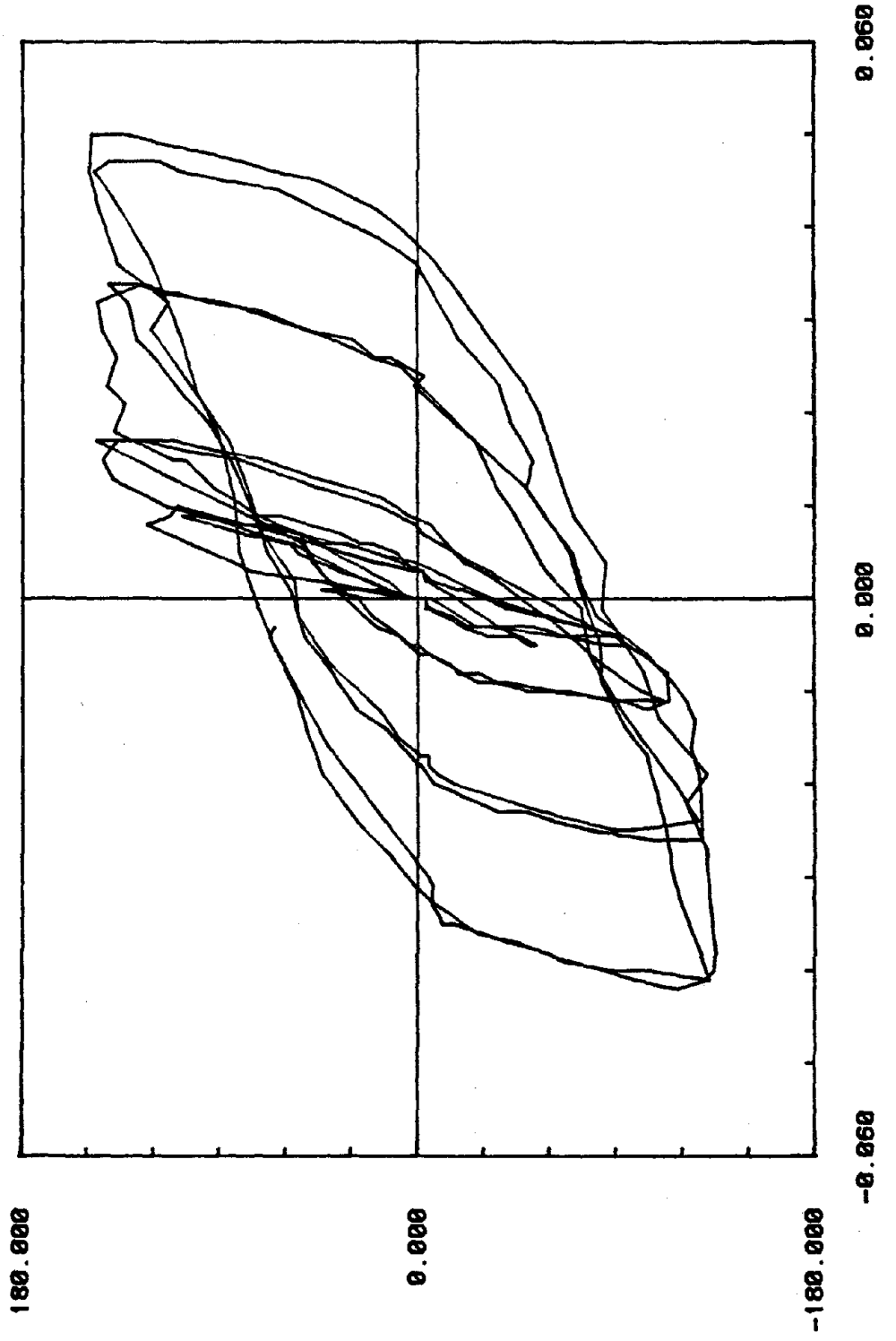

FIG. 3.16 Continued

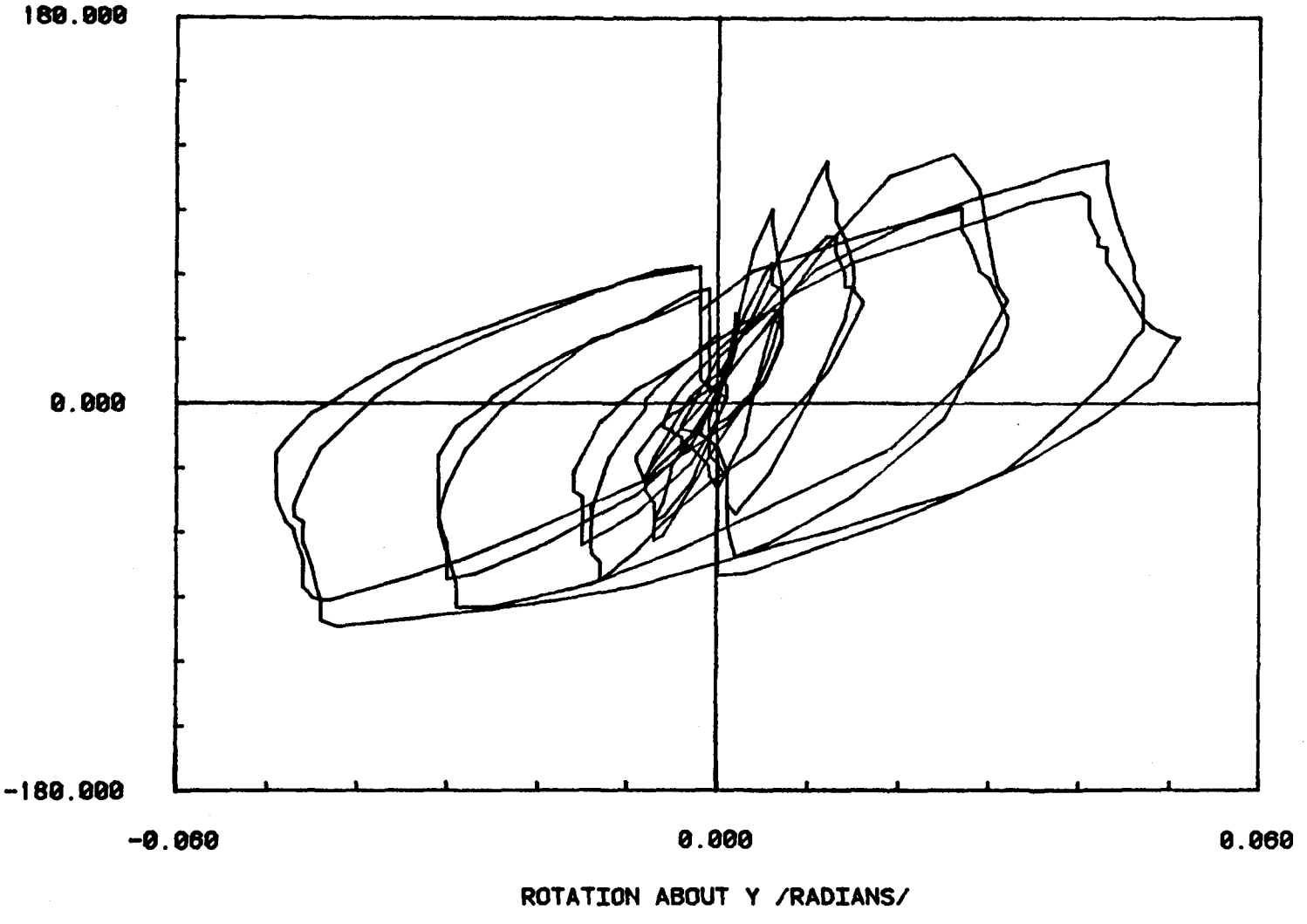

FIG. 3.17 Base Moment Versus Lower Column Rotation for Specimen 5

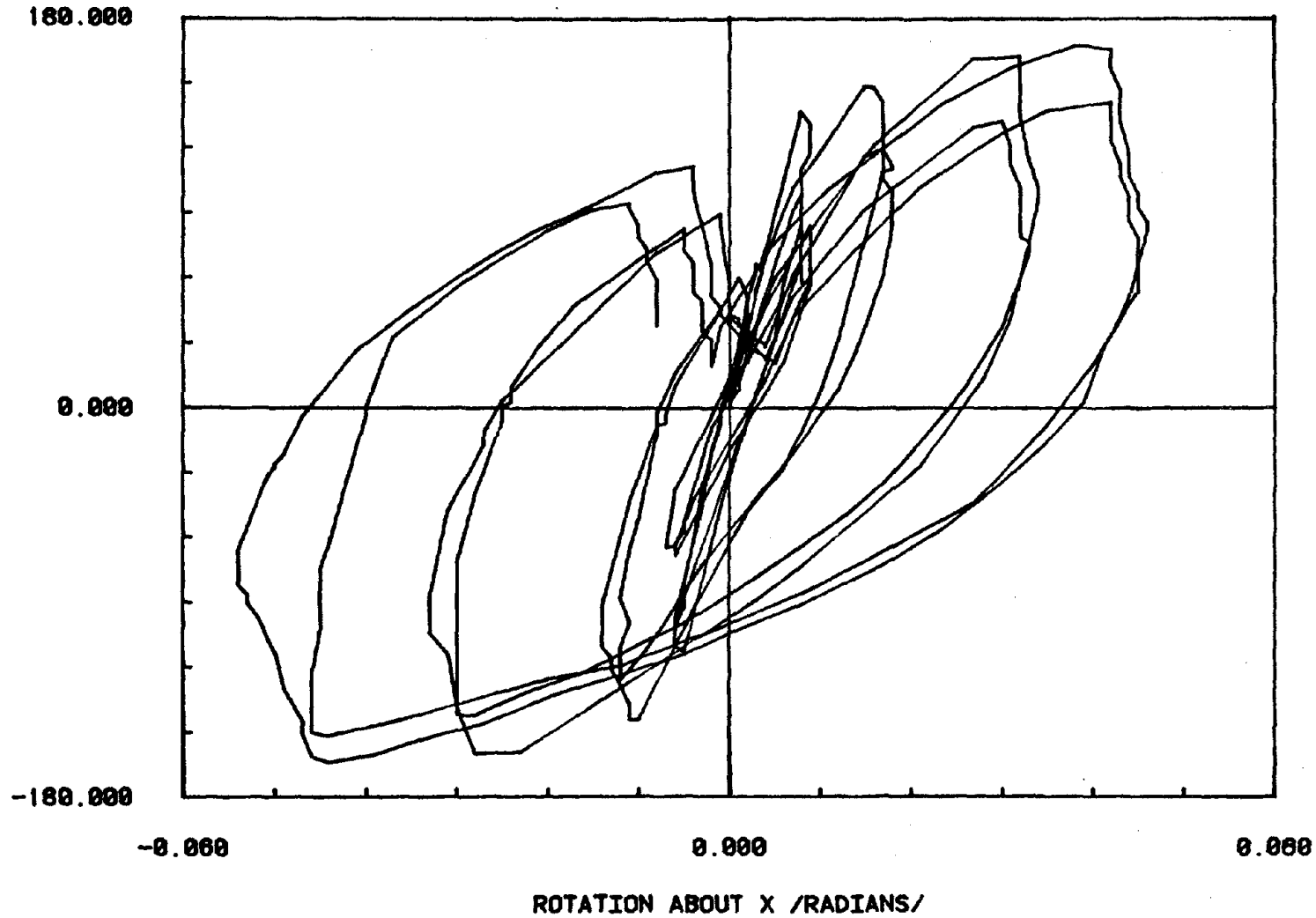

FIG. 3.17 Continued

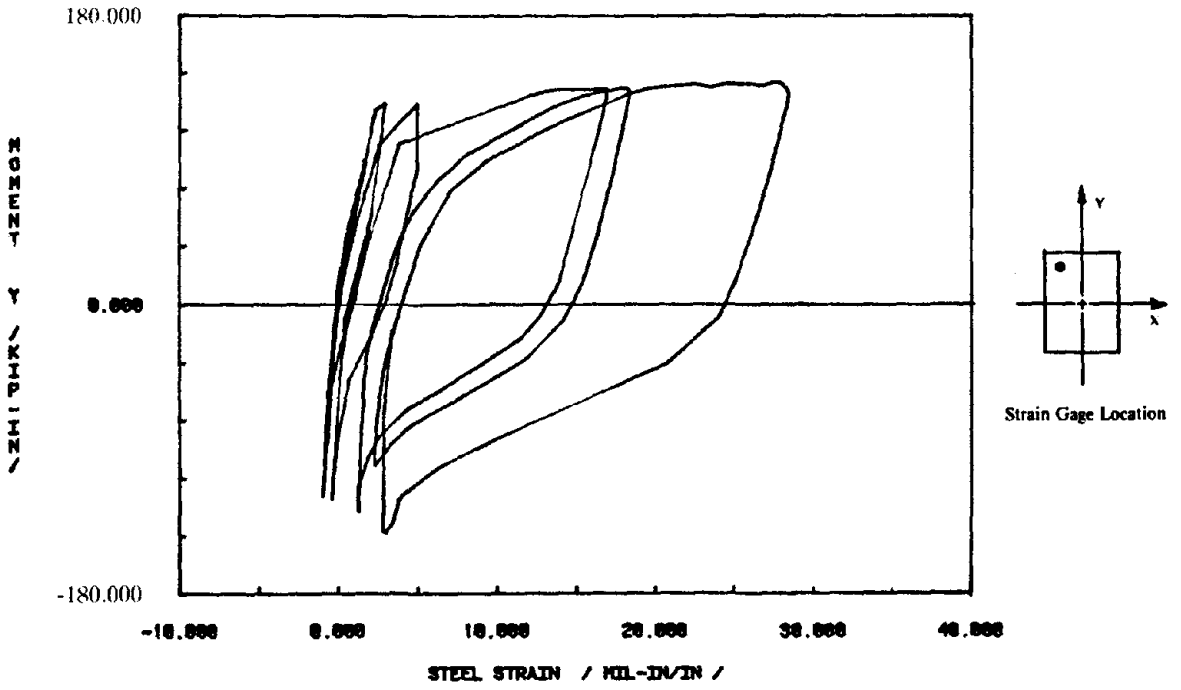

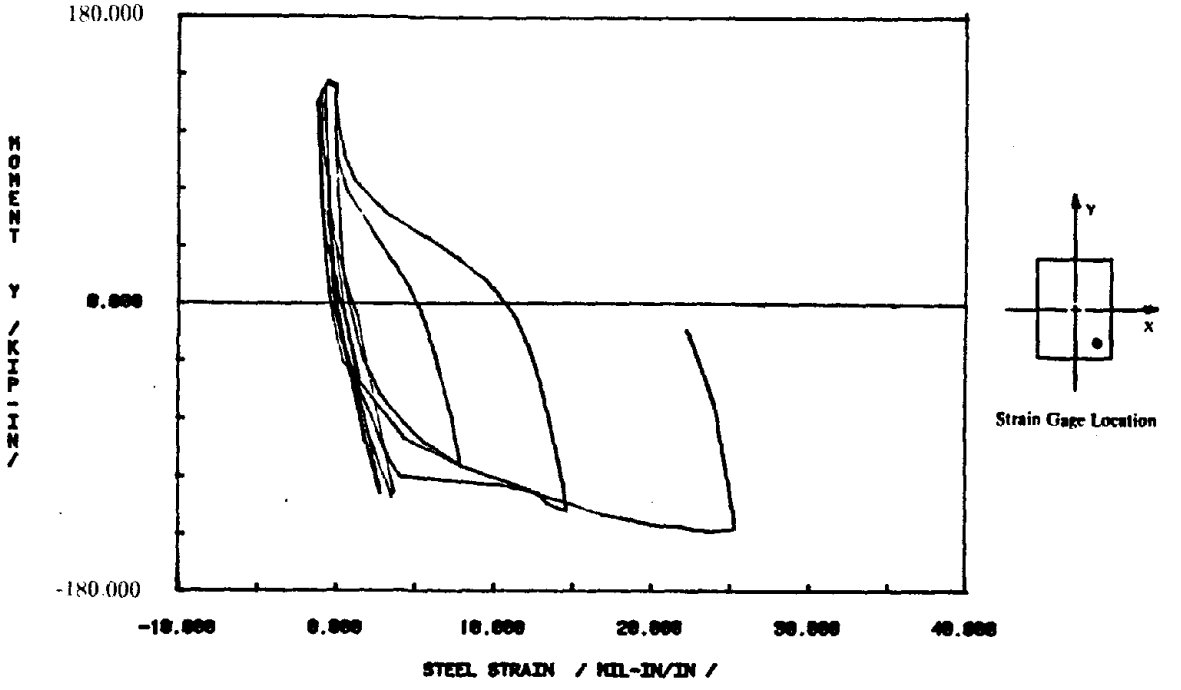

FIG. 3.18 Strain Histories for Specimen 1

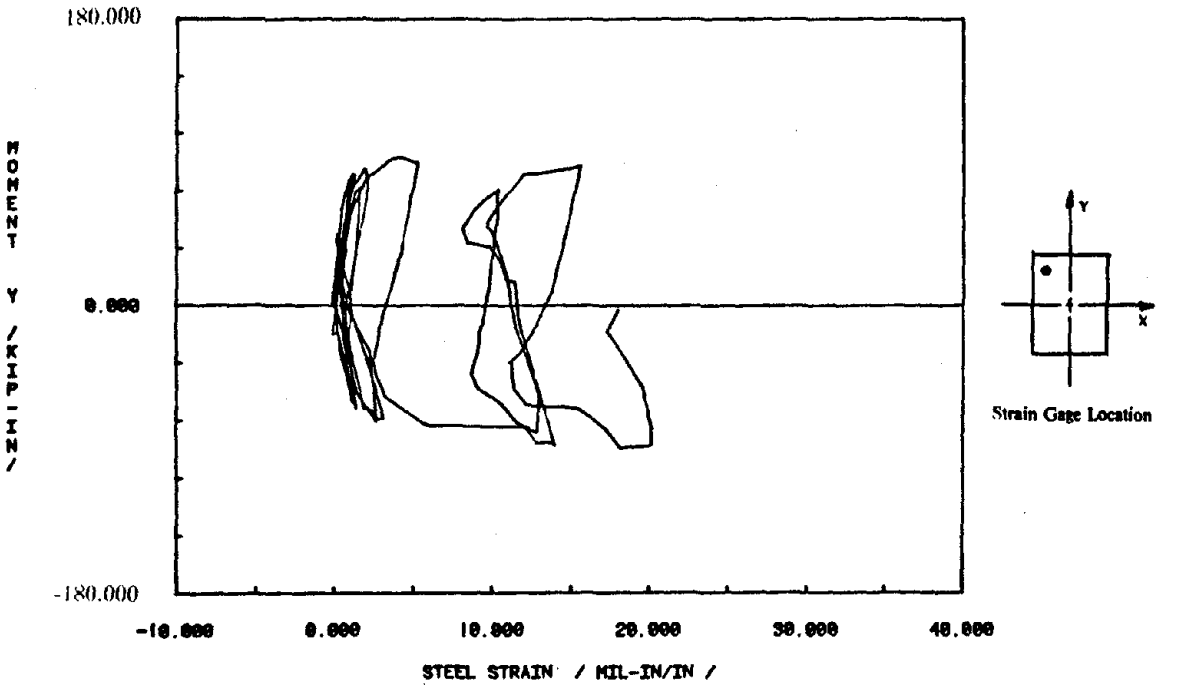

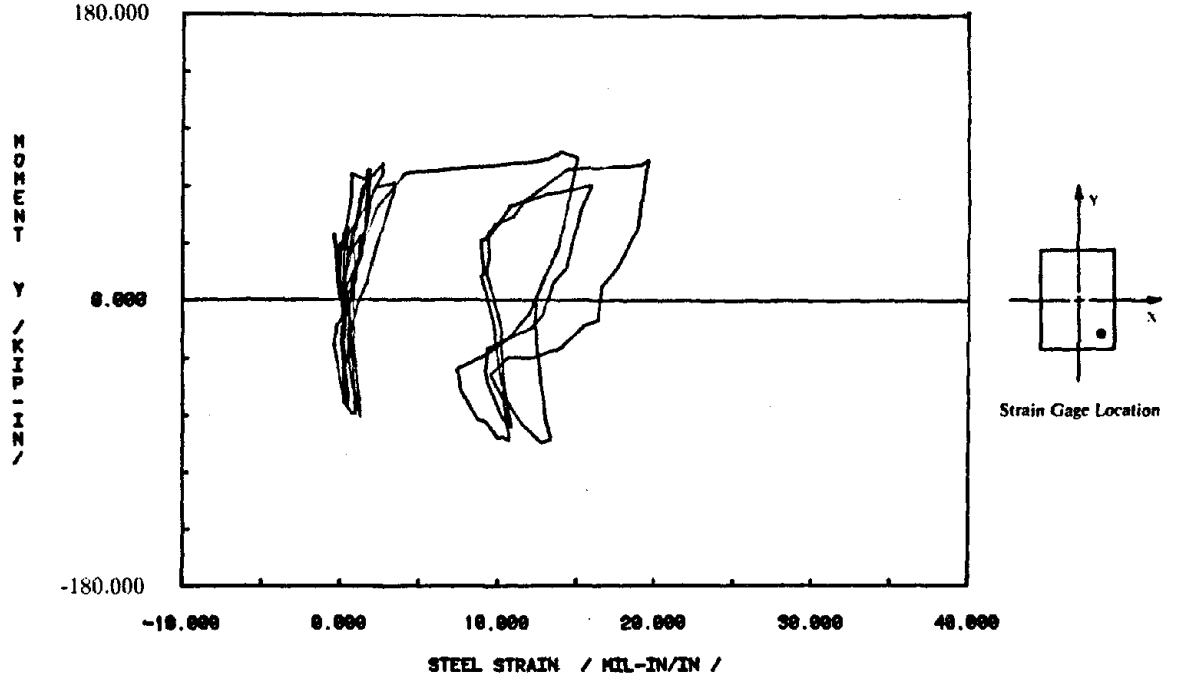

FIG. 3.19 Strain Histories for Specimen 2

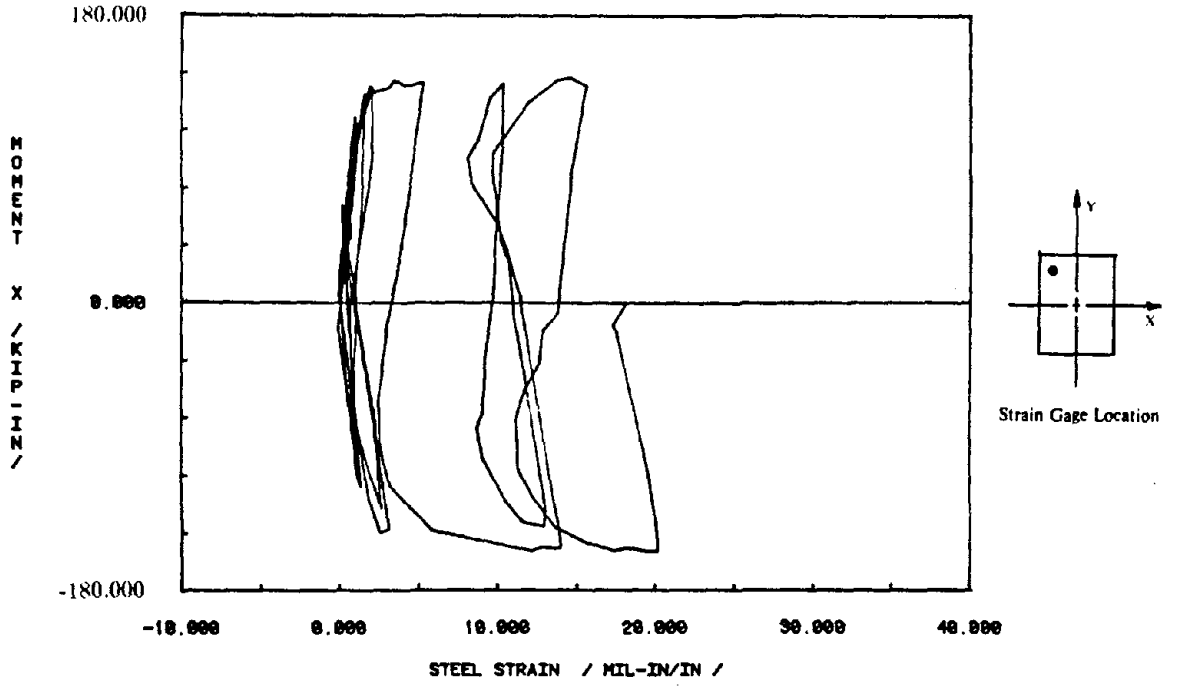

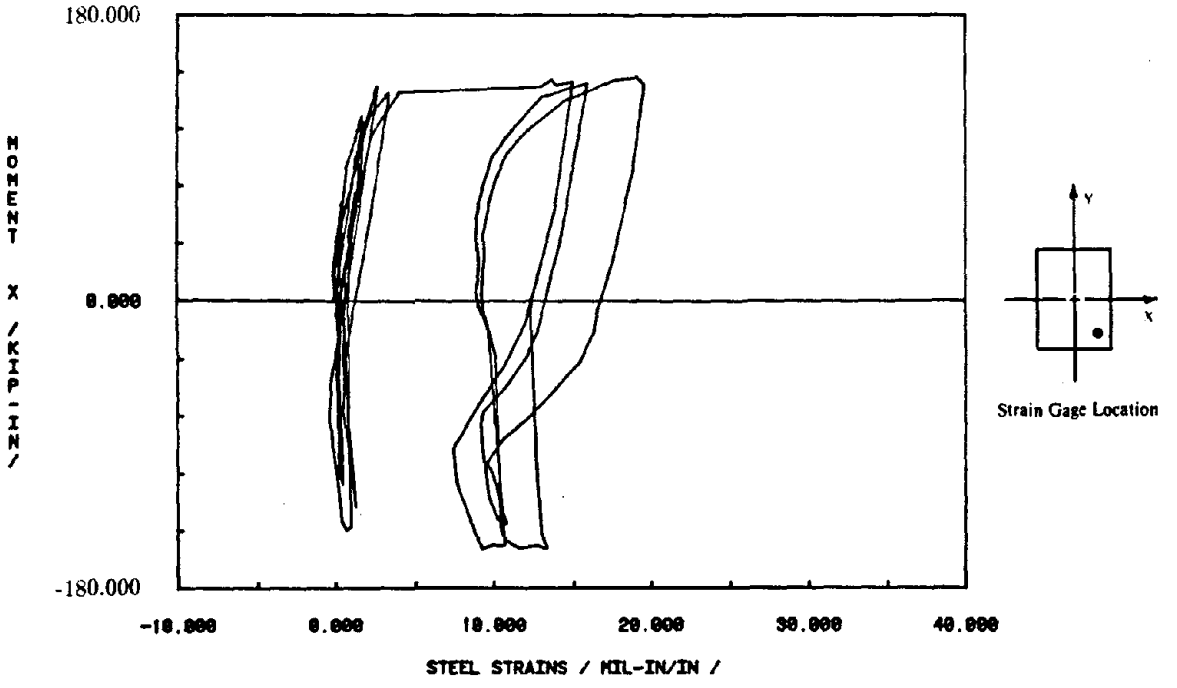

Fig. 3.19 Continue

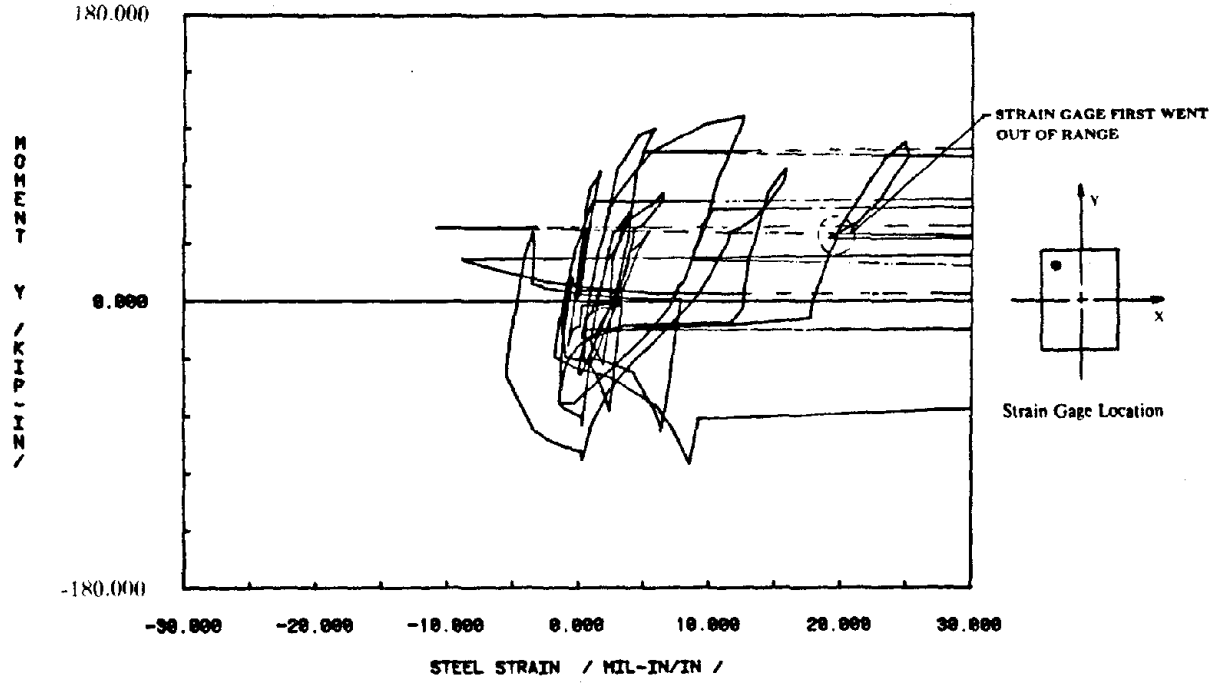

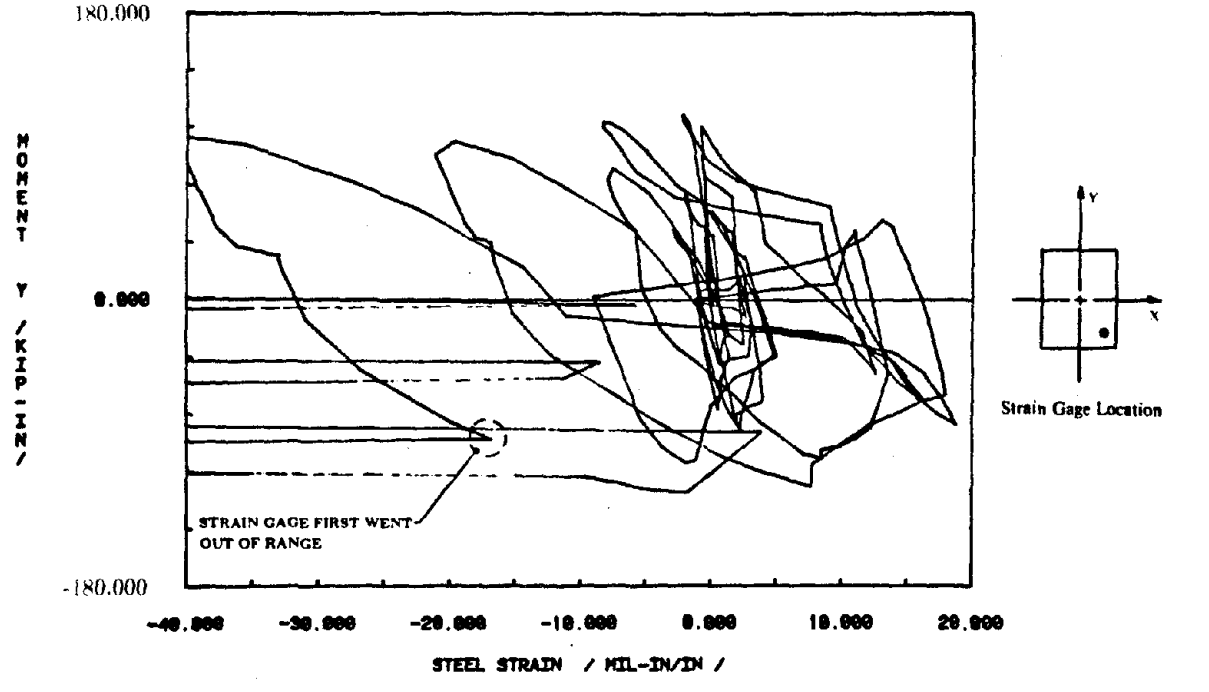

FIG. 3.20 Strain Histories for Specimen 3

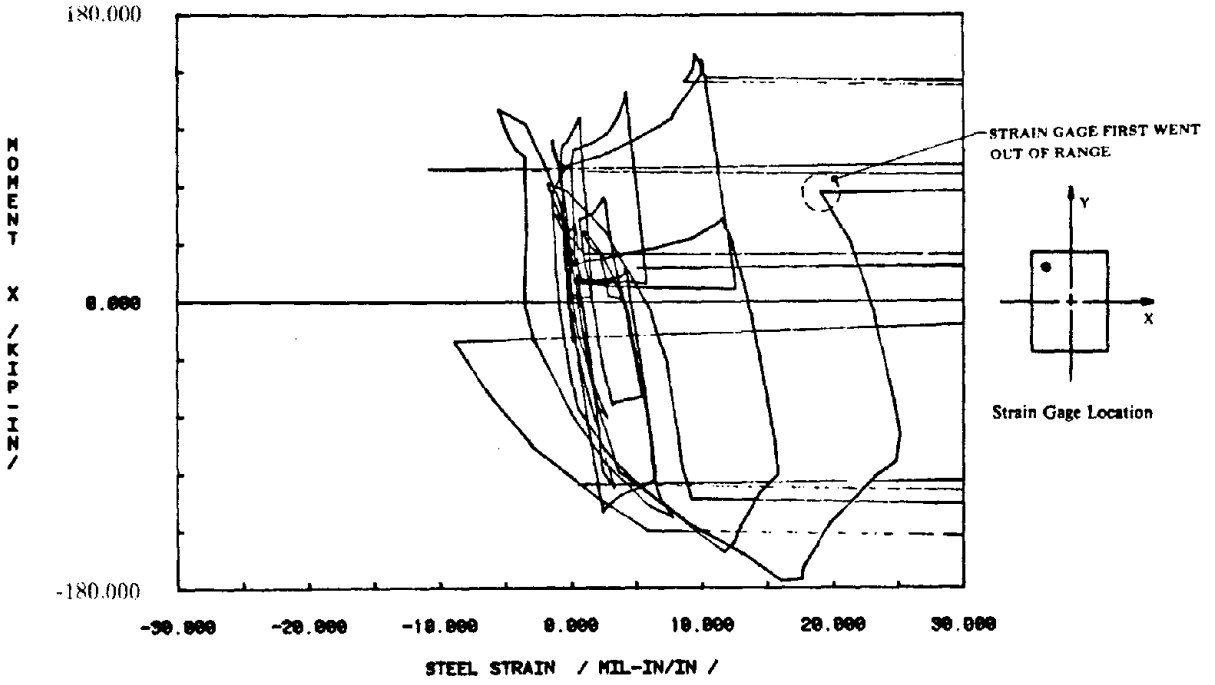

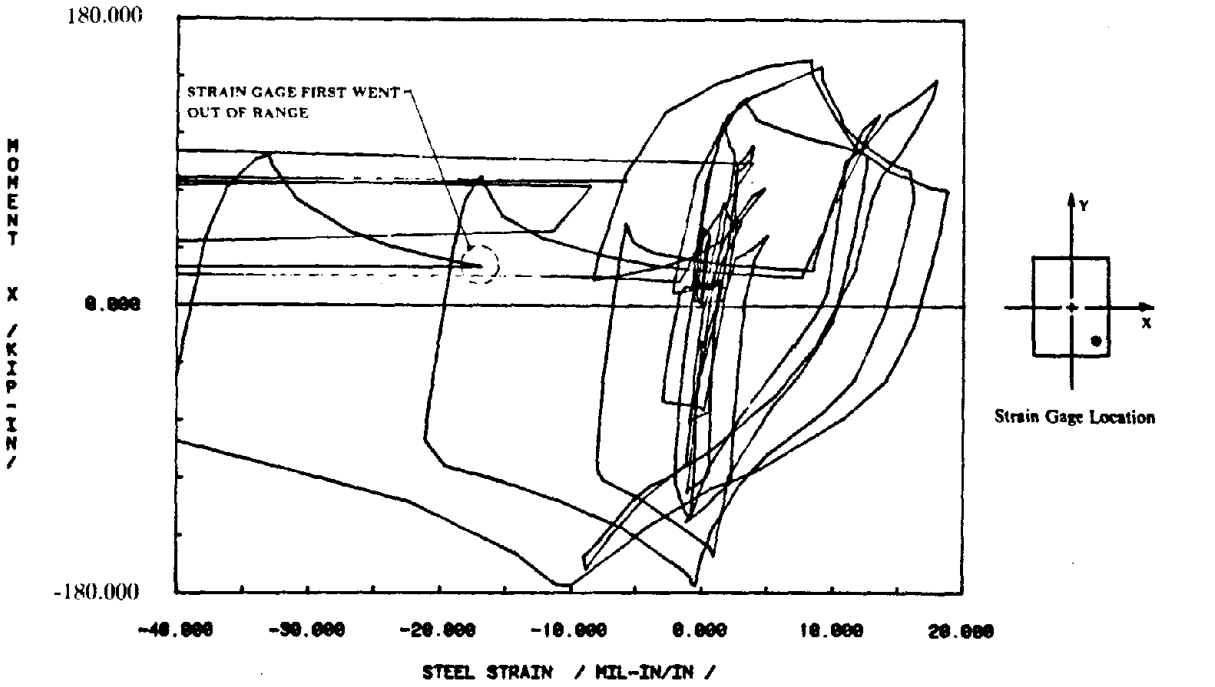

Fig. 3.20 Continue

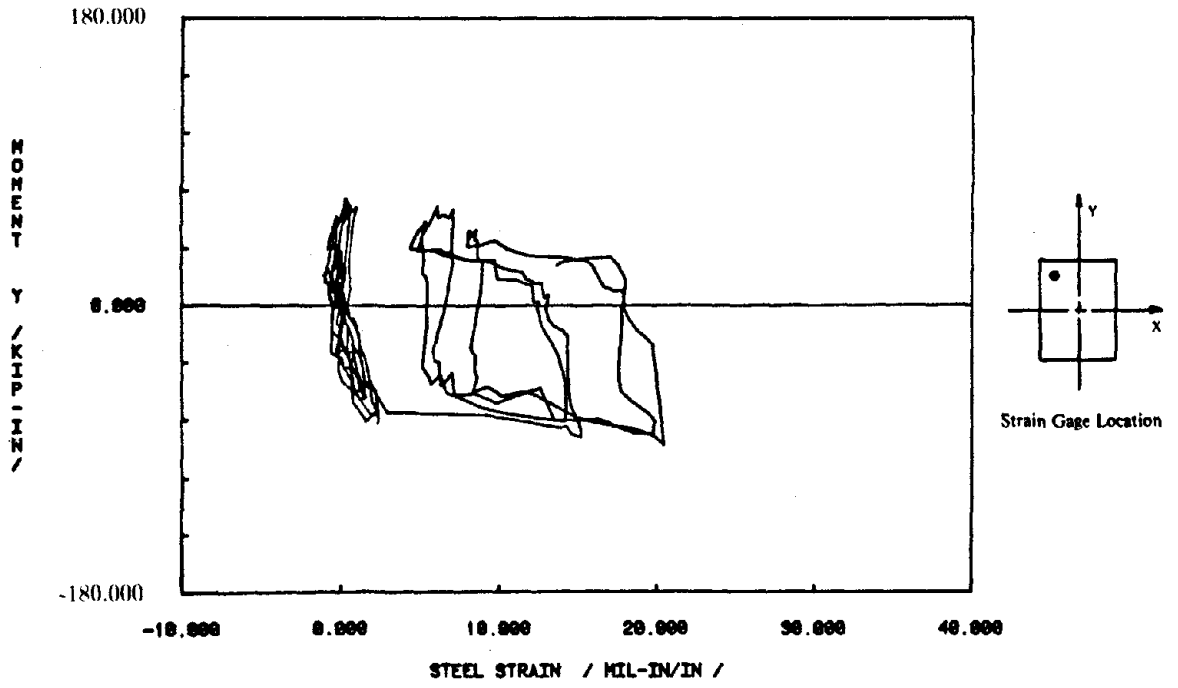

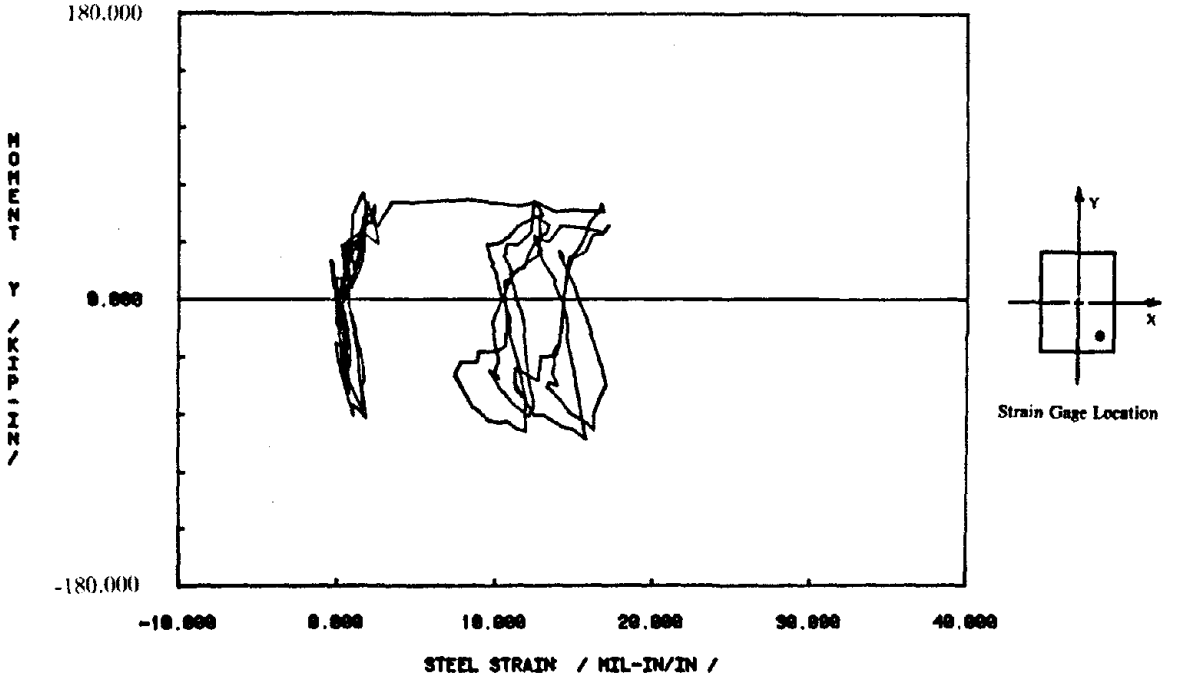

FIG. 3.21 Strain Histories for Specimen 4

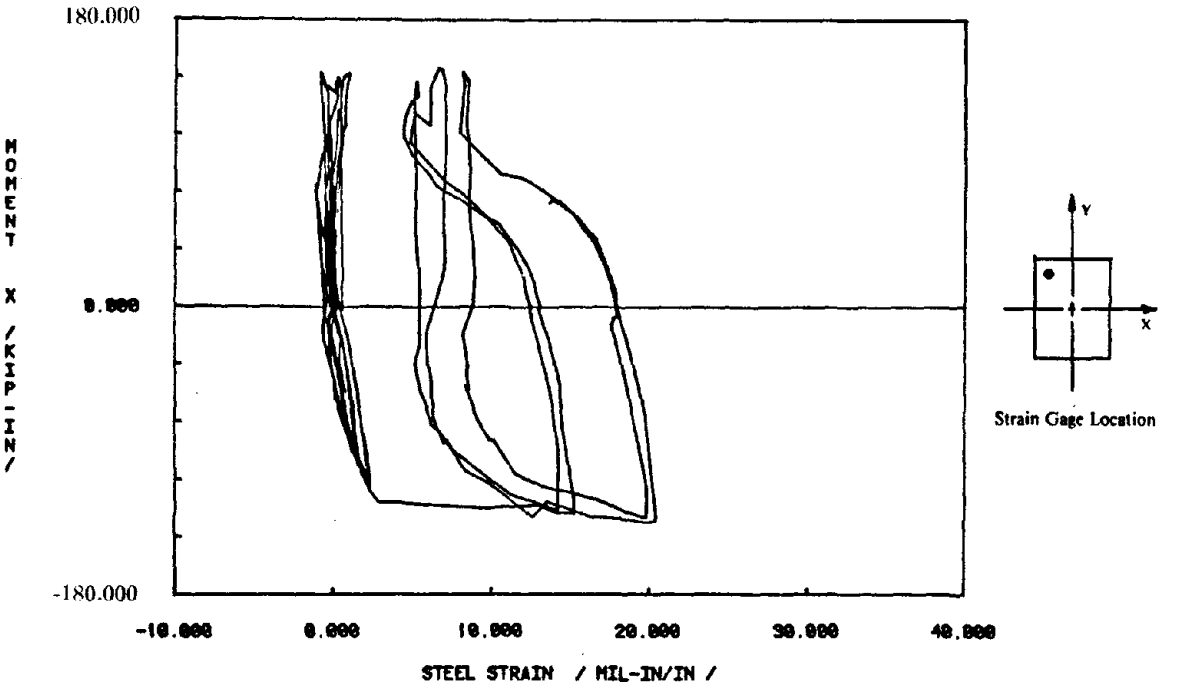

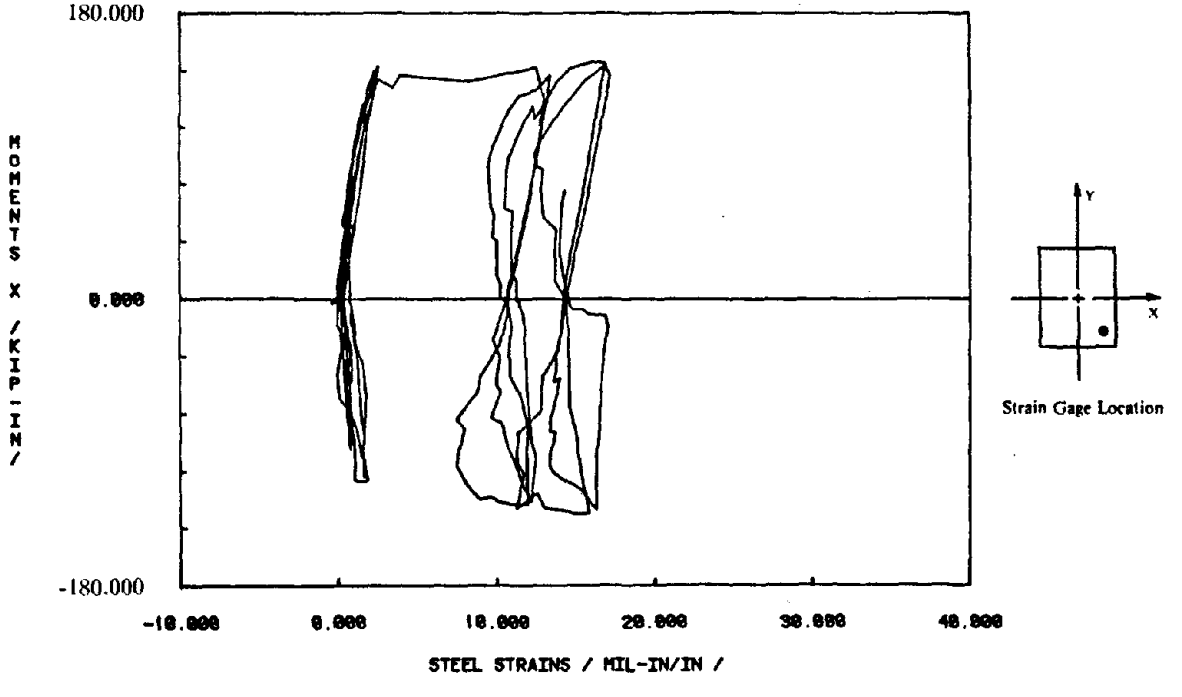

Fig. 3.21 Continue

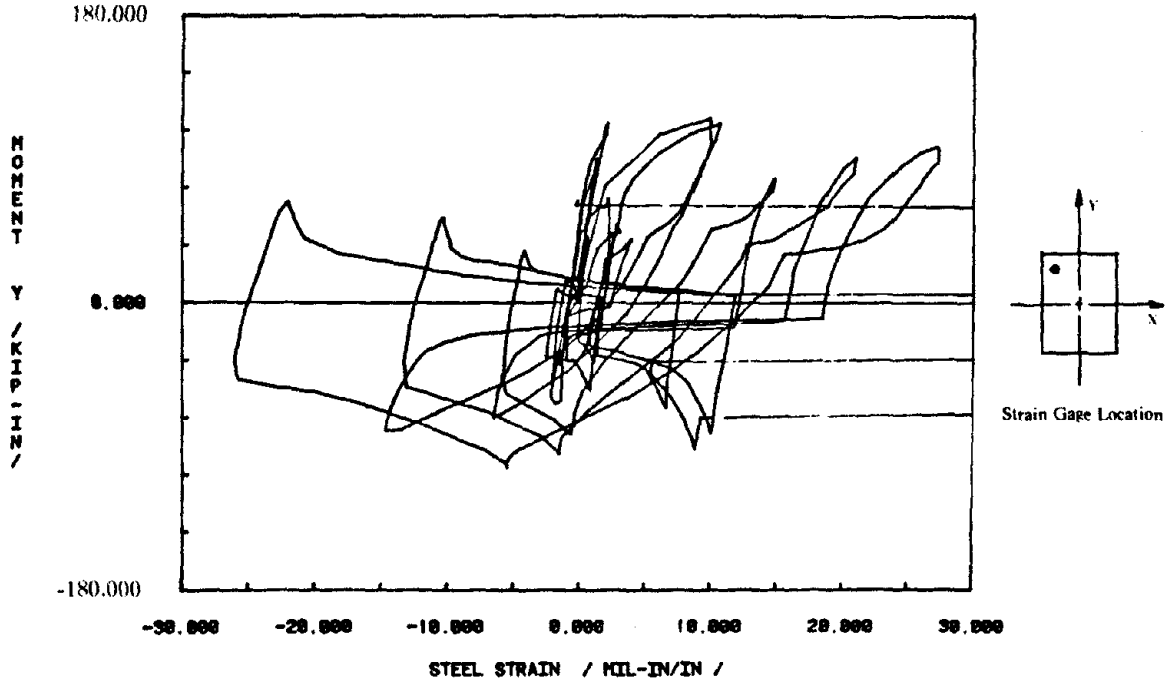

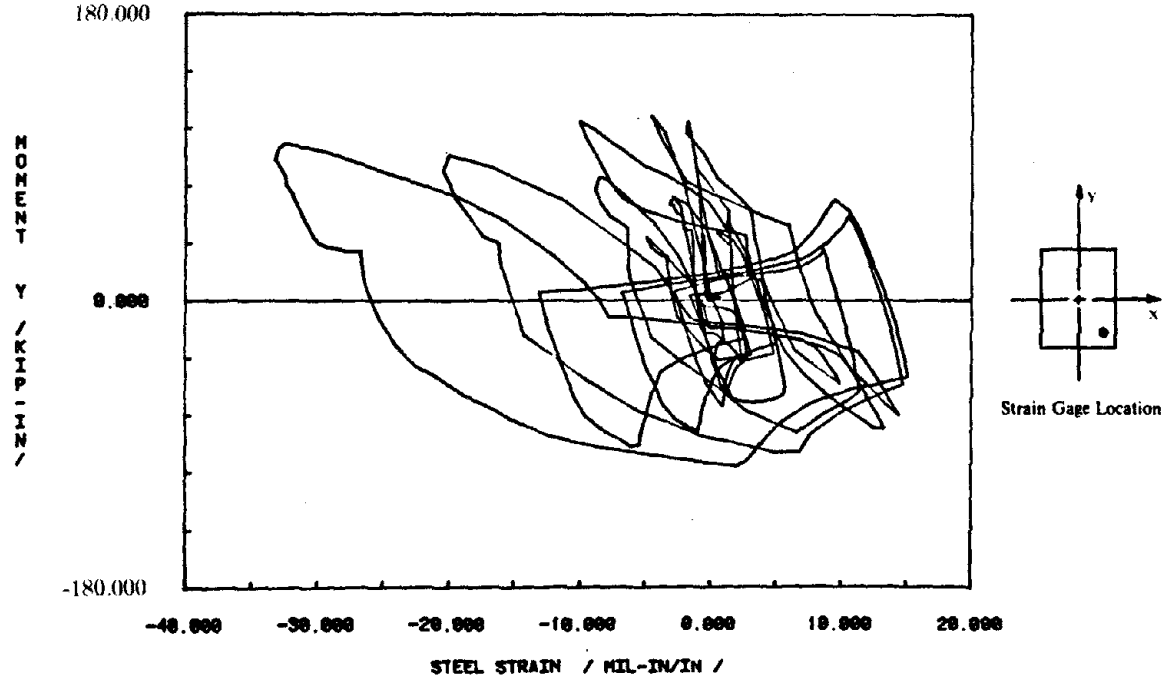

FIG. 3.22 Strain Histories for Specimen 5

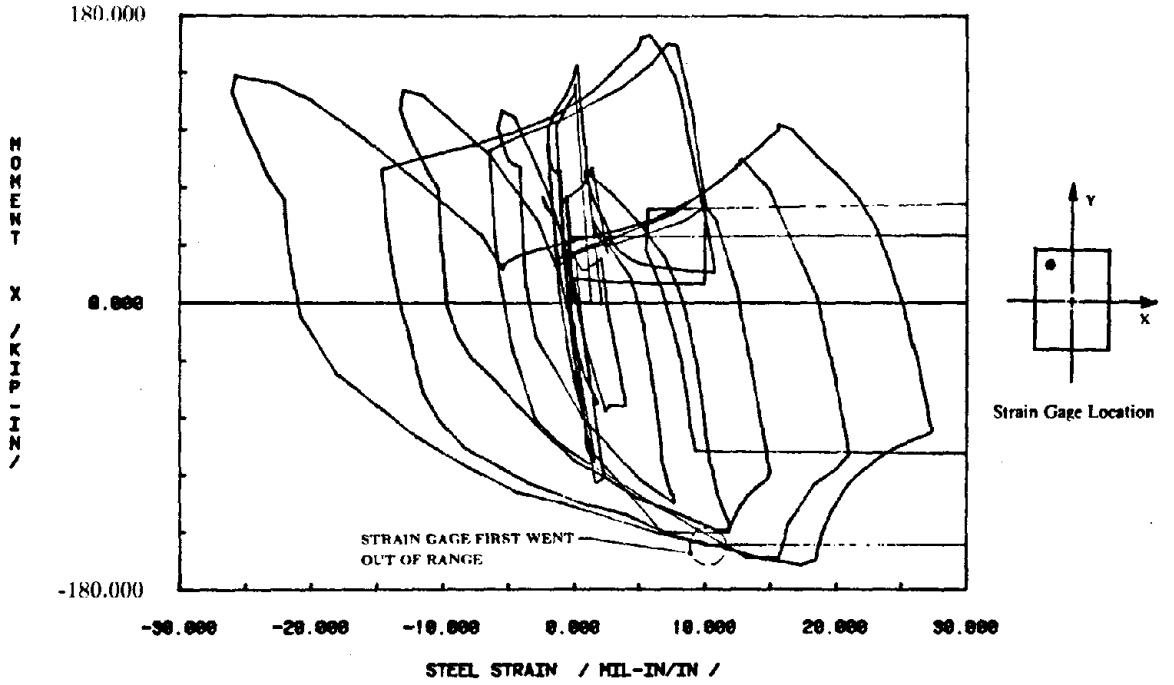

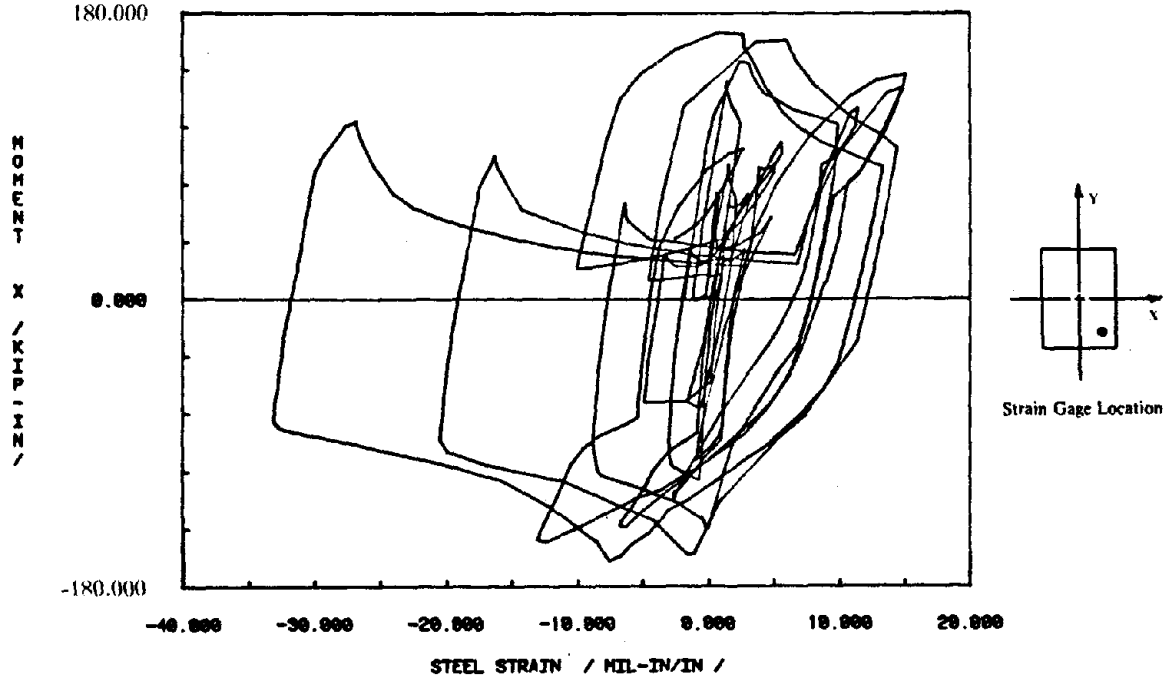

Fig. 3.22 Continue

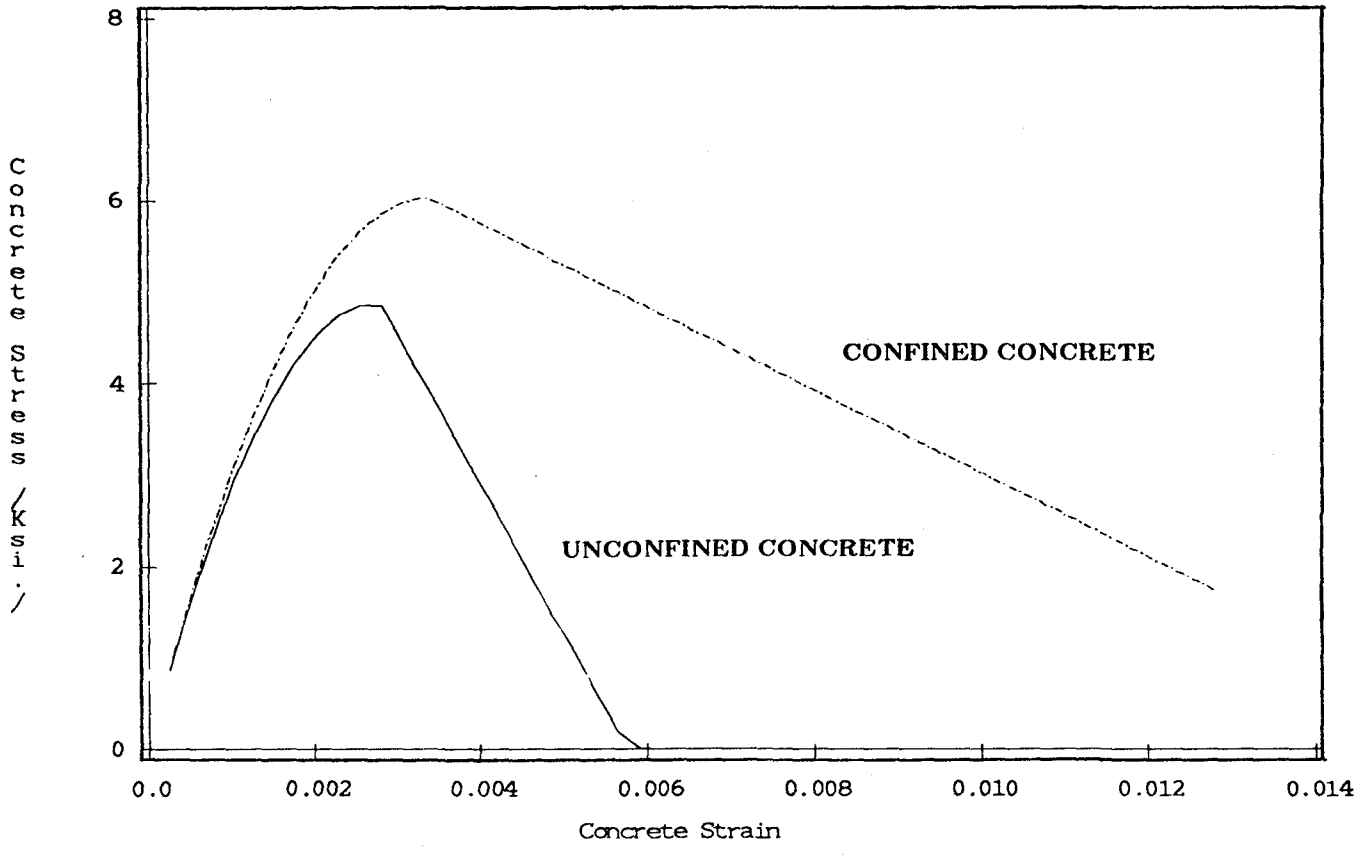

FIG. 4.1 Concrete Stress-Strain Relations Assumed for Moment-Curvature Calculations

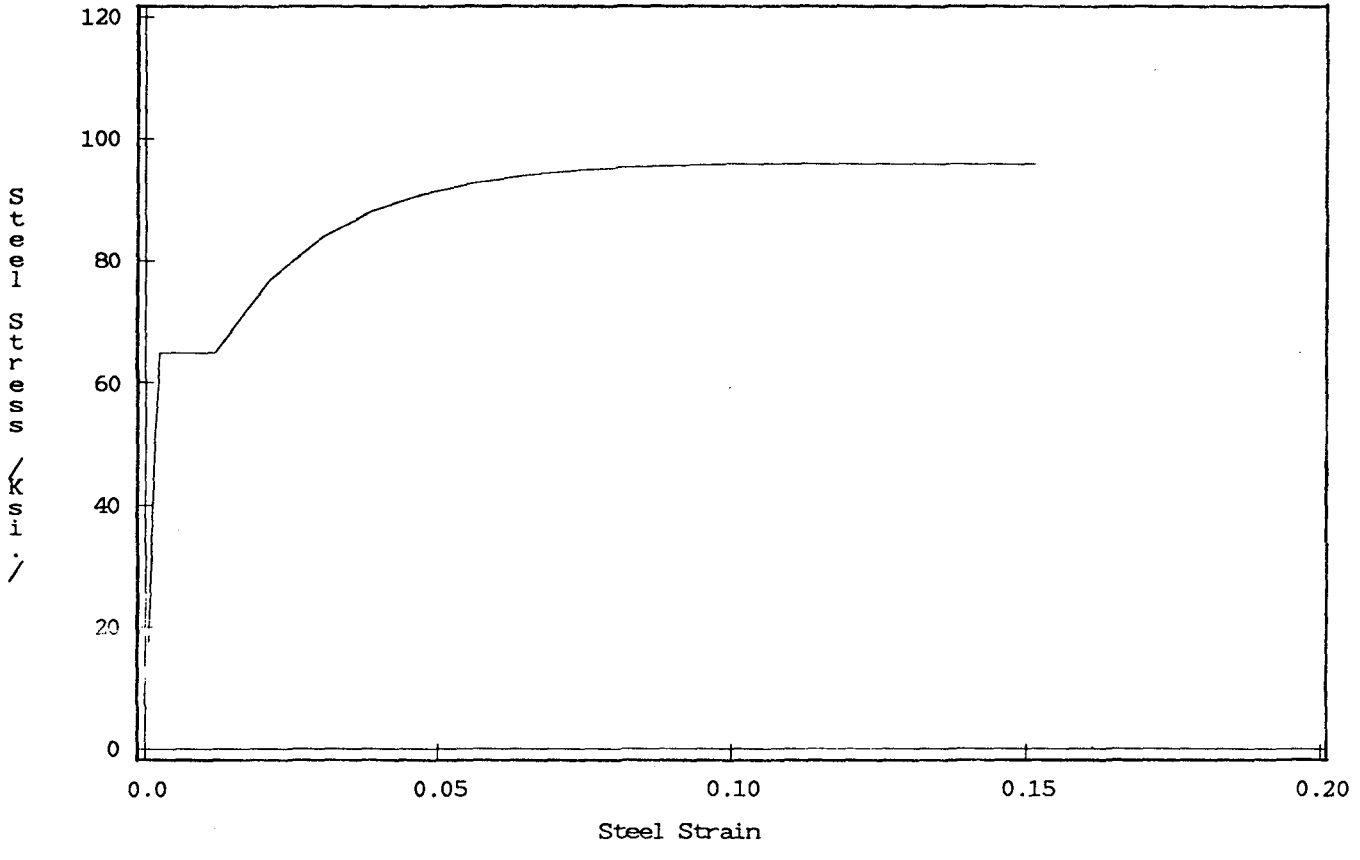

FIG. 4.2 **Steel Stress-Strain Relations Assumed for Moment-Curvature Calculations**

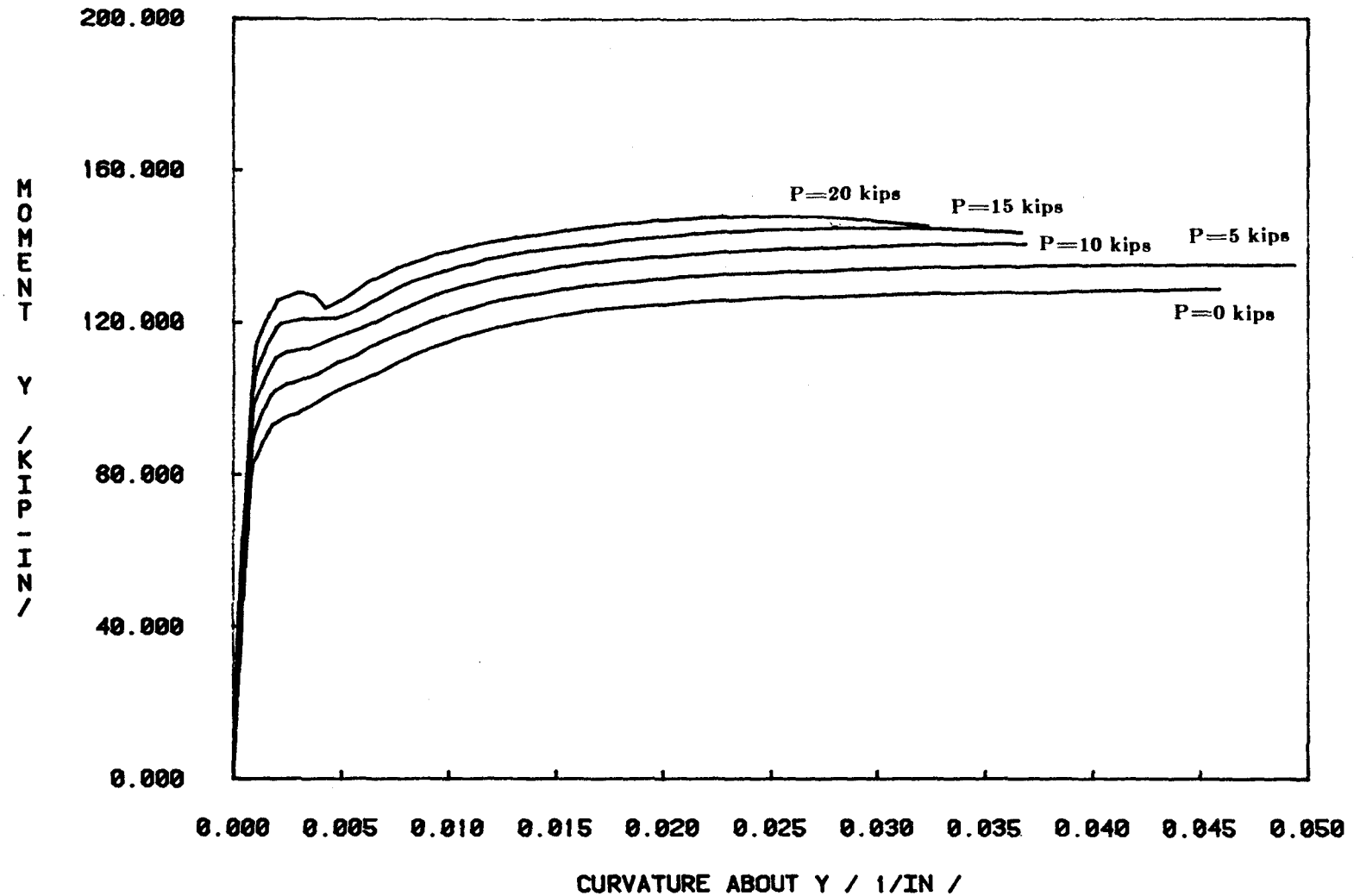

FIG. 4.3 Computed Moment-Curvature Relations

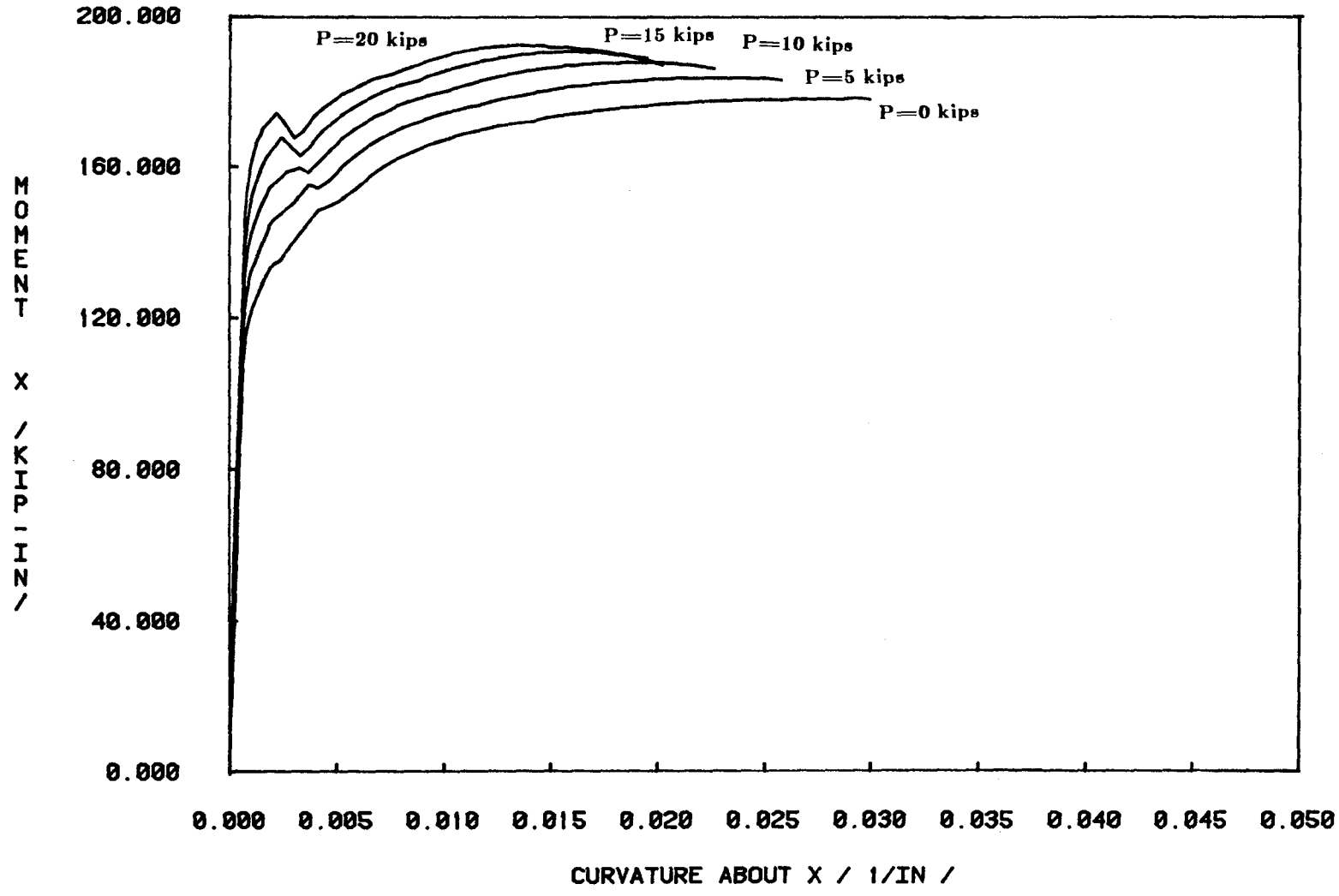

FIG. 4.3 Continued

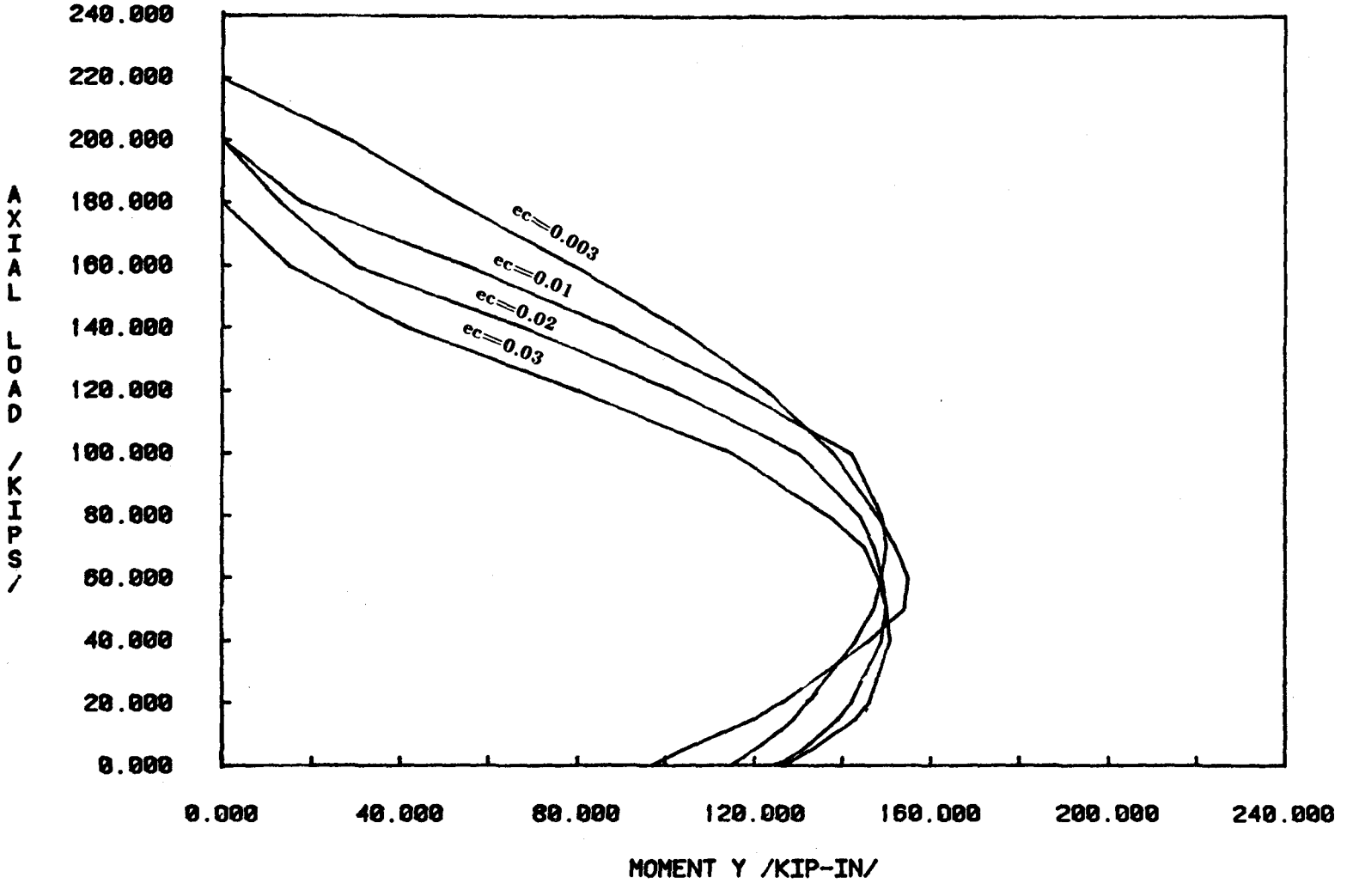

FIG. 4.4 Computed Uniaxial Moment-Axial Load Interaction Diagrams

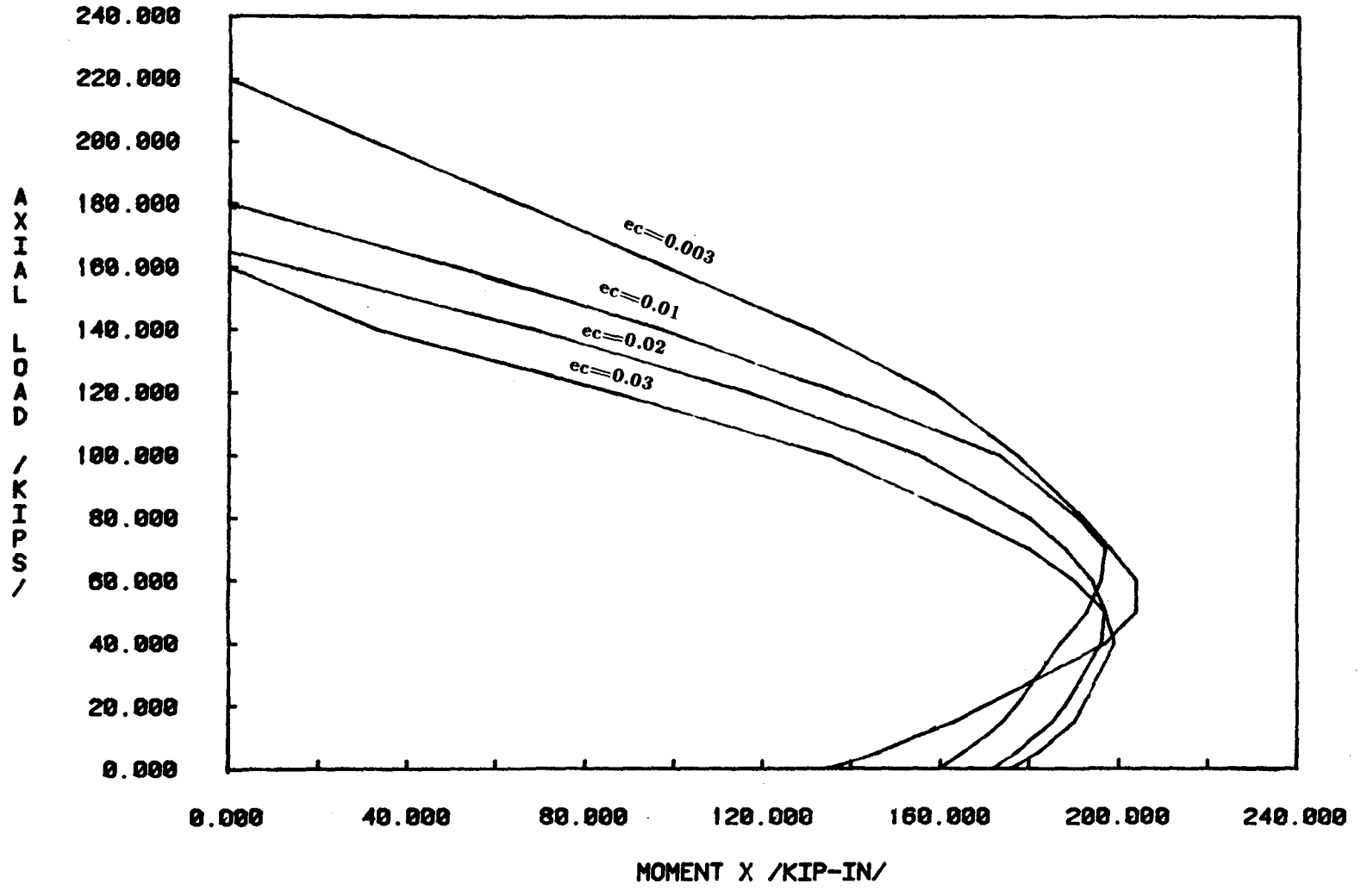

FIG. 4.4 Continued

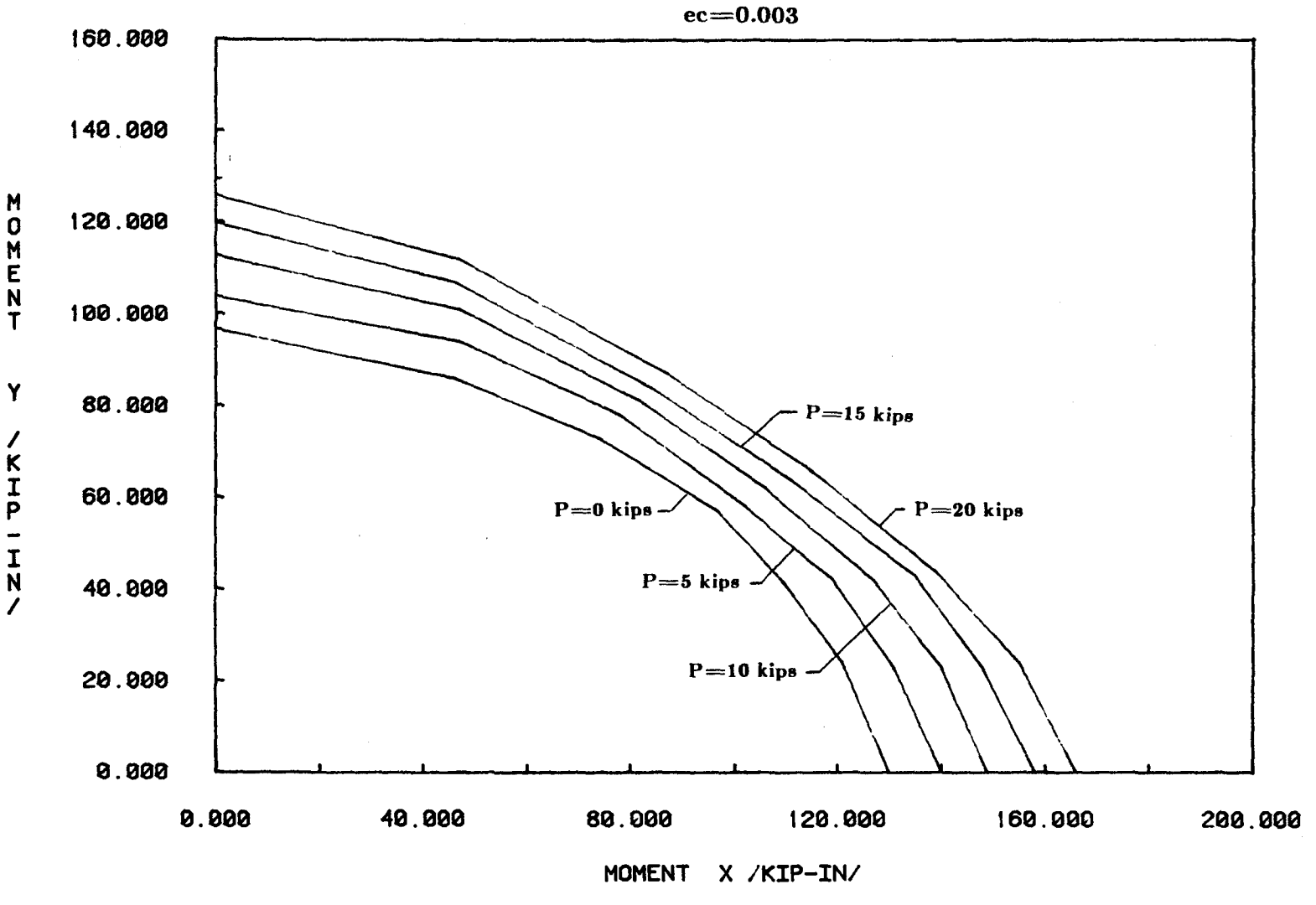

FIG. 4.5 Computed Biaxial Moment-Axial Load Interaction Diagrams

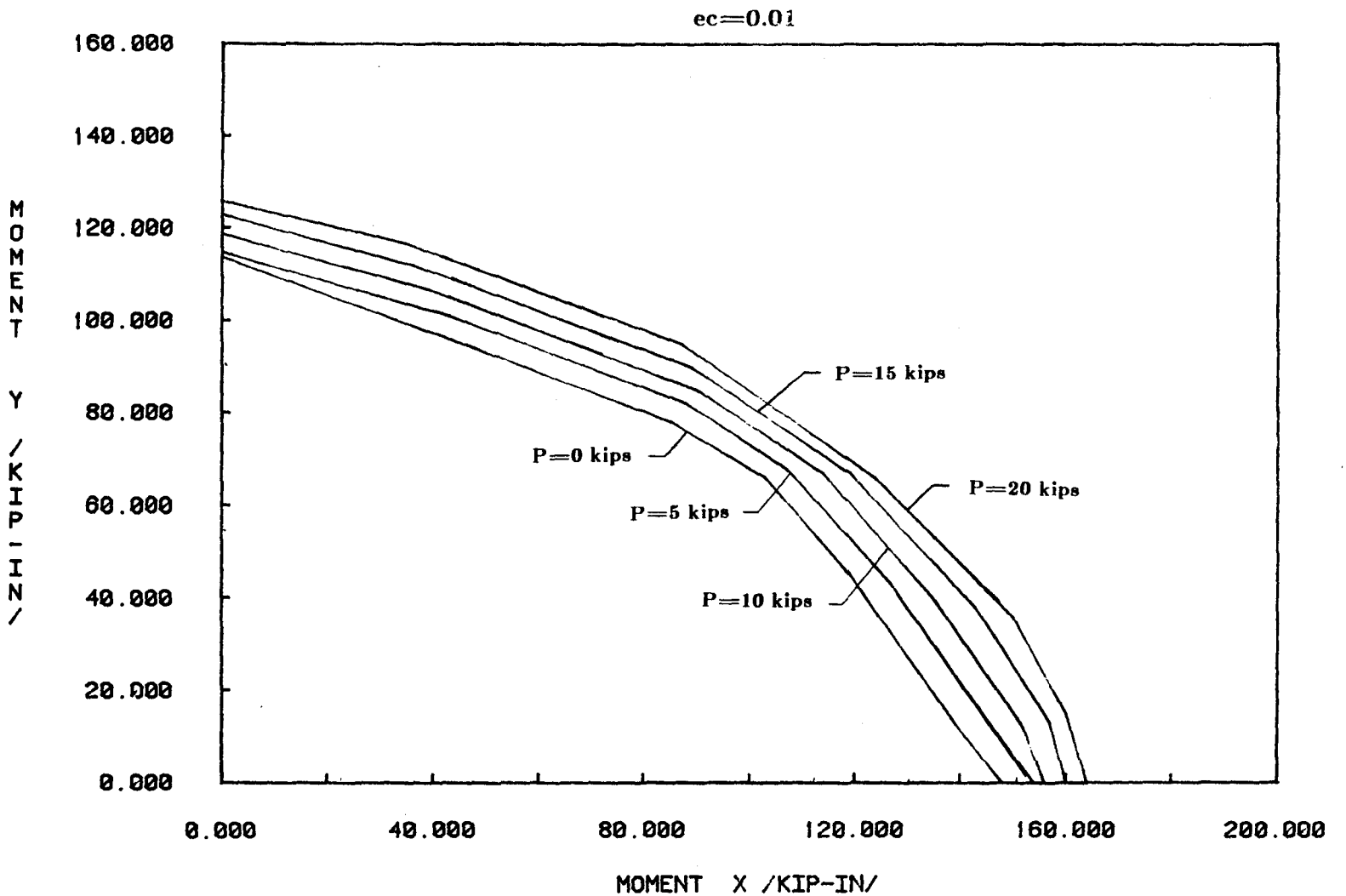

FIG. 4.5 Continued

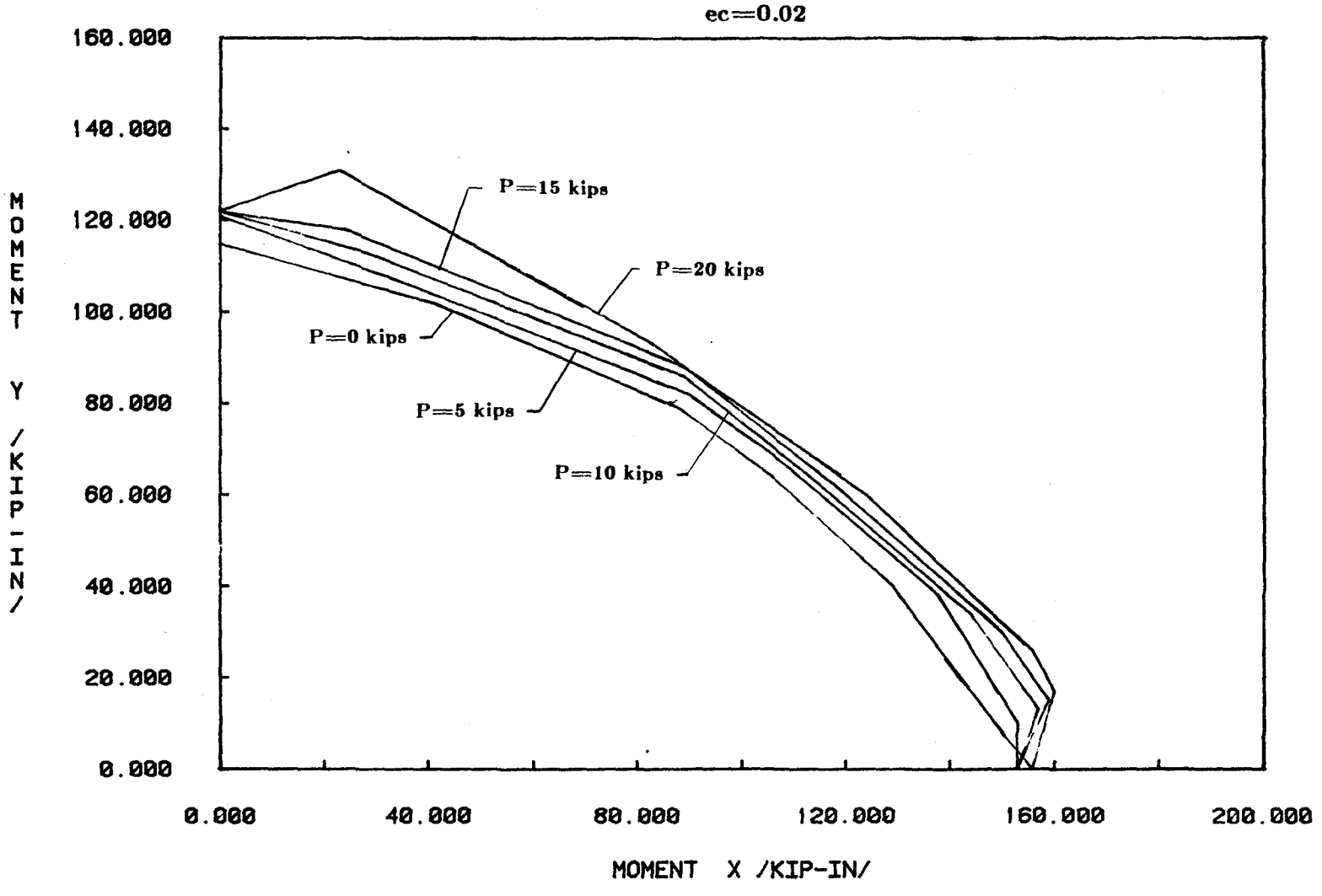

FIG. 4.5 Continued

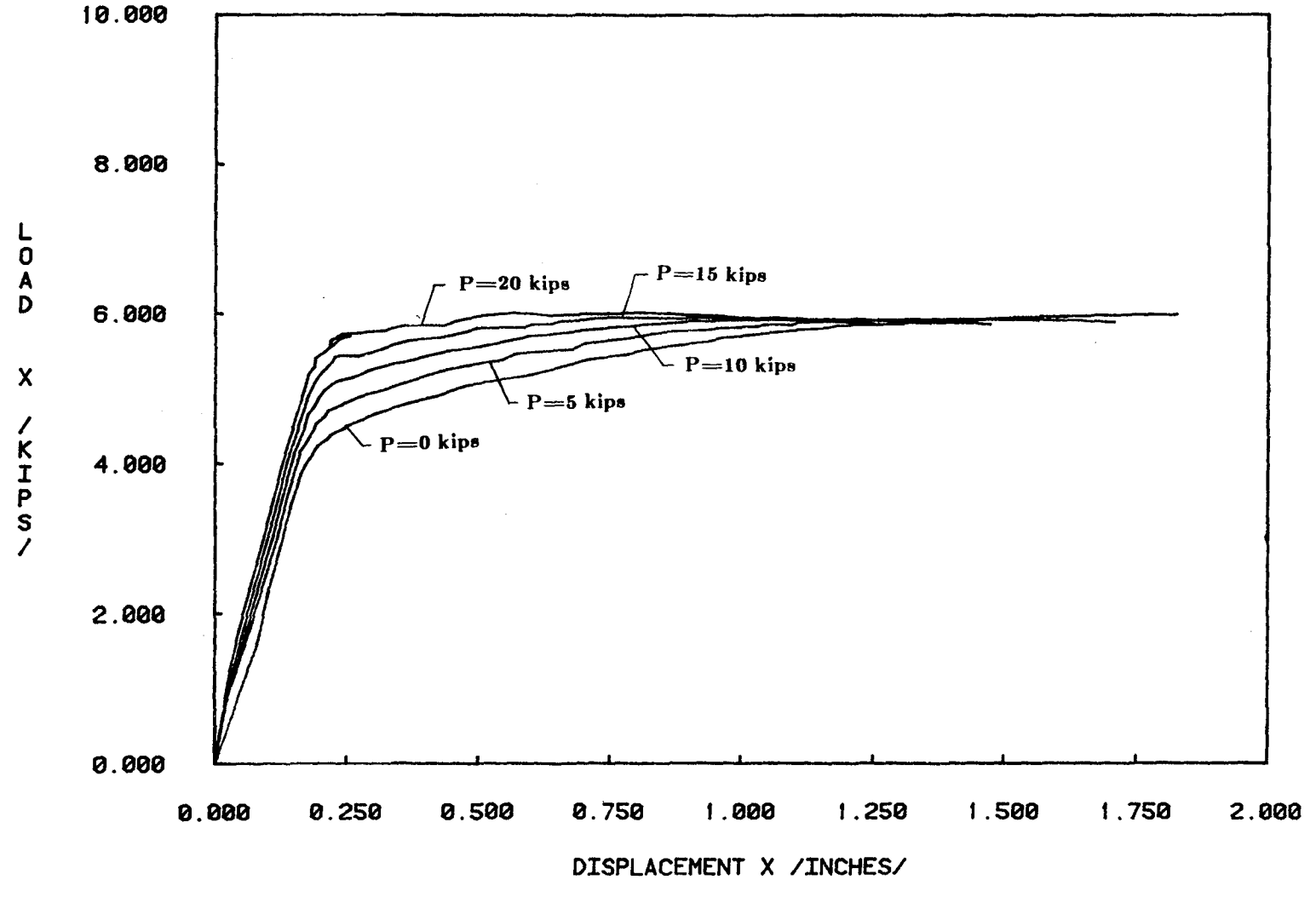

FIG. 4.6 Computed Monotonic Load-Displacement Relations

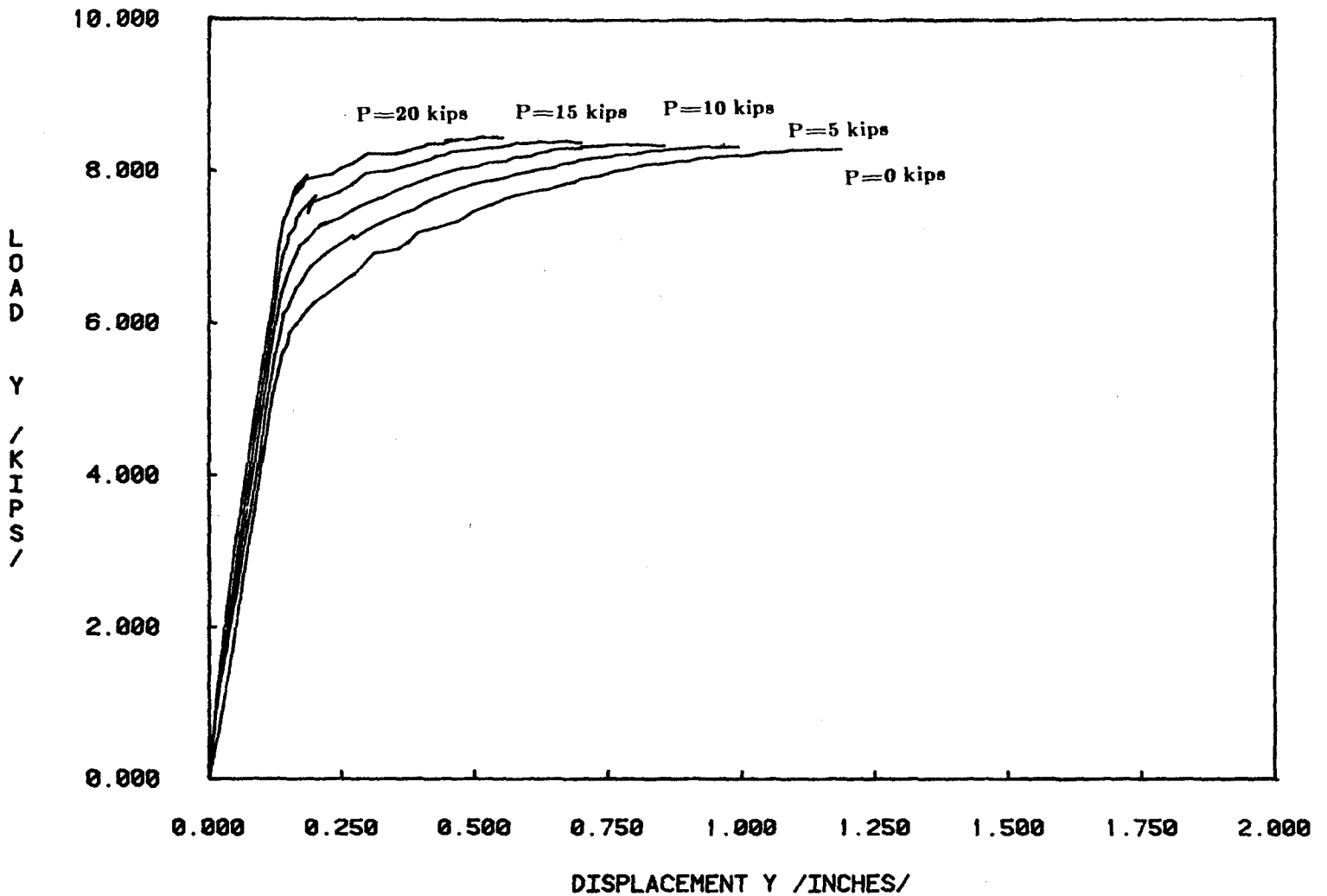

FIG. 4.6 Continued

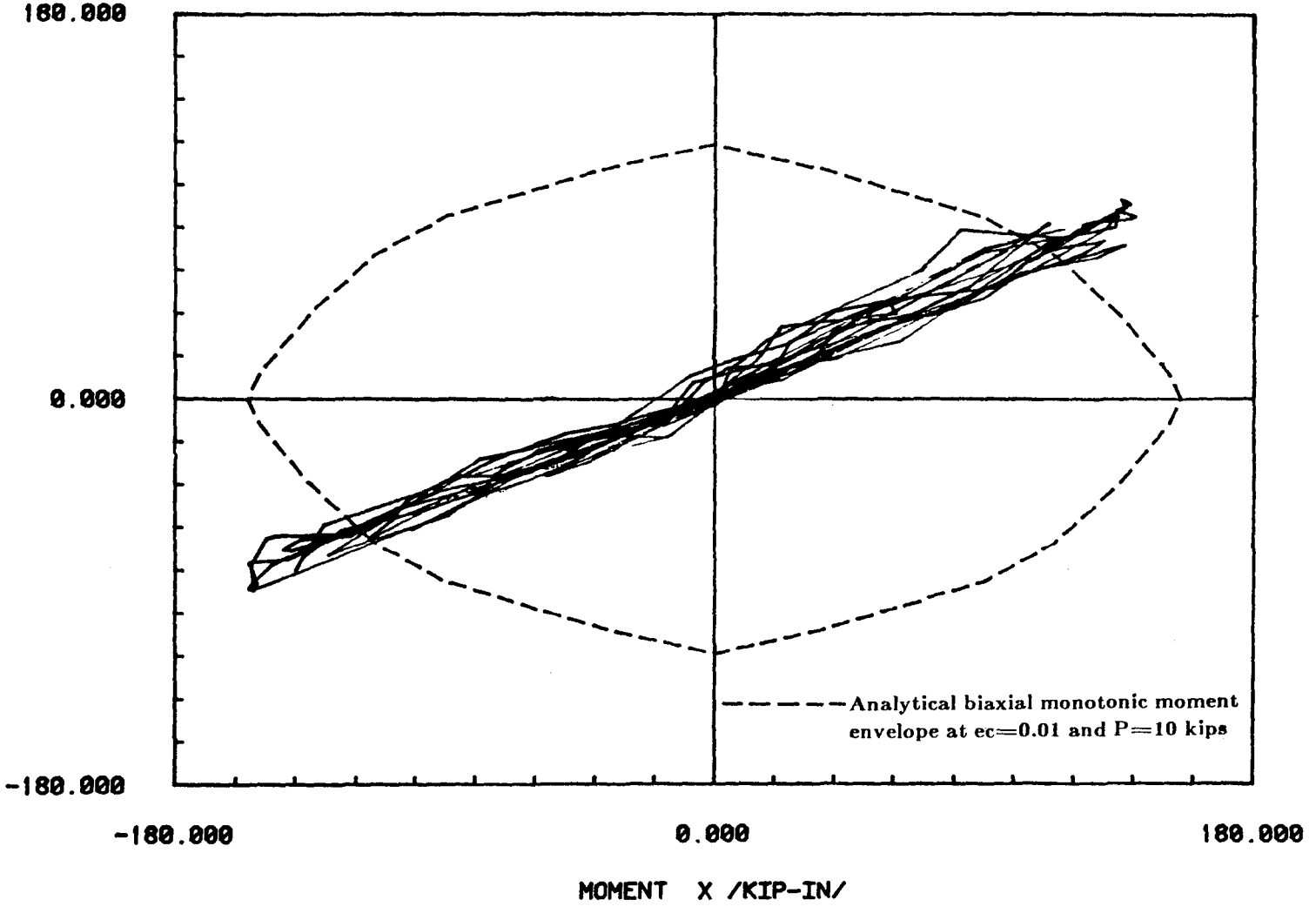

FIG. 4.7 Comparison Between Measured and Computed Base-Moment Strengths - Specimen 2

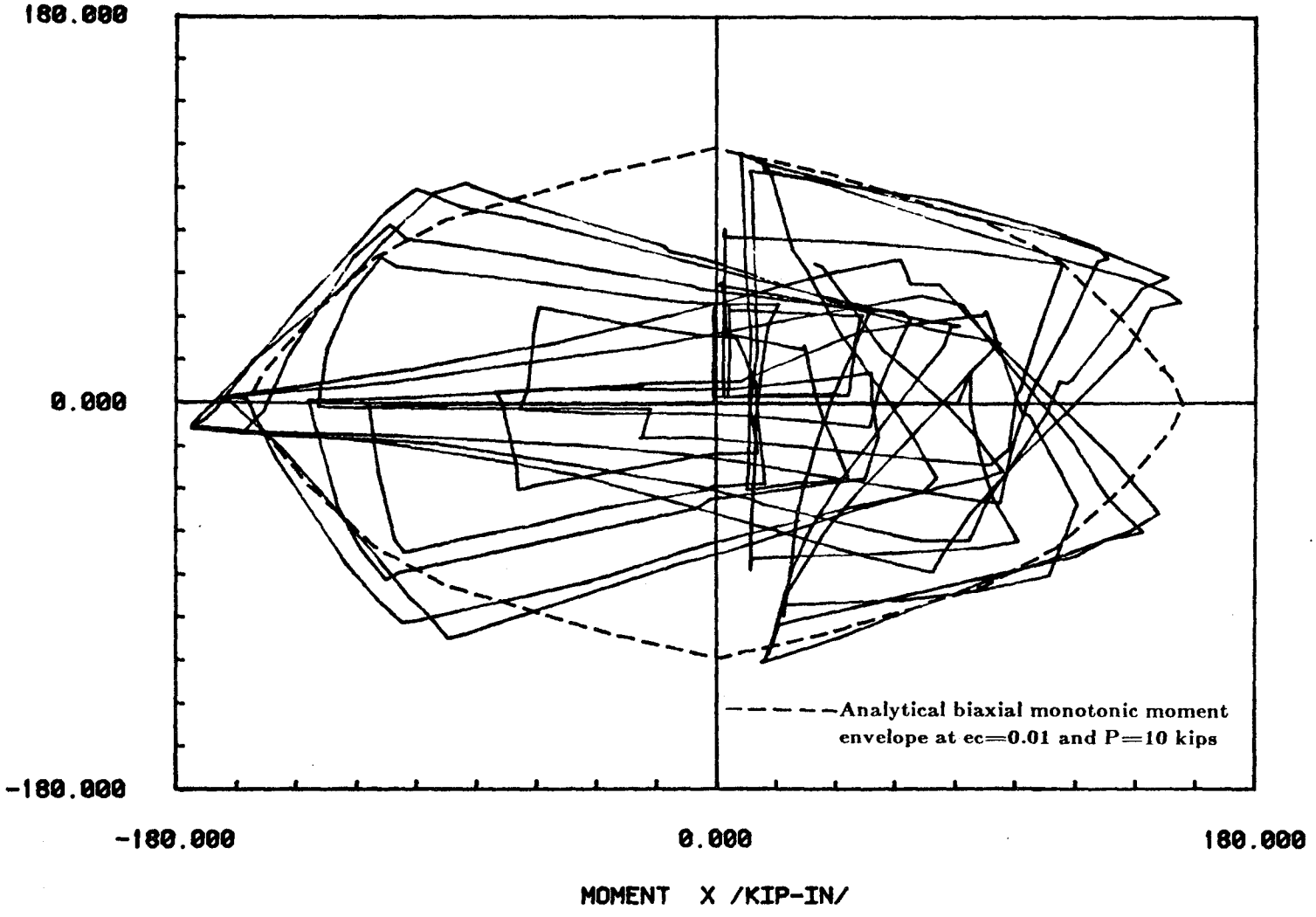

FIG. 4.7a Comparison Between Measured and Computed Base-Moment Strengths - Specimen 3

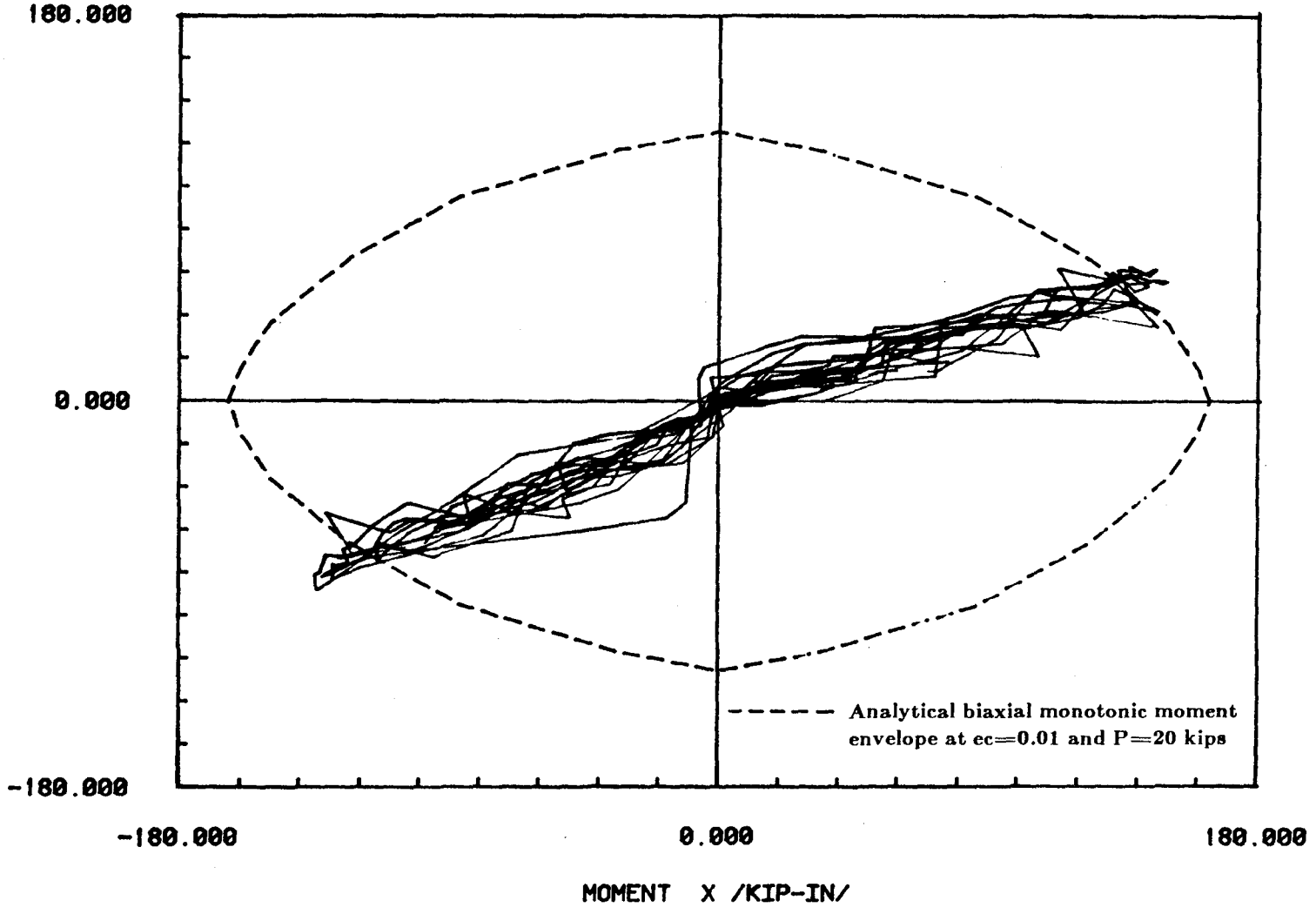

FIG. 4.7b Comparison Between Measured and Computed Base-Moment Strengths - Specimen 4

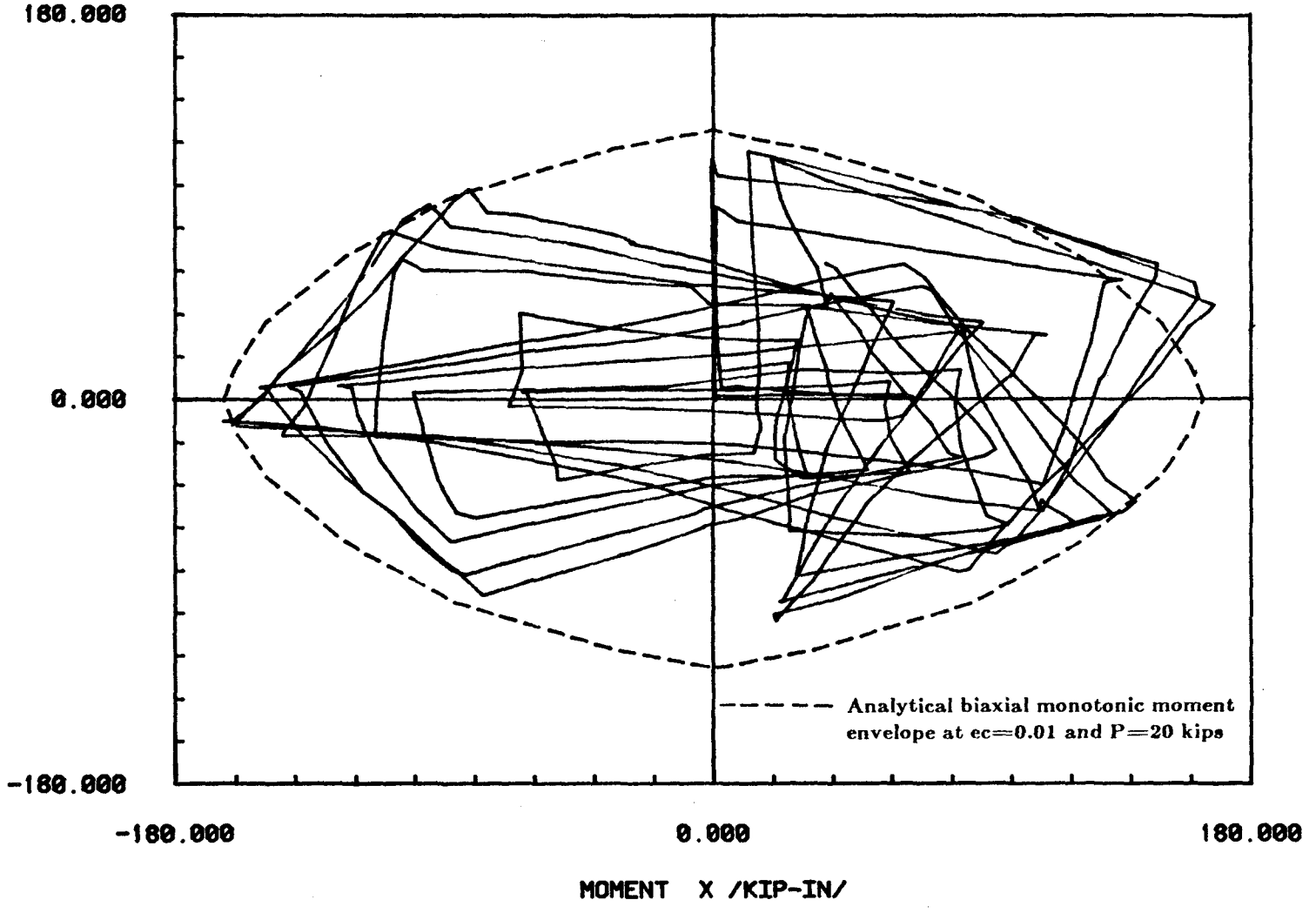

FIG. 4.7c Comparison Between Measured and Computed Base-Moment Strengths - Specimen 5

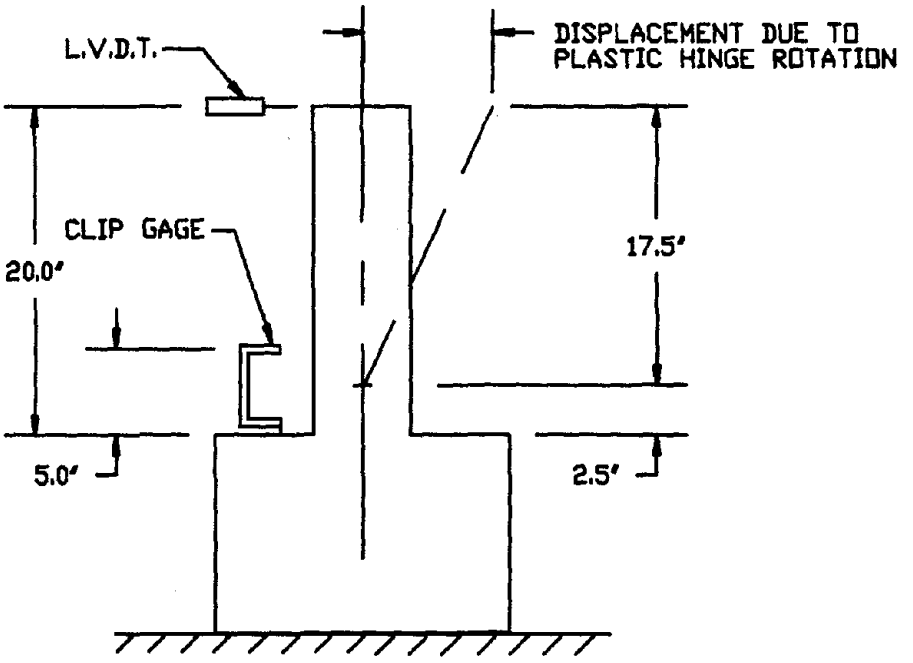

SPECIMEN	DIRECTION	MAXIMUM ROTATION (rad.)	DISPLACEMENT DUE TO MAX. ROTATION (in.)	MAXIMUM DISPLACEMENT L.V.D.T. (in.)
1	WEAK	0.060	1.02	1.12
2	WEAK	0.053	0.93	1.01
	STRONG	0.046	0.81	0.99
3	WEAK	0.051	0.90	1.01
	STRONG	0.051	0.90	1.01
4	WEAK	0.049	0.86	0.99
	STRONG	0.049	0.86	0.99
5	WEAK	0.049	0.86	1.01
	STRONG	0.049	0.86	1.01

FIG. 4.8 Contribution of Base Rotation to Total Column Deflection

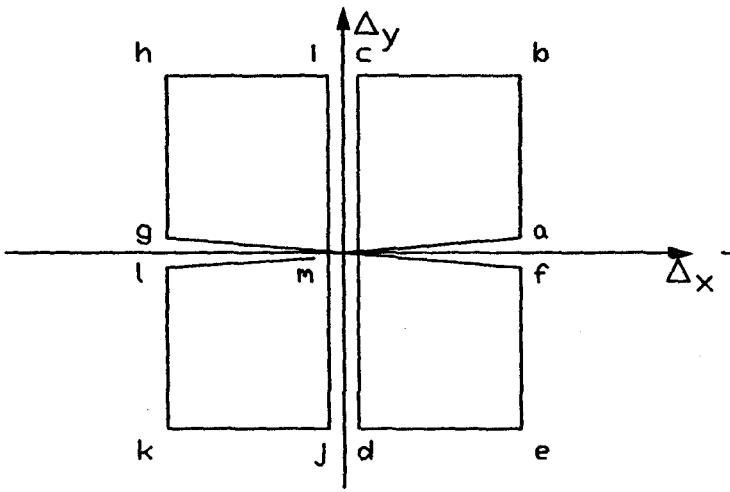

a.) Load History - One Cycle

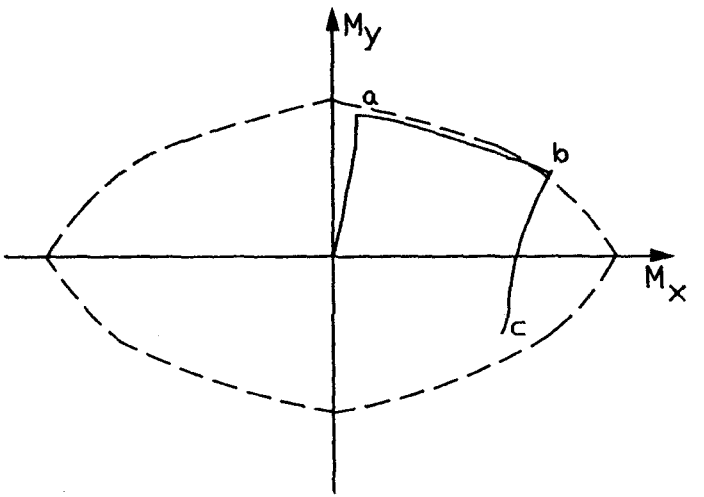

b.) Moment Versus Moment

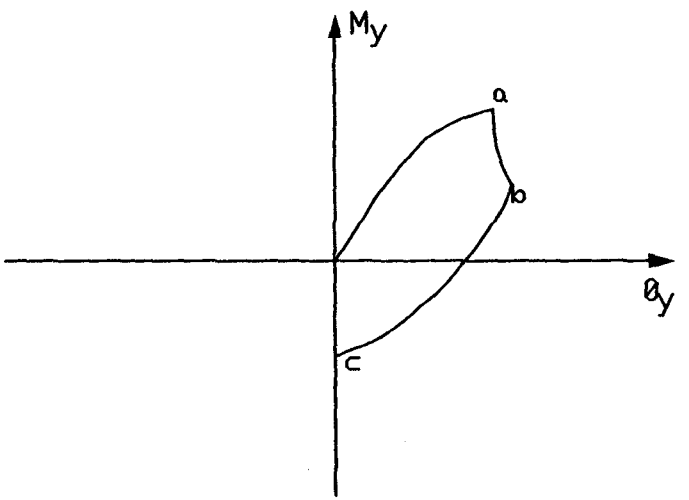

c.) Load-Deformation in "X" Direction

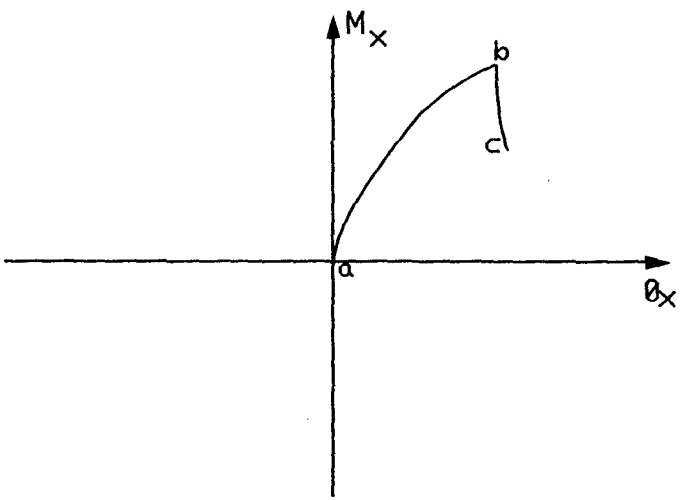

d.) Load-Deformation in "Y" Direction

FIG. 4.9 Idealized Biaxial Hysteresis Relations for Load Steps "a" through "c"

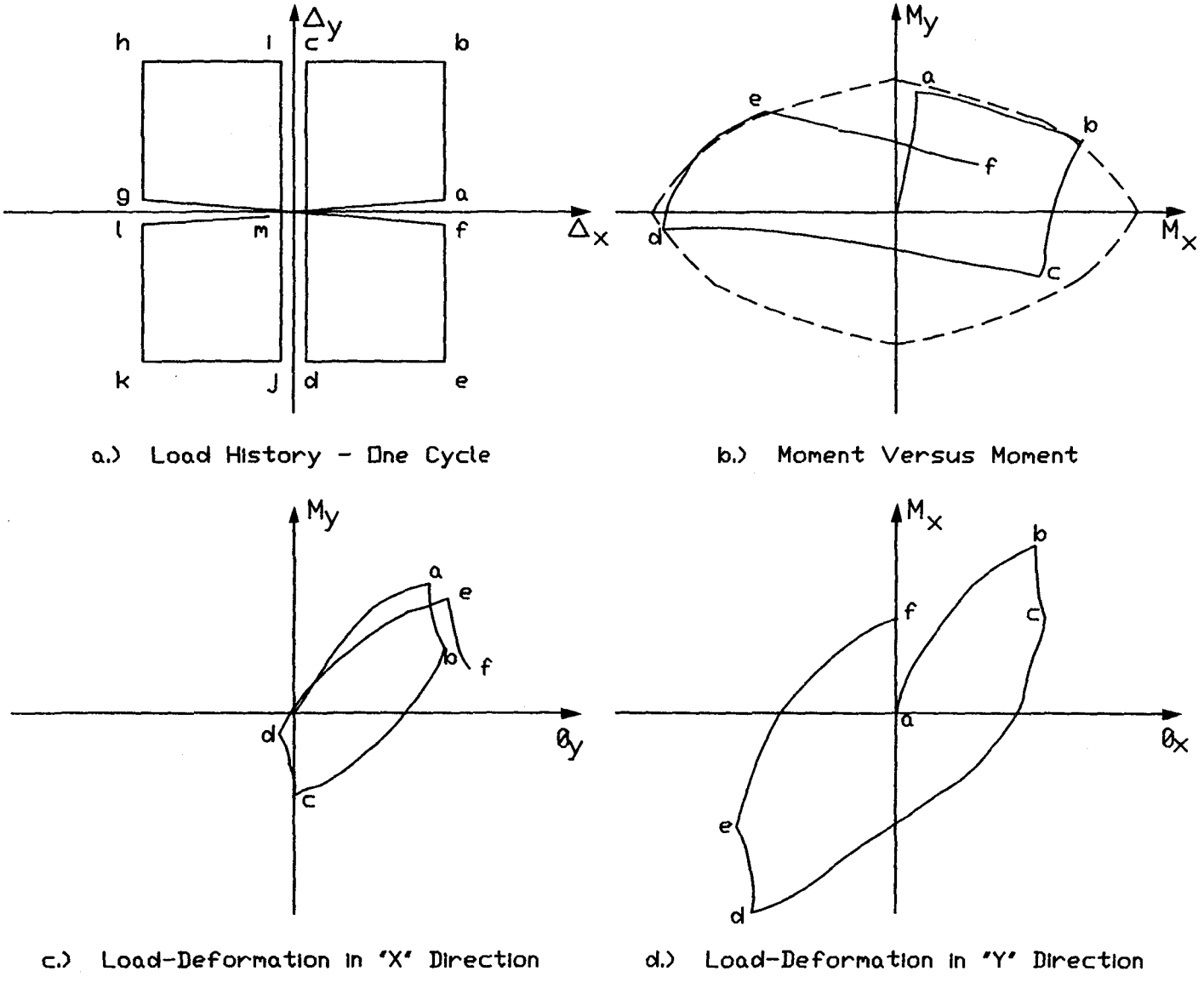

FIG. 4.10 Idealized Biaxial Hysteresis Relations for Load Steps "a" through "f"

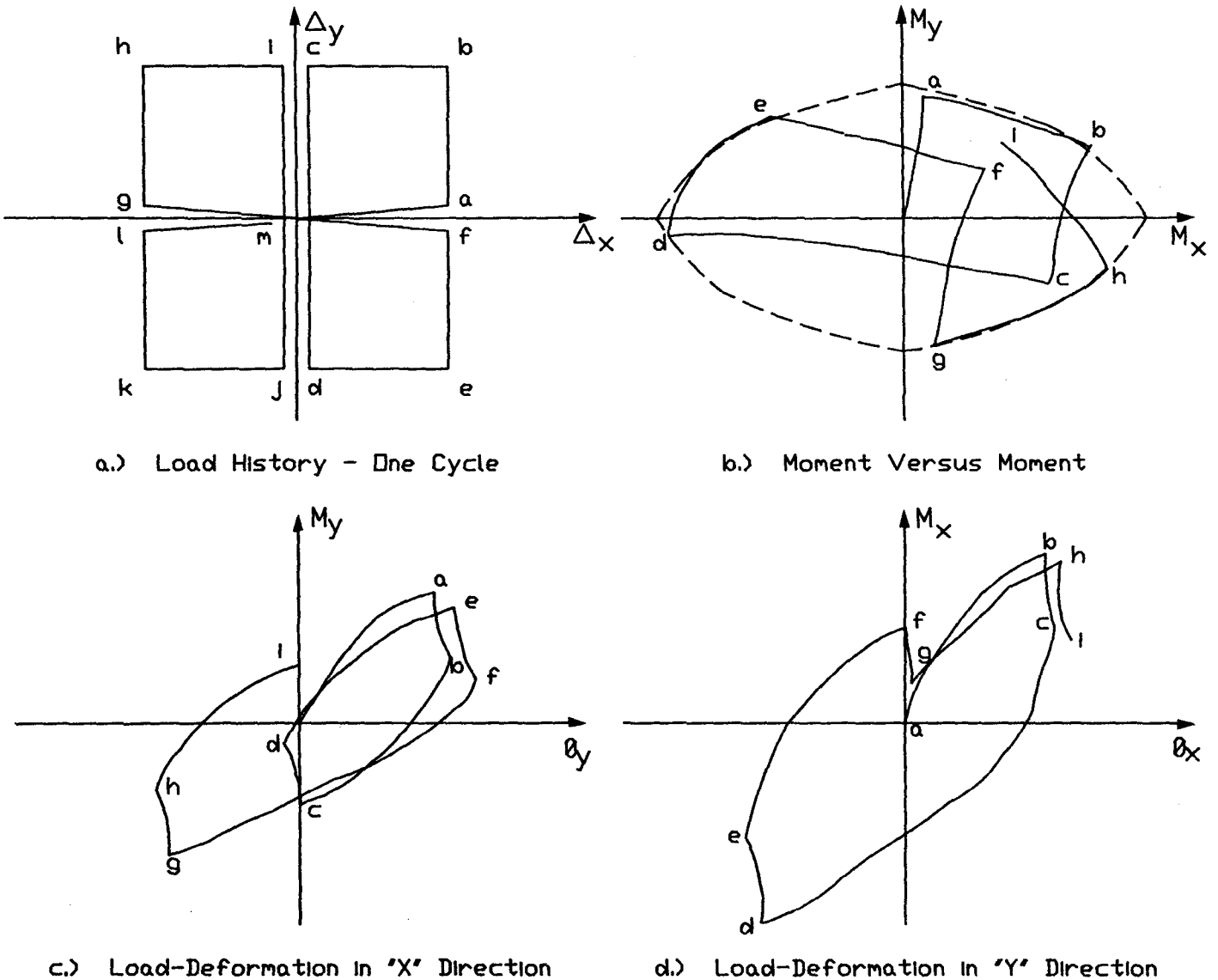

FIG. 4.11 Idealized Biaxial Hysteresis Relations for Load Steps "a" through "i"

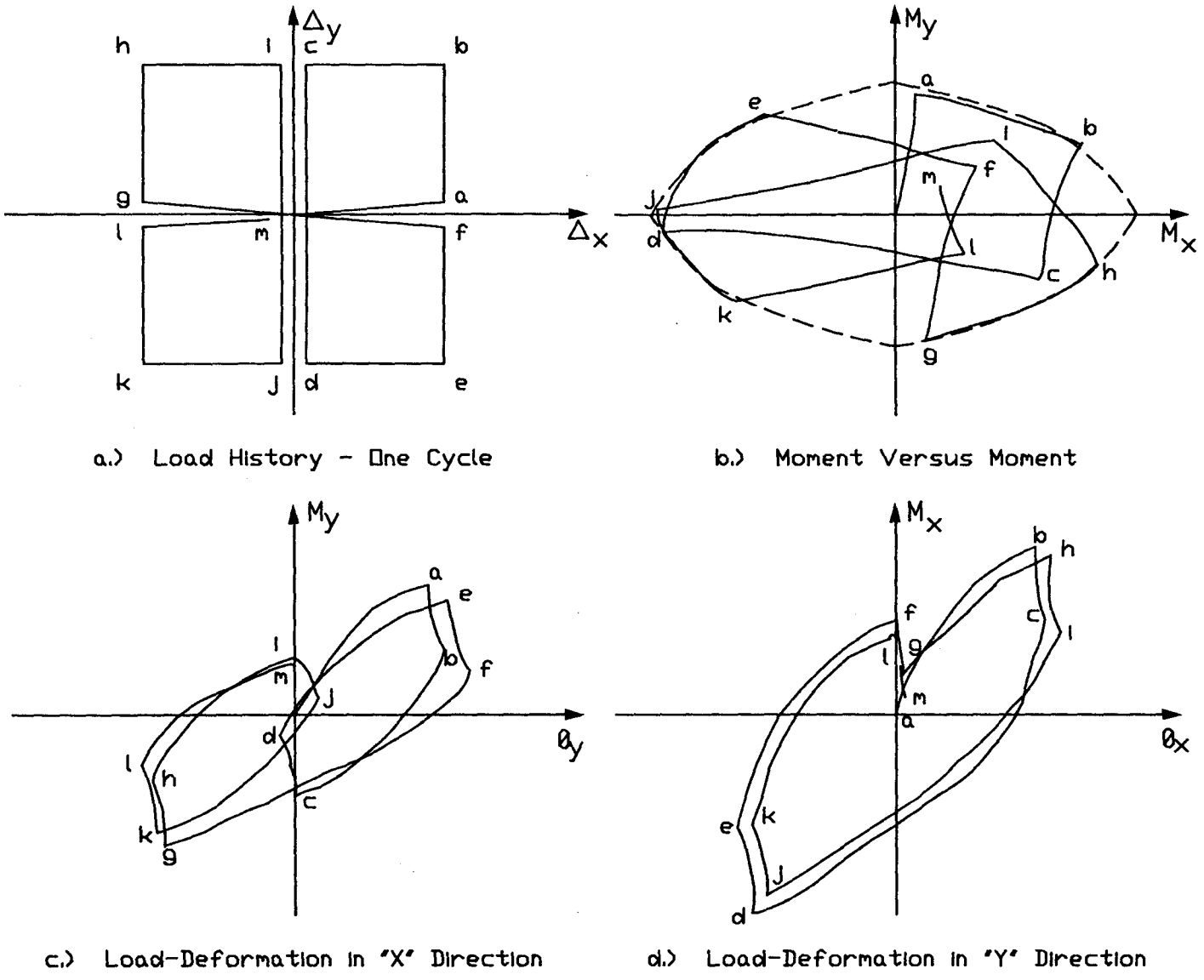

FIG. 4.12 Idealized Biaxial Hysteresis Relations for Load Steps "a" through "m"

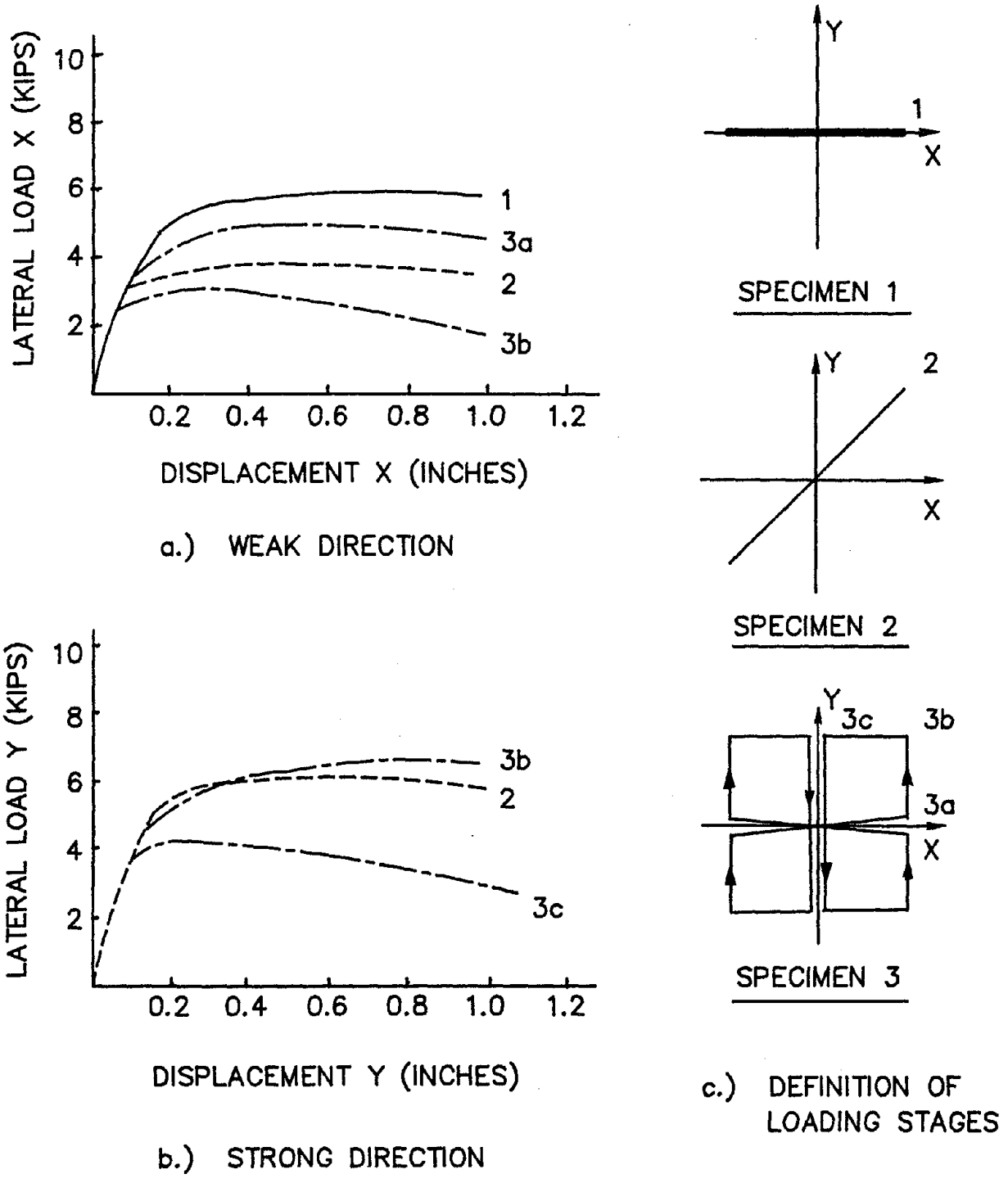

FIG. 4.13 Load Resistance Envelopes for Specimens 1, 2, and 3

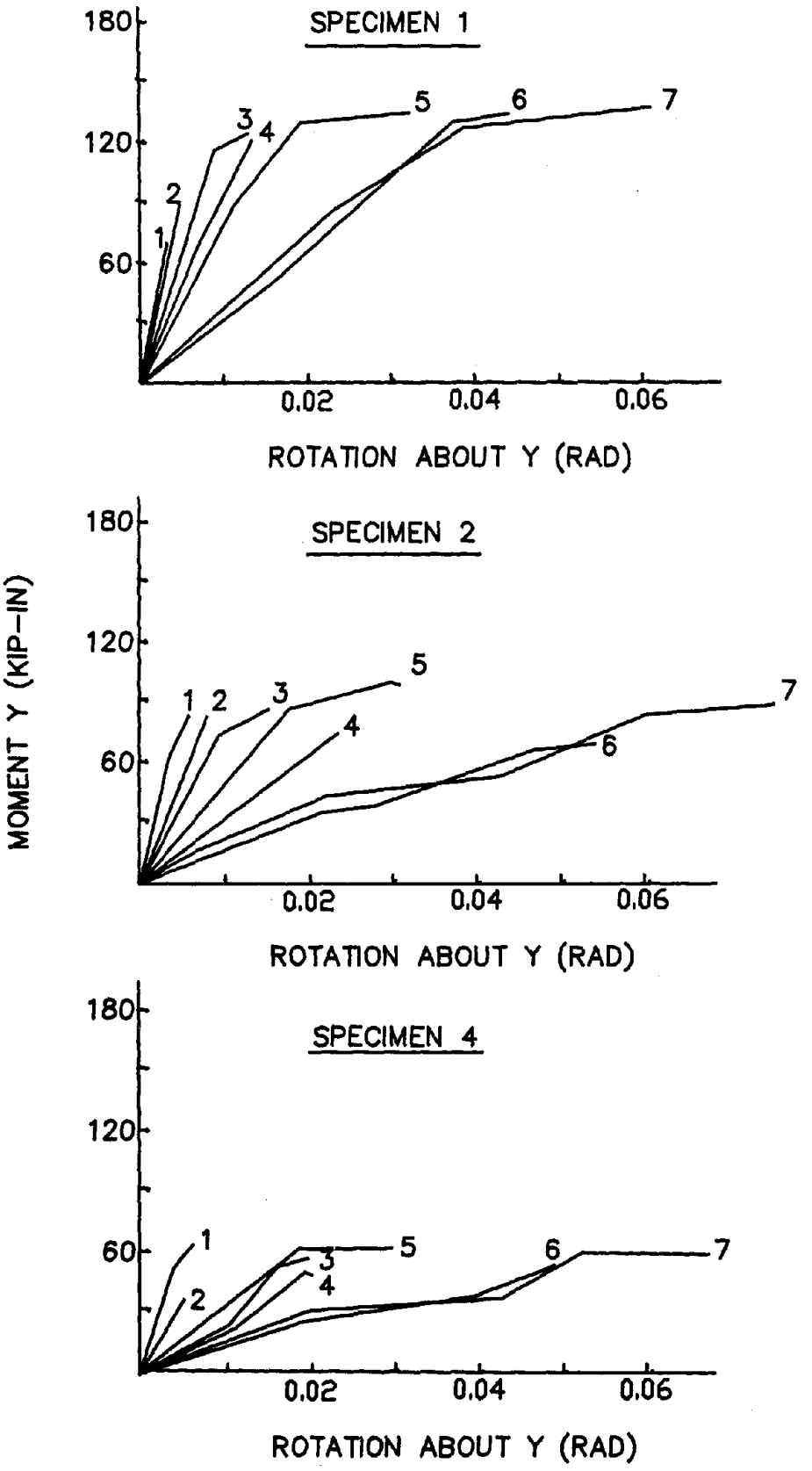

FIG. 4.14 Comparison of loading Stiffnesses

EARTHQUAKE ENGINEERING RESEARCH CENTER REPORT SERIES

EERC reports are available from the National Information Service for Earthquake Engineering(NISEE) and from the National Technical Information Service(NTIS). Numbers in parentheses are Accession Numbers assigned by the National Technical Information Service; these are followed by a price code. Contact NTIS, 5285 Port Royal Road, Springfield Virginia, 22161 for more information. Reports without Accession Numbers were not available from NTIS at the time of printing. For a current complete list of EERC reports (from EERC 67-1) and availablity information, please contact University of California, EERC, NISEE, 1301 South 46th Street, Richmond, California 94804.

UCB/EERC-80/01 "Earthquake Response of Concrete Gravity Dams Including Hydrodynamic and Foundation Interaction Effects," by Chopra, A.K., Chakrabarti, P. and Gupta, S., January 1980, (AD-A087297)A10.

UCB/EERC-80/02 "Rocking Response of Rigid Blocks to Earthquakes," by Yim, C.S., Chopra, A.K. and Penzien, J., January 1980, (PB80 166 002)A04.

UCB/EERC-80/03 "Optimum Inelastic Design of Seismic-Resistant Reinforced Concrete Frame Structures," by Zagajeski, S.W. and Bertero, V.V., January 1980, (PB80 164 635)A06.

UCB/EERC-80/04 "Effects of Amount and Arrangement of Wall-Panel Reinforcement on Hysteretic Behavior of Reinforced Concrete Walls," by Iliya, R. and Bertero, V.V., February 1980, (PB81 122 525)A09.

UCB/EERC-80/05 "Shaking Table Research on Concrete Dam Models," by Niwa, A. and Clough, R.W., September 1980, (PB81 122 368)A06.

UCB/EERC-80/06 "The Design of Steel Energy-Absorbing Restrainers and their Incorporation into Nuclear Power Plants for Enhanced Safety (Vol 1a): Piping with Energy Absorbing Restrainers: Parameter Study on Small Systems," by Powell, G.H., Oughourlian, C. and Simons, J., June 1980.

UCB/EERC-80/07 "Inelastic Torsional Response of Structures Subjected to Earthquake Ground Motions," by Yamazaki, Y., April 1980, (PB81 122 327)A08.

UCB/EERC-80/08 "Study of X-Braced Steel Frame Structures under Earthquake Simulation," by Ghanaat, Y., April 1980, (PB81 122 335)A11.

UCB/EERC-80/09 "Hybrid Modelling of Soil-Structure Interaction," by Gupta, S., Lin, T.W. and Penzien, J., May 1980, (PB81 122 319)A07.

UCB/EERC-80/10 "General Applicability of a Nonlinear Model of a One Story Steel Frame," by Sveinsson, B.I. and McNiven, H.D., May 1980, (PB81 124 877)A06.

UCB/EERC-80/11 "A Green-Function Method for Wave Interaction with a Submerged Body," by Kioka, W., April 1980, (PB81 122 269)A07.

UCB/EERC-80/12 "Hydrodynamic Pressure and Added Mass for Axisymmetric Bodies.," by Nilrat, F., May 1980, (PB81 122 343)A08.

UCB/EERC-80/13 "Treatment of Non-Linear Drag Forces Acting on Offshore Platforms," by Dao, B.V. and Penzien, J., May 1980, (PB81 153 413)A07.

UCB/EERC-80/14 "2D Plane/Axisymmetric Solid Element (Type 3-Elastic or Elastic-Perfectly Plastic) for the ANSR-II Program," by Mondkar, D.P. and Powell, G.H., July 1980, (PB81 122 350)A03.

UCB/EERC-80/15 "A Response Spectrum Method for Random Vibrations," by Der Kiureghian, A., June 1981, (PB81 122 301)A03.

UCB/EERC-80/16 "Cyclic Inelastic Buckling of Tubular Steel Braces," by Zayas, V.A., Popov, E.P. and Martin, S.A., June 1981, (PB81 124 885)A10.

UCB/EERC-80/17 "Dynamic Response of Simple Arch Dams Including Hydrodynamic Interaction," by Porter, C.S. and Chopra, A.K., July 1981, (PB81 124 000)A13.

UCB/EERC-80/18 "Experimental Testing of a Friction Damped Aseismic Base Isolation System with Fail-Safe Characteristics," by Kelly, J.M., Beucke, K.E. and Skinner, M.S., July 1980, (PB81 148 595)A04.

UCB/EERC-80/19 "The Design of Steel Emergy-Absorbing Restrainers and their Incorporation into Nuclear Power Plants for Enhanced Safety (Vol.1B): Stochastic Seismic Analyses of Nuclear Power Plant Structures and Piping Systems Subjected to Multiple Supported Excitations," by Lee, M.C. and Penzien, J., June 1980, (PB82 201 872)A08.

UCB/EERC-80/20 "The Design of Steel Energy-Absorbing Restrainers and their Incorporation into Nuclear Power Plants for Enhanced Safety (Vol 1C): Numerical Method for Dynamic Substructure Analysis," by Dickens, J.M. and Wilson, E.L., June 1980.

UCB/EERC-80/21 "The Design of Steel Energy-Absorbing Restrainers and their Incorporation into Nuclear Power Plants for Enhanced Safety (Vol 2): Development and Testing of Restraints for Nuclear Piping Systems," by Kelly, J.M. and Skinner, M.S., June 1980.

UCB/EERC-80/22 "3D Solid Element (Type 4-Elastic or Elastic-Perfectly-Plastic) for the ANSR-II Program," by Mondkar, D.P. and Powell, G.H., July 1980, (PB81 123 242)A03.

UCB/EERC-80/23 "Gap-Friction Element (Type 5) for the Ansr-II Program," by Mondkar, D.P. and Powell, G.H., July 1980, (PB81 122 285)A03.

UCB/EERC-80/24 "U-Bar Restraint Element (Type 11) for the ANSR-II Program," by Oughourlian, C. and Powell, G.H., July 1980, (PB81 122 293)A03.

UCB/EERC-80/25 "Testing of a Natural Rubber Base Isolation System by an Explosively Simulated Earthquake," by Kelly, J.M., August 1980, (PB81 201 360)A04.

UCB/EERC-80/26 "Input Identification from Structural Vibrational Response," by Hu, Y., August 1980, (PB81 152 308)A05.

UCB/EERC-80/27 "Cyclic Inelastic Behavior of Steel Offshore Structures," by Zayas, V.A., Mahin, S.A. and Popov, E.P., August 1980, (PB81 196 180)A15.

UCB/EERC-80/28 "Shaking Table Testing of a Reinforced Concrete Frame with Biaxial Response," by Oliva, M.G., October 1980, (PB81 154 304)A10.

UCB/EERC-80/29 "Dynamic Properties of a Twelve-Story Prefabricated Panel Building," by Bouwkamp, J.G., Kollegger, J.P. and Stephen, R.M., October 1980, (PB82 138 777)A07.

UCB/EERC-80/30 "Dynamic Properties of an Eight-Story Prefabricated Panel Building," by Bouwkamp, J.G., Kollegger, J.P. and Stephen, R.M., October 1980, (PB81 200 313)A05.

UCB/EERC-80/31 "Predictive Dynamic Response of Panel Type Structures under Earthquakes," by Kollegger, J.P. and Bouwkamp, J.G., October 1980, (PB81 152 316)A04.

UCB/EERC-80/32 "The Design of Steel Energy-Absorbing Restrainers and their Incorporation into Nuclear Power Plants for Enhanced Safety (Vol 3): Testing of Commercial Steels in Low-Cycle Torsional Fatique," by Spanner, P., Parker, E.R., Jongewaard, E. and Dory, M., 1980.

UCB/EERC-80/33 "The Design of Steel Energy-Absorbing Restrainers and their Incorporation into Nuclear Power Plants for Enhanced Safety (Vol 4): Shaking Table Tests of Piping Systems with Energy-Absorbing Restrainers," by Stiemer, S.F. and Godden, W.G., September 1980, (PB82 201 880)A05.

UCB/EERC-80/34 "The Design of Steel Energy-Absorbing Restrainers and their Incorporation into Nuclear Power Plants for Enhanced Safety (Vol 5): Summary Report," by Spencer, P., 1980.

UCB/EERC-80/35 "Experimental Testing of an Energy-Absorbing Base Isolation System," by Kelly, J.M., Skinner, M.S. and Beucke, K.E., October 1980, (PB81 154 072)A04.

UCB/EERC-80/36 "Simulating and Analyzing Artificial Non-Stationary Earth Ground Motions," by Nau, R.F., Oliver, R.M. and Pister, K.S., October 1980, (PB81 153 397)A04.

UCB/EERC-80/37 "Earthquake Engineering at Berkeley - 1980," by , September 1980, (PB81 205 674)A09.

UCB/EERC-80/38 "Inelastic Seismic Analysis of Large Panel Buildings," by Schricker, V. and Powell, G.H., September 1980, (PB81 154 338)A13.

UCB/EERC-80/39 "Dynamic Response of Embankment, Concrete-Gavity and Arch Dams Including Hydrodynamic Interation," by Hall, J.F. and Chopra, A.K., October 1980, (PB81 152 324)A11.

UCB/EERC-80/40 "Inelastic Buckling of Steel Struts under Cyclic Load Reversal.," by Black, R.G. , Wenger, W.A. and Popov, E.P., October 1980, (PB81 154 312)A08.

UCB/EERC-80/41 "Influence of Site Characteristics on Buildings Damage during the October 3,1974 Lima Earthquake," by Repetto, P., Arango, I. and Seed, H.B., September 1980, (PB81 161 739)A05.

UCB/EERC-80/42 "Evaluation of a Shaking Table Test Program on Response Behavior of a Two Story Reinforced Concrete Frame," by Blondet, J.M., Clough, R.W. and Mahin, S.A., December 1980, (PB82 196 544)A11.

UCB/EERC-80/43 "Modelling of Soil-Structure Interaction by Finite and Infinite Elements," by Medina, F., December 1980, (PB81 229 270)A04.

UCB/EERC-81/01 "Control of Seismic Response of Piping Systems and Other Structures by Base Isolation," by Kelly, J.M., January 1981, (PB81 200 735)A05.

UCB/EERC-81/02 "OPTNSR- An Interactive Software System for Optimal Design of Statically and Dynamically Loaded Structures with Nonlinear Response," by Bhatti, M.A., Ciampi, V. and Pister, K.S., January 1981, (PB81 218 851)A09.

UCB/EERC-81/03 "Analysis of Local Variations in Free Field Seismic Ground Motions," by Chen, J.-C., Lysmer, J. and Seed, H.B., January 1981, (AD-A099508)A13.

UCB/EERC-81/04 "Inelastic Structural Modeling of Braced Offshore Platforms for Seismic Loading. ," by Zayas, V.A., Shing, P.-S.B., Mahin, S.A. and Popov, E.P., January 1981, (PB82 138 777)A07.

UCB/EERC-81/05 "Dynamic Response of Light Equipment in Structures," by Der Kiureghian, A., Sackman, J.L. and Nour-Omid, B., April 1981, (PB81 218 497)A04.

UCB/EERC-81/06 "Preliminary Experimental Investigation of a Broad Base Liquid Storage Tank," by Bouwkamp, J.G., Kollegger, J.P. and Stephen, R.M., May 1981, (PB82 140 385)A03.

UCB/EERC-81/07 "The Seismic Resistant Design of Reinforced Concrete Coupled Structural Walls," by Aktan, A.E. and Bertero, V.V., June 1981, (PB82 113 358)A11.

UCB/EERC-81/08 "Unassigned," by Unassigned, 1981.

UCB/EERC-81/09 "Experimental Behavior of a Spatial Piping System with Steel Energy Absorbers Subjected to a Simulated Differential Seismic Input," by Stiemer, S.F., Godden, W.G. and Kelly, J.M., July 1981, (PB82 201 898)A04.

UCB/EERC-81/10 "Evaluation of Seismic Design Provisions for Masonry in the United States," by Sveinsson, B.I., Mayes, R.L. and McNiven, H.D., August 1981, (PB82 166 075)A08.

UCB/EERC-81/11 "Two-Dimensional Hybrid Modelling of Soil-Structure Interaction," by Tzong, T.-J., Gupta, S. and Penzien, J., August 1981, (PB82 142 118)A04.

UCB/EERC-81/12 "Studies on Effects of Infills in Seismic Resistant R/C Construction," by Brokken, S. and Bertero, V.V., October 1981, (PB82 166 190)A09.

UCB/EERC-81/13 "Linear Models to Predict the Nonlinear Seismic Behavior of a One-Story Steel Frame," by Valdimarsson, H., Shah, A.H. and McNiven, H.D., September 1981, (PB82 138 793)A07.

UCB/EERC-81/14 "TLUSH: A Computer Program for the Three-Dimensional Dynamic Analysis of Earth Dams," by Kagawa, T., Mejia, L.H., Seed, H.B. and Lysmer, J., September 1981, (PB82 139 940)A06.

UCB/EERC-81/15 "Three Dimensional Dynamic Response Analysis of Earth Dams," by Mejia, L.H. and Seed, H.B., September 1981, (PB82 137 274)A12.

UCB/EERC-81/16 "Experimental Study of Lead and Elastomeric Dampers for Base Isolation Systems," by Kelly, J.M. and Hodder, S.B., October 1981, (PB82 166 182)A05.

UCB/EERC-81/17 "The Influence of Base Isolation on the Seismic Response of Light Secondary Equipment," by Kelly, J.M., April 1981, (PB82 255 266)A04.

UCB/EERC-81/18 "Studies on Evaluation of Shaking Table Response Analysis Procedures," by Blondet, J. Marcial, November 1981, (PB82 197 278)A10.

UCB/EERC-81/19 "DELIGHT.STRUCT: A Computer-Aided Design Environment for Structural Engineering. ," by Balling, R.J., Pister, K.S. and Polak, E., December 1981, (PB82 218 496)A07.

UCB/EERC-81/20 "Optimal Design of Seismic-Resistant Planar Steel Frames," by Balling, R.J., Ciampi, V. and Pister, K.S., December 1981, (PB82 220 179)A07.

UCB/EERC-82/01 "Dynamic Behavior of Ground for Seismic Analysis of Lifeline Systems," by Sato, T. and Der Kiureghian, A., January 1982, (PB82 218 926)A05.

UCB/EERC-82/02 "Shaking Table Tests of a Tubular Steel Frame Model," by Ghanaat, Y. and Clough, R.W., January 1982, (PB82 220 161)A07.

UCB/EERC-82/03 "Behavior of a Piping System under Seismic Excitation: Experimental Investigations of a Spatial Piping System supported by Mechanical Shock Arrestors," by Schneider, S., Lee, H.-M. and Godden, W. G., May 1982, (PB83 172 544)A09.

UCB/EERC-82/04 "New Approaches for the Dynamic Analysis of Large Structural Systems," by Wilson, E.L., June 1982, (PB83 148 080)A05.

UCB/EERC-82/05 "Model Study of Effects of Damage on the Vibration Properties of Steel Offshore Platforms," by Shahrivar, F. and Bouwkamp, J.G., June 1982, (PB83 148 742)A10.

UCB/EERC-82/06 "States of the Art and Pratice in the Optimum Seismic Design and Analytical Response Prediction of R/C Frame Wall Structures," by Aktan, A.E. and Bertero, V.V., July 1982, (PB83 147 736)A05.

UCB/EERC-82/07 "Further Study of the Earthquake Response of a Broad Cylindrical Liquid-Storage Tank Model," by Manos, G.C. and Clough, R.W., July 1982, (PB83 147 744)A11.

UCB/EERC-82/08 "An Evaluation of the Design and Analytical Seismic Response of a Seven Story Reinforced Concrete Frame," by Charney, F.A. and Bertero, V.V., July 1982, (PB83 157 628)A09.

UCB/EERC-82/09 "Fluid-Structure Interactions: Added Mass Computations for Incompressible Fluid. ," by Kuo, J.S.-H., August 1982, (PB83 156 281)A07.

UCB/EERC-82/10 "Joint-Opening Nonlinear Mechanism: Interface Smeared Crack Model," by Kuo, J.S.-H., August 1982, (PB83 149 195)A05.

UCB/EERC-82/11 "Dynamic Response Analysis of Techi Dam," by Clough, R.W., Stephen, R.M. and Kuo, J.S.-H., August 1982, (PB83 147 496)A06.

UCB/EERC-82/12 "Prediction of the Seismic Response of R/C Frame-Coupled Wall Structures," by Aktan, A.E., Bertero, V.V. and Piazzo, M., August 1982, (PB83 149 203)A09.

UCB/EERC-82/13 "Preliminary Report on the Smart 1 Strong Motion Array in Taiwan," by Bolt, B.A. , Loh, C.H., Penzien, J. and Tsai, Y.B., August 1982, (PB83 159 400)A10.

UCB/EERC-82/14 "Shaking-Table Studies of an Eccentrically X-Braced Steel Structure," by Yang, M.S., September 1982, (PB83 260 778)A12.

UCB/EERC-82/15 "The Performance of Stairways in Earthquakes," by Roha, C., Axley, J.W. and Bertero, V.V., September 1982, (PB83 157 693)A07.

UCB/EERC-82/16 "The Behavior of Submerged Multiple Bodies in Earthquakes," by Liao, W.-G., September 1982, (PB83 158 709)A07.

UCB/EERC-82/17 "Effects of Concrete Types and Loading Conditions on Local Bond-Slip Relationships," by Cowell, A.D., Popov, E.P. and Bertero, V.V., September 1982, (PB83 153 577)A04.

UCB/EERC-82/18 "Mechanical Behavior of Shear Wall Vertical Boundary Members: An Experimental Investigation," by Wagner, M.T. and Bertero, V.V., October 1982, (PB83 159 764)A05.

UCB/EERC-82/19 "Experimental Studies of Multi-support Seismic Loading on Piping Systems," by Kelly, J.M. and Cowell, A.D., November 1982.

UCB/EERC-82/20 "Generalized Plastic Hinge Concepts for 3D Beam-Column Elements," by Chen, P. F.-S. and Powell, G.H., November 1982, (PB83 247 981)A13.

UCB/EERC-82/21 "ANSR-II: General Computer Program for Nonlinear Structural Analysis," by Oughourlian, C.V. and Powell, G.H., November 1982, (PB83 251 330)A12.

UCB/EERC-82/22 "Solution Strategies for Statically Loaded Nonlinear Structures," by Simons, J.W. and Powell, G.H., November 1982, (PB83 197 970)A06.

UCB/EERC-82/23 "Analytical Model of Deformed Bar Anchorages under Generalized Excitations," by Ciampi, V., Eligehausen, R., Bertero, V.V. and Popov, E.P., November 1982, (PB83 169 532)A06.

UCB/EERC-82/24 "A Mathematical Model for the Response of Masonry Walls to Dynamic Excitations," by Sucuoglu, H., Mengi, Y. and McNiven, H.D., November 1982, (PB83 169 011)A07.

UCB/EERC-82/25 "Earthquake Response Considerations of Broad Liquid Storage Tanks," by Cambra, F.J., November 1982, (PB83 251 215)A09.

UCB/EERC-82/26 "Computational Models for Cyclic Plasticity, Rate Dependence and Creep," by Mosaddad, B. and Powell, G.H., November 1982, (PB83 245 829)A08.

UCB/EERC-82/27 "Inelastic Analysis of Piping and Tubular Structures," by Mahasuverachai, M. and Powell, G.H., November 1982, (PB83 249 987)A07.

UCB/EERC-83/01 "The Economic Feasibility of Seismic Rehabilitation of Buildings by Base Isolation," by Kelly, J.M., January 1983, (PB83 197 988)A05.

UCB/EERC-83/02 "Seismic Moment Connections for Moment-Resisting Steel Frames.," by Popov, E.P., January 1983, (PB83 195 412)A04.

UCB/EERC-83/03 "Design of Links and Beam-to-Column Connections for Eccentrically Braced Steel Frames," by Popov, E.P. and Malley, J.O., January 1983, (PB83 194 811)A04.

UCB/EERC-83/04 "Numerical Techniques for the Evaluation of Soil-Structure Interaction Effects in the Time Domain," by Bayo, E. and Wilson, E.L., February 1983, (PB83 245 605)A09.

UCB/EERC-83/05 "A Transducer for Measuring the Internal Forces in the Columns of a Frame-Wall Reinforced Concrete Structure," by Sause, R. and Bertero, V.V., May 1983, (PB84 119 494)A06.

UCB/EERC-83/06 "Dynamic Interactions Between Floating Ice and Offshore Structures," by Croteau, P., May 1983, (PB84 119 486)A16.

UCB/EERC-83/07 "Dynamic Analysis of Multiply Tuned and Arbitrarily Supported Secondary Systems. ," by Igusa, T. and Der Kiureghian, A., July 1983, (PB84 118 272)A11.

UCB/EERC-83/08 "A Laboratory Study of Submerged Multi-body Systems in Earthquakes," by Ansari, G.R., June 1983, (PB83 261 842)A17.

UCB/EERC-83/09 "Effects of Transient Foundation Uplift on Earthquake Response of Structures," by Yim, C.-S. and Chopra, A.K., June 1983, (PB83 261 396)A07.

UCB/EERC-83/10 "Optimal Design of Friction-Braced Frames under Seismic Loading," by Austin, M.A. and Pister, K.S., June 1983, (PB84 119 288)A06.

UCB/EERC-83/11 "Shaking Table Study of Single-Story Masonry Houses: Dynamic Performance under Three Component Seismic Input and Recommendations," by Manos, G.C., Clough, R.W. and Mayes, R.L., July 1983, (UCB/EERC-83/11)A08.

UCB/EERC-83/12 "Experimental Error Propagation in Pseudodynamic Testing," by Shiing, P.B. and Mahin, S.A., June 1983, (PB84 119 270)A09.

UCB/EERC-83/13 "Experimental and Analytical Predictions of the Mechanical Characteristics of a 1/5-scale Model of a 7-story R/C Frame-Wall Building Structure," by Aktan, A.E., Bertero, V.V., Chowdhury, A.A. and Nagashima, T., June 1983, (PB84 119 213)A07.

UCB/EERC-83/14 "Shaking Table Tests of Large-Panel Precast Concrete Building System Assemblages," by Oliva, M.G. and Clough, R.W., June 1983, (PB86 110 210/AS)A11.

UCB/EERC-83/15 "Seismic Behavior of Active Beam Links in Eccentrically Braced Frames," by Hjelmstad, K.D. and Popov, E.P., July 1983, (PB84 119 676)A09.

UCB/EERC-83/16 "System Identification of Structures with Joint Rotation," by Dimsdale, J.S., July 1983, (PB84 192 210)A06.

UCB/EERC-83/17 "Construction of Inelastic Response Spectra for Single-Degree-of-Freedom Systems," by Mahin, S. and Lin, J., June 1983, (PB84 208 834)A05.

UCB/EERC-83/18 "Interactive Computer Analysis Methods for Predicting the Inelastic Cyclic Behaviour of Structural Sections," by Kaba, S. and Mahin, S., July 1983, (PB84 192 012)A06.

UCB/EERC-83/19 "Effects of Bond Deterioration on Hysteretic Behavior of Reinforced Concrete Joints," by Filippou, F.C., Popov, E.P. and Bertero, V.V., August 1983, (PB84 192 020)A10.

UCB/EERC-83/20 "Analytical and Experimental Correlation of Large-Panel Precast Building System Performance," by Oliva, M.G., Clough, R.W., Velkov, M. and Gavrilovic, P., November 1983.

UCB/EERC-83/21 "Mechanical Characteristics of Materials Used in a 1/5 Scale Model of a 7-Story Reinforced Concrete Test Structure," by Bertero, V.V., Aktan, A.E., Harris, H.G. and Chowdhury, A.A., October 1983, (PB84 193 697)A05.

UCB/EERC-83/22 "Hybrid Modelling of Soil-Structure Interaction in Layered Media," by Tzong, T.-J. and Penzien, J., October 1983, (PB84 192 178)A08.

UCB/EERC-83/23 "Local Bond Stress-Slip Relationships of Deformed Bars under Generalized Excitations," by Eligehausen, R., Popov, E.P. and Bertero, V.V., October 1983, (PB84 192 848)A09.

UCB/EERC-83/24 "Design Considerations for Shear Links in Eccentrically Braced Frames," by Malley, J.O. and Popov, E.P., November 1983, (PB84 192 186)A07.

UCB/EERC-84/01 "Pseudodynamic Test Method for Seismic Performance Evaluation: Theory and Implementation," by Shing, P.-S. B. and Mahin, S.A., January 1984, (PB84 190 644)A08.

UCB/EERC-84/02 "Dynamic Response Behavior of Kiang Hong Dian Dam," by Clough, R.W., Chang, K.-T., Chen, H.-Q. and Stephen, R.M., April 1984, (PB84 209 402)A08.

UCB/EERC-84/03 "Refined Modelling of Reinforced Concrete Columns for Seismic Analysis," by Kaba, S.A. and Mahin, S.A., April 1984, (PB84 234 384)A06.

UCB/EERC-84/04 "A New Floor Response Spectrum Method for Seismic Analysis of Multiply Supported Secondary Systems," by Asfura, A. and Der Kiureghian, A., June 1984, (PB84 239 417)A06.

UCB/EERC-84/05 "Earthquake Simulation Tests and Associated Studies of a 1/5th-scale Model of a 7-Story R/C Frame-Wall Test Structure," by Bertero, V.V., Aktan, A.E., Charney, F.A. and Sause, R., June 1984, (PB84 239 409)A09.

UCB/EERC-84/06 "R/C Structural Walls: Seismic Design for Shear," by Aktan, A.E. and Bertero, V.V., 1984.

UCB/EERC-84/07 "Behavior of Interior and Exterior Flat-Plate Connections subjected to Inelastic Load Reversals," by Zee, H.L. and Moehle, J.P., August 1984, (PB86 117 629/AS)A07.

UCB/EERC-84/08 "Experimental Study of the Seismic Behavior of a Two-Story Flat-Plate Structure. ," by Moehle, J.P. and Diebold, J.W., August 1984, (PB86 122 553/AS)A12.

UCB/EERC-84/09 "Phenomenological Modeling of Steel Braces under Cyclic Loading," by Ikeda, K., Mahin, S.A. and Dermitzakis, S.N., May 1984, (PB86 132 198/AS)A08.

UCB/EERC-84/10 "Earthquake Analysis and Response of Concrete Gravity Dams," by Fenves, G. and Chopra, A.K., August 1984, (PB85 193 902/AS)A11.

UCB/EERC-84/11 "EAGD-84: A Computer Program for Earthquake Analysis of Concrete Gravity Dams," by Fenves, G. and Chopra, A.K., August 1984, (PB85 193 613/AS)A05.

UCB/EERC-84/12 "A Refined Physical Theory Model for Predicting the Seismic Behavior of Braced Steel Frames," by Ikeda, K. and Mahin, S.A., July 1984, (PB85 191 450/AS)A09.

UCB/EERC-84/13 "Earthquake Engineering Research at Berkeley - 1984," by , August 1984, (PB85 197 341/AS)A10.

UCB/EERC-84/14 "Moduli and Damping Factors for Dynamic Analyses of Cohesionless Soils," by Seed, H.B., Wong, R.T., Idriss, I.M. and Tokimatsu, K., September 1984, (PB85 191 468/AS)A04.

UCB/EERC-84/15 "The Influence of SPT Procedures in Soil Liquefaction Resistance Evaluations," by Seed, H.B., Tokimatsu, K., Harder, L.F. and Chung, R.M., October 1984, (PB85 191 732/AS)A04.

UCB/EERC-84/16 "Simplified Procedures for the Evaluation of Settlements in Sands Due to Earthquake Shaking," by Tokimatsu, K. and Seed, H.B., October 1984, (PB85 197 887/AS)A03.

UCB/EERC-84/17 "Evaluation of Energy Absorption Characteristics of Bridges under Seismic Conditions," by Imbsen, R.A. and Penzien, J., November 1984.

UCB/EERC-84/18 "Structure-Foundation Interactions under Dynamic Loads," by Liu, W.D. and Penzien, J., November 1984, (PB87 124 889/AS)A11.

UCB/EERC-84/19 "Seismic Modelling of Deep Foundations," by Chen, C.-H. and Penzien, J., November 1984, (PB87 124 798/AS)A07.

UCB/EERC-84/20 "Dynamic Response Behavior of Quan Shui Dam," by Clough, R.W., Chang, K.-T., Chen, H.-Q., Stephen, R.M., Ghanaat, Y. and Qi, J.-H., November 1984, (PB86 115177/AS)A07.

UCB/EERC-85/01 "Simplified Methods of Analysis for Earthquake Resistant Design of Buildings," by Cruz, E.F. and Chopra, A.K., February 1985, (PB86 112299/AS)A12.

UCB/EERC-85/02 "Estimation of Seismic Wave Coherency and Rupture Velocity using the SMART 1 Strong-Motion Array Recordings," by Abrahamson, N.A., March 1985, (PB86 214 343)A07.

UCB/EERC-85/03 "Dynamic Properties of a Thirty Story Condominium Tower Building," by Stephen, R.M., Wilson, E.L. and Stander, N., April 1985, (PB86 118965/AS)A06.

UCB/EERC-85/04 "Development of Substructuring Techniques for On-Line Computer Controlled Seismic Performance Testing," by Dermitzakis, S. and Mahin, S., February 1985, (PB86 132941/AS)A08.

UCB/EERC-85/05 "A Simple Model for Reinforcing Bar Anchorages under Cyclic Excitations," by Filippou, F.C., March 1985, (PB86 112 919/AS)A05.

UCB/EERC-85/06 "Racking Behavior of Wood-framed Gypsum Panels under Dynamic Load," by Oliva, M.G., June 1985.

UCB/EERC-85/07 "Earthquake Analysis and Response of Concrete Arch Dams," by Fok, K.-L. and Chopra, A.K., June 1985, (PB86 139672/AS)A10.

UCB/EERC-85/08 "Effect of Inelastic Behavior on the Analysis and Design of Earthquake Resistant Structures," by Lin, J.P. and Mahin, S.A., June 1985, (PB86 135340/AS)A08.

UCB/EERC-85/09 "Earthquake Simulator Testing of a Base-Isolated Bridge Deck," by Kelly, J.M., Buckle, I.G. and Tsai, H.-C., January 1986, (PB87 124 152/AS)A06.

UCB/EERC-85/10 "Simplified Analysis for Earthquake Resistant Design of Concrete Gravity Dams," by Fenves, G. and Chopra, A.K., June 1986, (PB87 124 160/AS)A08.

UCB/EERC-85/11 "Dynamic Interaction Effects in Arch Dams," by Clough, R.W., Chang, K.-T., Chen, H.-Q. and Ghanaat, Y., October 1985, (PB86 135027/AS)A05.

UCB/EERC-85/12 "Dynamic Response of Long Valley Dam in the Mammoth Lake Earthquake Series of May 25-27, 1980," by Lai, S. and Seed, H.B., November 1985, (PB86 142304/AS)A05.

UCB/EERC-85/13 "A Methodology for Computer-Aided Design of Earthquake-Resistant Steel Structures," by Austin, M.A., Pister, K.S. and Mahin, S.A., December 1985, (PB86 159480/AS)A10 .

UCB/EERC-85/14 "Response of Tension-Leg Platforms to Vertical Seismic Excitations," by Liou, G.-S., Penzien, J. and Yeung, R.W., December 1985, (PB87 124 871/AS)A08.

UCB/EERC-85/15 "Cyclic Loading Tests of Masonry Single Piers: Volume 4 - Additional Tests with Height to Width Ratio of 1," by Sveinsson, B., McNiven, H.D. and Sucuoglu, H., December 1985.

UCB/EERC-85/16 "An Experimental Program for Studying the Dynamic Response of a Steel Frame with a Variety of Infill Partitions," by Yanev, B. and McNiven, H.D., December 1985.

UCB/EERC-86/01 "A Study of Seismically Resistant Eccentrically Braced Steel Frame Systems," by Kasai, K. and Popov, E.P., January 1986, (PB87 124 178/AS)A14.

UCB/EERC-86/02 "Design Problems in Soil Liquefaction," by Seed, H.B., February 1986, (PB87 124 186/AS)A03.

UCB/EERC-86/03 "Implications of Recent Earthquakes and Research on Earthquake-Resistant Design and Construction of Buildings," by Bertero, V.V., March 1986, (PB87 124 194/AS)A05.

UCB/EERC-86/04 "The Use of Load Dependent Vectors for Dynamic and Earthquake Analyses," by Leger, P., Wilson, E.L. and Clough, R.W., March 1986, (PB87 124 202/AS)A12.

UCB/EERC-86/05 "Two Beam-To-Column Web Connections," by Tsai, K.-C. and Popov, E.P., April 1986 , (PB87 124 301/AS)A04.

UCB/EERC-86/06 "Determination of Penetration Resistance for Coarse-Grained Soils using the Becker Hammer Drill," by Harder, L.F. and Seed, H.B., May 1986, (PB87 124 210/AS)A07.

UCB/EERC-86/07 "A Mathematical Model for Predicting the Nonlinear Response of Unreinforced Masonry Walls to In-Plane Earthquake Excitations," by Mengi, Y. and McNiven, H.D., May 1986, (PB87 124 780/AS)A06.

UCB/EERC-86/08 "The 19 September 1985 Mexico Earthquake: Building Behavior," by Bertero, V.V., July 1986.

UCB/EERC-86/09 "EACD-3D: A Computer Program for Three-Dimensional Earthquake Analysis of Concrete Dams," by Fok, K.-L., Hall, J.F. and Chopra, A.K., July 1986, (PB87 124 228/AS)A08.

UCB/EERC-86/10 "Earthquake Simulation Tests and Associated Studies of a 0.3-Scale Model of a Six-Story Concentrically Braced Steel Structure," by Uang, C.-M. and Bertero, V.V., December 1986.

UCB/EERC-86/11 "Mechanical Characteristics of Base Isolation Bearings for a Bridge Deck Model Test," by Kelly, J.M., Buckle, I.G. and Koh, C.-G., 1987.

UCB/EERC-86/12 "Modelling of Dynamic Response of Elastomeric Isolation Bearings," by Koh, C.-G. and Kelly, J.M., 1987.

UCB/EERC-87/01 "FPS Earthquake Resisting System: Experimental Report," by Zayas, V.A., Low, S.S. and Mahin, S.A., June 1987.

UCB/EERC-87/02 "Earthquake Simulator Tests and Associated Studies of a 0.3-Scale Model of a Six-Story Eccentrically Braced Steel Structure," by Whittaker, A., Uang, C.-M. and Bertero, V.V., July 1987.

UCB/EERC-87/03 "A Displacement Control and Uplift Restraint Device for Base-Isolated Structures," by Kelly, J.M., Griffith, M.C. and Aiken, I.G., April 1987.

UCB/EERC-87/04 "Earthquake Simulator Testing of a Combined Sliding Bearing and Rubber Bearing Isolation System," by Kelly, J.M. and Chalhoub, M.S., 1987.

UCB/EERC-87/05 "Three-Dimensional Inelastic Analysis of Reinforced Concrete Frame-Wall Structures," by Moazzami, S. and Bertero, V.V., May 1987.

UCB/EERC-87/06 "Experiments on Eccentrically Braced Frames With Composite Floors," by Ricles, J. and Popov, E., June 1987.

UCB/EERC-87/07 "Dynamic Analysis of Seismically Resistant Eccentrically Braced Frames," by Ricles, J. and Popov, E., June 1987.

UCB/EERC-87/08 "Undrained Cyclic Triaxial Testing of Gravels - The Effect of Membrane Compliance, " by Evans, M.D. and Seed, H.B., July 1987.

UCB/EERC-87/09 "Hybrid Solution Techniques For Generalized Pseudo-Dynamic Testing," by Thewalt, C. and Mahin, S. A., July 1987.

UCB/EERC-87/10 "Investigation of Ultimate Behavior of AISC Group 4 and 5 Heavy Steel Rolled-Section Splices with Full and Partial Penetration Butt Welds," by Bruneau, M. and Mahin, S.A., July 1987.

UCB/EERC-87/11 "Residual Strength of Sand From Dam Failures in the Chilean Earthquake of March 3, 1985," by De Alba, P., Seed, H. B., Retamal, E. and Seed, R. B., September 1987.

UCB/EERC-87/12 "Inelastic Response of Structures With Mass And/Or Stiffness Eccentricities In Plan Subjected to Earthquake Excitation," by Bruneau, M., September 1987.

UCB/EERC-87/13 "CSTRUCT: An Interactive Computer Environment For the Design and Analysis of Earthquake Resistant Steel Structures," by Austin, M.A., Mahin, S.A. and Pister, K.S., September 1987.

UCB/EERC-87/14 "Experimental Study of Reinforced Concrete Columns Subjected to Multi-Axial Loading," by Low, S.S. and Moehle, J.P., September 1987.